Charge injection into dielectric liquids

Jalalur Rahman

CHARGE INJECTION INTO DIELECTRIC LIQUIDS

being a Thesis submitted for the Degree of

DOCTOR OF PHILOSOPHY

in the Department of Applied Physics and Electronics

University of Durham

by

JALALUR RAHMAN, B.Sc. (Hons), M.Sc. (Dac).

December 1970.

A B S T R A C T

This work was aimed at finding suitable conditions for increased charge injection into liquid hexane. Experiments have been carried out on charge injection by both photoelectric and high-field processes. Photoelectric injection in very pure and highly degassed hexane depends mainly on the condition of the photocathode. Immediately after the preparation of the photocathode, the current increases continuously with applied voltage and it is shown to be mainly due to the emission of photoelectrons. Both cathode and liquid deteriorate over several days and a larger proportion of the current becomes due to bulk ionisation. Simultaneous d.c. and pulse measurements are used to prove that the initial photocurrent not only originates at the cathode but that its magnitude is also limited by the rate of emission of photoelectrons which subsequently form heavy negative carriers. The field dependence of the photocurrent has been explained in terms of the probability of heavy carrier formation by the electrons passing over an image barrier. The observed carrier mobility is in close agreement with that of other workers.

Field-injection from razor blade electrodes resulted in high conduction currents at comparatively low applied voltages. The current is only slightly higher when the blade is negative. In pure hexane the current is found to be independent of bulk movement of the liquid so that it must be limited by electrode processes which are probably electron emission and electron extraction for negative and positive polarities respectively. In commercial and water or alcohol doped hexane, the current increases with liquid flow when the blade is negative but decreases when it is positive.

These effects are explained in terms of field dissociation of the impurities and the formation of space charge at the high-field electrode. The present measurements suggest that the high injection currents reported elsewhere are mainly due to field ionisation of impurities rather than electron emission.

CONTENTS

CHAPTER I

INTRODUCTION

1.1 Background to the Thesis

The study of dielectric materials started with the practical need for good insulators in the very early experiments on electrostatics and it has progressed steadily since those times. Improvements in these materials have not been as rapid in recent years as they have in the related semiconductor materials, although there has been a steady and increasing demand for difficult applications of insulators in various branches of science and technology. There is still a great deal that is unknown about the basic electrical processes in insulators and particularly in insulating liquids for which there is no completely accepted theory. This thesis attempts to make a small contribution to this subject.

Of all the known liquid dielectrics, saturated hydrocarbons ($CH_3 - (CH_2)_n - CH_3$) are the best insulators. As their common name 'paraffin' (parum affines) indicates, they have the lowest chemical affinity of all hydrocarbons. When extremely pure, they have resistivities as high as 10^{20} ohm cm and breakdown strengths of the order of 10^6 V/cm. These compounds have the molecular shape of long zig-zag chains with almost the same cross-section for all molecules in the homologous series. The chain length increases in proportion to the number of CH_2 groups. In the solid state each molecular chain lies in one plane but in the liquid there can be rotation about each bond and the molecules can then be thought of as randomly bent cylinders.[1]

Paraffins in the form of long chains without branches are known as 'normal paraffins', designated n-pentane, n-hexane, etc. Normal hexane (C_6H_{14}) remains a liquid over a wide range of convenient temperatures ($-95^{o}C$ - $+69^{o}C$) and it has therefore received the greatest attention in the past. In the present work it is also chosen as the experimental liquid.

The electrical properties of dielectric liquids have been studied by many scientists for a long time. Of the various properties, one of the most important and probably the least understood is the mechanism of electrical conduction in these liquids. Conduction in dielectric liquids in general, and hexane in particular, remains largely unexplained due to

(a) contradictions between various experiments because of impurity effects, and

(b) lack of understanding of the role of the electrodes.

Previous work in this laboratory has helped to elucidate some of the impurity effects, and a further study of electrode effects is overdue. The cathode is of primary importance in this because the injection of negative carriers is believed to play a very important part in the conduction mechanism.

In view of the small magnitude and complex character of the 'natural' current, it has become common to study conduction processes in hexane by enhancing the conduction artificially by the injection of charge carriers into the liquid. The resulting conduction and its dependence on the electric field strength is then related to the type of excess carriers employed and so to their method of production.

Chapter II of this thesis briefly reviews some of the relevant previous work on the natural and enhanced conduction of dielectric liquids.

1.2 Scope of this Thesis

The original aim of the present work was to examine and hope to identify the charge carriers in hexane by electron spin resonance (ESR). With the existing spectrometers in the Department, this requires a charge density of greater than 10^{12} cm^{-3}, so that any such experiment must have enhanced conduction in the liquid. Increase of conductivity by bulk ionisation is not desirable as it gives rise to deterioration of the liquid and it is also not representative of 'natural' conduction. It is therefore necessary to increase the density of carriers in the liquid by enhanced cathode injection to obtain sufficient charge density for ESR work to be done. The study of the injection processes themselves, however, became the main objective of the present work when it was realised that charge densities of the required order would be very difficult to achieve in pure liquids. This study has turned out to have been of at least equal value to anything that could have been found out by ESR.

The present work is thus concentrated on increasing the cathode injection by the following two methods:-

a) photoinjection from a plane electrode

b) high-field injection from a sharply pointed electrode.

The photoinjection measurements described in Chapter IV were aimed at extending the work of Pugh[2] and Bloor[3] in order to find out more about the mechanism of charge injection. The effect of dissolved gas (oxygen) on photoinjection, as observed by Morant[4], gave both Pugh and Bloor the idea of measurements in highly degassed hexane. Pugh also found that true photo-injection is possible only with the following conditions:-

a) extremely pure liquids, specially purified so as not to absorb ultraviolet light in the wave-length range 2700 - 4000 Å,

b) highly degassed liquids,

c) a freshly prepared photocathode,

d) the use of UV radiation of the correct wavelength range.

Unless all these conditions are met, the photocurrents, if any, are not due to photoinjection from the cathode.

The present work proves that under these conditions the photocurrent is definitely limited by the cathode injection process and this is probably the only work in hexane for which this has been established to a high degree of certainty.

Field injection of charge carriers (previously examined by Hughes[5] at Bangor) has been investigated here in detail, as described in Chapter V. This has interest both for the basic study of injection process and for possibilities of its application in electrostatic machines. Accordingly, the latter part of the present work was devoted to studying high field injection in both pure (dried and filtered) and impure (as supplied or doped with water and alcohol) hexane samples.

The characteristics of field injection in flowing liquids have been found to be very complicated. The large field injected currents reported by Hughes are shown to be due to impurities (and probably water) in solution. The complex characteristics of the field injected currents are explained qualitatively in Chapter VII.

This study is of practical importance to the design of electrostatic generators and motors which have been proposed recently. It shows that

high injected currents are due to impurity ionisation and this is obviously undesirable in machines as it may lead to deterioration of the liquid and decay of performance. It will be interesting to see whether prolonged use of these machines confirms this.

Both the injection processes are found to be very complicated. In each case electrons are emitted from the metal surface but they are thought to remain free for extremely short periods of time before being trapped to form low-mobility carriers in the liquid. In the present work it was not possible to put forward any precise quantitative theory of this cathode injection although some progress has been made in this direction, as described in Chapter VI. Further understanding of the cathode processes will eventually be required to explain 'natural' conduction processes leading to high-field conduction and eventually breakdown. The conclusions of the present work in this wider context will be described in Chapter VIII.

CHAPTER II

REVIEW OF CONDUCTION AND INJECTION PROCESSES IN HEXANE

The conduction mechanism in dielectric liquids, such as hexane, may be classified under two main headings. At the lower field-strengths (less than 100 KV/cm), the conduction current is very small (10^{-16} - 10^{-12} A)[1] and is often attributed to the impurities present, including the dissolved air. At higher field-strengths electron emission from the cathode may play the main reason for the increase in the conduction current. The mechanism of conduction in the high-field region is thus often taken as an electronic one. The various possible mechanisms, both in low and high electric fields, are summarised in section one of this Chapter.

To study the conduction mechanism of these poorly conducting liquids, various experiments have been devised by workers in the field. One of their main efforts has been to increase the conductivity to more readily measurable values by introducing free electrons into the liquids. Section two describes the different methods by which such electron injection may be achieved.

2.1 Natural Conduction in Hexane

The conductivity of commercial liquids varies from 10^{-16}-10^{-12} mho/cm.[1] This wide variation is mainly due to the impurity content of the liquid. After the application of a voltage, the current decreases with time for several hours, with the removal of electrolytic impurities from the liquid. Zaky et al[6] observed this so called "electrical purification" up to a field strength of 100 KV/cm. Using a pair of oxygen-free electrodes, House[7] and Zaky et al[6] measured conduction current up to

1.5 MV/cm and 900 KV/cm respectively in gassy spectroscopic grade hexane. They[6] obtained a current-voltage curve with three distinct regions. A small linear of current increase was found up to 250 KV/cm, until saturation was reached, and then after 350 KV/cm, the current increased steadily again. Above a stress of 840 KV/cm, the current readings were unstable and the gap broke down at about 900 KV/cm.

Low-field conductivity measurements by Guizonnier[8] in these insulating liquids have also been found to obey the relation

$$I = A \exp(-w/kT) \qquad (1)$$

where A is a constant, T is absolute temperature, k the Boltzmann constant and w ($\simeq$ 4.1 eV), the activation energy which is independent of the nature of the liquids. This common value of w led to the conclusion that the conductivity of these liquids has a common cause and this was attributed to the moisture contained in the liquids. The same value of activation energy calculated from conductivity measurement in deionised water may have confirmed the presence of moisture in such liquids. The appearance of a minimum conductivity towards 30 - 40^{o}C[9] and the variation in the field distribution[10] in the liquid may also be explained by the presence of water in liquids. Dissolved water is thus an important source of electrolytic impurity[11]. Although the solubility of water in hexane is extremely small (about 100 ppm), the conductivity of a water saturated sample may be as high as 5.5 x 10^{-8} mho/cm. Standhommer and Seyer[12] found that the number of ions per unit volume is increased from 200 in a dry sample to 1.6 x 10^{5} in water saturated hexane (measured at 50^{o}C), and that the ion concentrations produced per unit time and per unit volume are a linear function of water concentration. Mobility measurements in benzene containing a high percentage of water gave a

value of 10^{-3} cm^2/volt sec for the mobility of a negative charge carrier. The mobility for positive carriers was slightly greater and was found to decrease with increasing temperature[13].

Increase in the conductivity of these liquids can also be achieved by adding other impurities than water. For such purpose, compounds such as alcohol which are miscible with hexane at all proportions have been preferred[14]. A plot of the logarithm of the conductivity against alcohol concentrations from 4% to 12% was found to be approximately linear but with a slight tendency towards saturation at higher concentration. The conductivity was 2.0×10^{-12} mho/cm for 4% alcohol and increased to 2.5×10^{-10} mho/cm for 12%.

Stannett[15] observed a high increase in conductivity by adding minute carbon particles to hydrocarbon transformer oil. The motion of such conducting particles in electrically stressed hexane has been examined[16,17] and a quantitative agreement with the measured conduction current in gassy hexane has been found by Krasucki[18]. However, this does not account for the considerable difference between the conduction in degassed and gassy hexane. It was assumed that the particles initially became charged while in contact with one of the electrodes, the consequent force exerted on them by the field caused the motion. Air bubbles of dimensions less than a μm lodged on hydrophobic particles which can exist indefinitely in water[19], may also be present in hexane and take part in conduction. The non-linear relationship between the logarithm of the natural conductivity with inverse of absolute temperature indicates the existence of at least two mechanisms for the thermal activation of the conduction[20,21].

The high-field conduction in commercial hexane may be due to electron emission or a field dependent dissociation of impurities or of liquid

molecules[22]. Measurements made with similar liquids indicated a modified thermϕionic emission[23,24]. The conduction current was found to depend on the impurity content and on the temperature of the liquid but not on pressure exerted on the liquid surface for field-strengths up to 90% of breakdown[25]. The most important factor determining the current appears to be a surface layer on the cathode[26,27]. A study of the potential distribution showed that at higher fields, the curve loses its linearity due to space charge buildup near the electrodes[28]. Recent measurement in degassed liquid using a 'charge-probe' also showed slight field distortion[29].

When in the state of highest purity, hexane shows an electrical conductivity of the order of 10^{-20}-10^{-19} mho/cm.[1] This natural or self conduction has been shown to be primarily due to cosmic rays although micro-particles irremovable from the liquid may also take part, particularly at the lower field-strengths[6]. Kahan[16] found that up to a field of 150 KV/cm, the conduction current remained below 10^{-12}A. With rise of stress, the I-V curve bends upwards until at about 350 KV/cm, it was found to flatten off at a current value between 10^{-7}A and 10^{-6}A. He observed no dependence of current on inter-electrode gap, electrode geometry, or polarity reversal and there was no change in current when either or both of the electrodes were changed from an optical finish to a comparatively rough state. Measurements of conduction current, particularly at high field, however, showed a marked effect of dissolved oxygen. In degassed liquid, currents sometimes fluctuated more and more as the field was increased, and the currents were always much higher than those in air-saturated samples. The gassy liquid on the other hand was found to give a stable current up to 1.2 MV/cm. The electric strength of degassed liquid decreased as the gas

pressure was reduced whereas gassy liquid showed little dependence[30]. Hesketh and Lewis[31] using a crossed-wire electrode system, observed a current increase of more than three orders in outgassed liquid over the air saturated one in a volume of liquid not greater than 5×10^{-4} cm.^{3}

A great number of studies have been made of electrical breakdown in hexane. The work has included the effects of cathode material,[30,32] temperature, pressure and additives,[33] dissolved gas (oxygen)[34,35,36] voltage pulse duration[37,38] and electrode gap[26,30] on the breakdown strength, but the mechanism of breakdown is yet to be defined clearly. The measurement of formative time lags for breakdown may be used as an indirect way of calculating the carrier mobility at breakdown voltages[39].

The breakdown strength of pure and degassed hexane is between 600 - 700 KV/cm. The higher values reported (1.3 - 1.56 MV/cm) correspond to the strength with dissolved oxygen[40].

2.2 Injection Processes in Dielectric Liquids.

Ideally a pure non-polar liquid such as hexane should not conduct at all, but the closest approach so far attained in practice gives a conductivity~10^{-20} mho/cm. in a highly degassed sample. This low value of conductivity makes it extremely difficult to investigate the mechanism of conduction and to measure the carrier mobility or mobilities in such liquids. Although a number of theories have been put forward by different workers, the mechanism of electrical conduction and the exact nature of the charge carriers are not yet fully understood. The values of carrier mobility calculated by different workers also vary over a wide range (from .07[41] down to 1.5×10^{-4} cm^2/volt sec.[42] for negative carriers in hexane). The experimental difficulties can be overcome by increasing the conductivity by the introduction of free electrons. The techniques so far used to

enhance conduction artificially without liquid contamination are (a) the photoelectric effect using ultraviolet radiation (b) field emission (c) injection due to high-energy radiation of an electrode (d) electron injection through the surface of the liquid and (e) electron emission from a tunnel cathode.

2.2.1. Injection by the photoelectric effect

The mechanism of the photoelectric effect has been utilized by many workers since the beginning of this century to inject electrons into dielectric liquids. In this laboratory Pugh[2] made an extensive study of photoinjection into hexane with ultraviolet radiation and gave a detailed review of previous work. Only a brief account of the subject is given in this sub-section.

The injection of electrons into dielectric liquids by this method depends on the cathode condition and the purity of the liquid. A fresh layer of aluminium deposited in vacuum was found to be the best photo-cathode[43]. A medium-power mercury discharge lamp is generally used as a source of radiation. Morant[4] observed an increase in the current through hexane by a factor of up to 10^3 by focussing such radiation on a good cathode. By irradiating the cathode through a semi-transparent anode and through the liquid, a photocurrent of $\sim 10^{-12}$A was obtained for a field strength of a few KV/cm. From the transient growth of current, immediately after illuminating the cathode, the mobility of the charge carriers was calculated to be 9.8×10^{-4} cm^2/volt sec[44].

The possibility of photoionisation and photoexcitation of the liquid can be avoided by suitable filtering of the radiation. Le Blanc[45] radiated the cathode through the liquid whereas Swan[46] directed

radiation through a silica window on the inside of which was deposited a thin film of Al. The former method suffered from poor collimation of the light beam and considerable reflections occurring in the cell. Also the possibility of ion production in the liquid subjected to electric stress cannot be ruled out. Swan observed a photocurrent of $\sim 10^{-12}$A for a field strength of a few KV/cm and a carrier mobility of about 8.0×10^{-4} cm^2/volt sec.

Pugh[2] irradiated the photocathode obliquely through the liquid and measured photocurrents from freshly evaporated layers of Al, Mg and Au. Within a few minutes of cathode preparation a photocurrent of $\sim 10^{-10}$A was obtained with both Al and Mg cathodes for an applied field of 3 KV/cm. The current with the Au cathode was much smaller for the same field strength. The activity of these layers decreased with time[43] but the decay could be retarded by subsequent immersion in highly degassed hexane. Measureable photocurrents were obtained for a few days after cathode preparation and the photocurrents could be partly revived by depositing a fresh layer of evaporant. The photocurrents obtained with filtered radiation were much higher for forward voltages than for reverse voltages but the currents with unfiltered radiation showed no polarity effect and were ionic in character. The ionic mobility, assuming volume recombination, was calculated to be 6.0×10^{-4} cm^2/volt sec for negative ions. One of Pugh's conclusions was that true photoinjection from an electrode was only obtainable with a fresh surface and in hexane pure enough to be transparent to the filtered u.v. radiation that had to be used. A photocurrent of the same magnitude as Pugh's was obtained by Hughes[5] in dry and degassed hexane by irradiating a Mg cylinder and using

an applied field as high as 20 KV/cm . In highly purified and well degassed (at a pressure of $\leq 2 \times 10^{-8}$ torr) liquid, photocurrents up to 10^{-9}A were obtained from an evaporated Ba film and an applied field of a few KV/cm[41]. By mechanically chopping the light beam and measuring the time of flight, a carrier mobility even greater than 1 cm^2/volt sec was calculated.

Pulses of u-v radiation have also been used to inject electrons from such cathodes into liquids. The transient current observed from such pulses were of the order of 10^{-12}A for a field strength of a few KV/cm. The mobility of the charge carriers, calculated from transit time measurements, was 1.1×10^{-3} cm^2/volt sec[45]. Chong et al[47] used light pulses from an air gap discharge to inject photoelectrons from a Mg cathode. In pure n-hexane they found a field independent carrier mobility of 8.5×10^{-4} cm^2/volt sec. Addition of 1% alcohol in hexane decreased the carrier mobility to half of this value.

Using pulses of u-v radiation, Bloor[3] injected photoelectrons from a freshly prepared aluminium cathode into highly degassed as well as gassy hexane, and measured the carrier mobility and field distortion. His main observances were that (a) the mobility of the charge carrier in hexane does not change due to degassing, (b) the mobility is $\sim 10^{-3}$ cm^2/volt sec and is independent of applied field up to 140 KV/cm, (c) oxygen dissolved in hexane reduces the number of photoinjected carriers without changing the shape of the transient current pulse and (d) the oxygen effect is a surface rather than a volume phenomenon. There seemed to be strong coupling between the carriers and the neutral molecules and curvature in the current transients was attributed to liquid movement within the test cell. With a

good photo-cathode Bloor was able to inject charge up to a value of 10^{-10} coulombs.

Kalinowski,[48] in his photoinjection experiments, used a special chamber in which one electrode was a silver net with 50% transmission placed against a quartz window, the other being a nickel-plated electrode. U-v radiation from a mercury lamp was selected to give photoemission from either electrode, without being absorbed by the experimental liquids (cyclohexane and n-heptane). A photocurrent of $\sim 10^{-12}$A was obtained for a field strength of a few KV/cm by irradiating either electrode. The photocurrents increased with temperature but a change observed at about 40^{o}C in pure liquids implied a new process of carrier generation.

Current-stress curves in pure hexane and for filtered radiation seem to follow the general law

$$I = AE^{n} \qquad (2)$$

The constant A has been found to depend on the nature of the cathode, the purity of liquid, the intensity of illumination and spectral composition of the radiation. The values of n found by different workers[1] range from 1 to 1.38. Terlecki observed that I-V curves for true photo-emission maintain their upward trend up to a field strength of at least 300 KV/cm[41]. The measurements of Morant[4] with unfiltered radiation (giving bulk ionisation) show saturation for an applied field of a few hundred volts/cm.

2.2.2. Charge injection using field emitters

In the photoelectric method, a significant charge injection is only possible if the liquid is thoroughly degassed[4]. For air saturated liquid a good alternative is to use a field injection from a sharp point to

enhance the conduction current[49]. The high field developed at the point causes local ionisation of the liquid and currents of up to a few micro-amps per tip have been obtained by a multipoint corona emitter of this type. A further increase in the current is accomplished by replacing point ionisers by line-emitters[50]. Currents of up to 55 μA have been reported with three such emitters, each of 2 cm long, held at a negative potential of 14 KV with respect to a collector placed about a millimetre away.

The methods mentioned above, although yielding a high current output, result in chemical degradation of the experimental liquid after a prolonged period of operation. To increase charge injection without liquid ionisation (and consequent deterioration), Coe et al[51] devised a new technique of high injection. They used sharpened stainless steel razor-blade edges (Ever Ready Personna Co.) as field emitters for copious emission of electrons into hexane. Such emitters consisted of razor-blades mounted against a metallic plate with only a few millimetres gap between the blade tips and the plate. The whole assembly was well immersed in the experimental liquid. Applying a negative potential of a few KV to the razor-blades with respect to the plate, gives emission of electrons from the blade tips into the liquid. Due to the geometry of the blade-plate diode, the field strength drops sharply away from the tips, thus reducing the possibility of ionisation of the stressed liquid.

To increase the charge injection, Coe et al used a number of blades connected in an array. With an applied voltage of only 9.5 KV and a tip to counter electrode spacing of 1 mm, currents up to 20 μA/blade (corresponding to an emission current density of $0.25 A/cm^2$) have been recorded in hexane. The conduction current increased with the number of blades in the emitter

array. The emitter-tips showed a self-screening effect and blades had to be spaced at least 4 mm apart, if such effects were to be avoided. Using an array of 43 blades, they obtained a current of 550 μA with the above electrode spacing and applied voltage. After a certain threshold voltage (about 3.5 KV) the current was found to increase as the third power of applied voltage. The conduction current was further increased by using a perforated grid as collector instead of a solid plate. Mechanical pumping of the liquid to a velocity of 0.5 m/sec, in the same direction as the charge migration, enhanced the conduction current by a factor of between 5 and 10.

In order to measure the mobility of these carriers, Essex & Seeker[52] designed a test cell with an additional grid (called the 'injector grid') in between the emitter and collector grids. Dried and degassed (at 10^{-2} torr) hexane was introduced into the cell and an electric field was applied across the drift gap (between injector and collector grids). The carriers move towards the collector grid by the action of the drift field. The time required for such a charge-front to cross the gap was measured and the apparent mobility calculated. By applying higher voltages across the injector diode, the mobility was found to increase with increasing carrier injection. Taking account of bulk liquid motion[53] associated with the high carrier injection, the true mobility was found to be 2.7×10^{-4} cm^2/volt sec. In a later experiment[42] they measured the mobility of carriers in a number of saturated hydrocarbons for different drift-gaps and injection levels. Extrapolation of the apparent mobility curve to the critical injection voltage (zero power input and no induced liquid motion) gave a true carrier mobility of $1.5 \pm 0.5 \times 10^{-4}$ cm^2/volt sec in hexane.

The large increase in the conduction current that can be obtained by pumping the liquid led Hughes and Secker[54] to construct a liquid-filled electrostatic generator. The charge injection system consisted of three razor-blades mounted 2 mm away from and perpendicular to a mesh-grid. The charge collector, a cylindrical brass plug with a number of holes, and the injector were incorporated in a closed loop system containing a circulating pump. Hexane acted as a charge transporting medium as well as the effective insulator. The linear arrangement was later changed to a coaxial injector diode[5] with the liquid being pumped through small emitter-grid channels at a velocity of up to 59 m/sec. This high velocity liquid at the emitting edges resulted in up to 15 μA of current leaving the injector diode and a generated voltage of 200 KV was obtained. Two other injector arrangements had been tried, but the generated voltage was then limited by insulation failure of the hexane.

For the collection of charges from the flowing stream of liquid, a number of collector arrangements were tried. A ball bearing collector gave 100% collection efficiency when the charge density in liquid exceeded a certain threshold value.

In a recent experiment with sharp razor-blades (tip radius < 600 Å) Secker and Aplin[55] obtained a current of the order of microamps for an applied voltage of 11 KV across a razor-blade / flat plate diode in BDH fraction from petroleum hexane. They also observed a charge injection region (for voltages > 4 KV across 2 mm gap) where the forward current is up to 100 times as high as the reverse current. With Koch-Light Puriss grade of hexane an increase in current of up to three times[56] was noticed with the same electrode system and applied voltage. The forward to reverse ratio was reduced considerably at higher voltages.

2.2.3. Other methods of charge injection

The two methods of charge-injection described above were also investigated in the present work. Further methods, not used here, can now be briefly described. These methods include injection (a) by means of high energy radiations, (b) from a thermionic cathode and (c) from a tunnel cathode.

(a) Injection due to high energy radiations.

Research on induced conduction by irradiating the bulk of the liquid with X-rays, γ -rays, α , β particles, etc. have been carried out by a number of workers[1]. An ionisation chamber is generally used and the induced currents have been found to follow the relation

$$i = i_o + CE \qquad (3)$$

The constant 'C' depends on the number of ions produced in the liquid, the electrode spacing and the physical and chemical property of the liquid. A current of $\sim 10^{-9}$ A/cm^2 can be induced in such chambers with a field strength of a few KV/cm. In hexane, ionised by X-rays, Adamczewski[1] identified two kinds of positive ion but only kind of negative ion, and these had mobilities of 8.4×10^{-4}, 4.5×10^{-4} and 2.8×10^{-4} cm^2/volt sec respectively.

To inject a layer of charges without bulk ionisation, Secker[57] used a well collimated beam of X-rays striking an aluminium foil at a glancing angle and forming a plasma region close to the foil. A current of $\sim 10^{-10}$A was obtained by applying a field strength of a few KV/cm between the foil and the collector electrode. Transit time measurements of positive and negative carriers, using a pulse of X-rays[58] gave apparent mobilities of 1×10^{-3} and 2×10^{-3} cm^2/volt sec respectively, with a

high degree of scatter. The mobilities were found to increase with increase in the conduction current produced by high-intensity beams.

Gzowski & Chybicki[59] coated one of the electrodes of their ionisation chamber with a β -radiating source to emit a thin layer of charges. When the radioactive electrode was negative, the currents obtained were greater by a small constant value than those measured with positive polarity. Currents were of the same order of magnitude as those with bulk irradiation and the current-voltage curve also followed the relation (3).

(b) Charge injection from a thermionic cathode.

Sato et al[60] devised a method of injecting electrons from a tungsten filament in a partially evacuated vessel onto the free surface of transformer oil with only the collector electrode immersed. The transconductance of the vacuum diode was large in comparison with the conductance of the liquid used so that virtually the whole of the applied voltage was across the liquid. Under the influence of a field, electrons travelled to the collector in the form of heavy negative ions. A current of $\sim 10^{-8}$A was obtained for an applied field of a few KV./cm and at a pressure of 2×10^{-3} torr above the oil surface. The mobility calculated from the slope of I vs V^2/d^3 curves varied from $0.6 - 1.1 \times 10^{-4}$ cm^2/volt sec. Values calculated from the transit time of the carriers, generated by applying a pulse voltage to the filament, were also of the same order. Charge-injection from such an emitter into benzene and liquid gases showed a space charge limited behaviour for currents greater than 10^{-9}A[61]. By introducing a grid in between the filament and the collector and applying a suitable emitter-grid bias, a conduction current of up to microamps could be obtained in transformer oil for an applied voltage of a few KV[62].

To ensure uniformity of charge injection and to measure the surface voltage due to charge build up, Watson and Clancy[63] used an electron beam for both purposes. An electron beam scanned across the dielectric (10^{-2}cm thick) and the voltage due to the surface charge was measured by observing the deflection of a second beam directed parallel to the dielectric surface. For an injection density ranging from 10^{-10}A/cm^2 up to 10^{-7}A/cm^2, the surface potential varied from 10V to 100V. As the system was operated at a pressure of 10^{-7} - 10^{-6} torr, only liquids with very low vapour pressures could be studied.

(c) Injection from a tunnel cathode

The difficulty of making an ohmic contact to a liquid dielectric has recently been overcome by the development of a 'tunnel cathode'. Essentially this consists of two metallic electrodes separated by a thin oxide layer. The theory and operation of these cathodes can be found elsewhere[64]. Its advantage over other methods is that there is no high field in the liquid. With only 15V across such a diode (Al - Al_2O_3 - Au/Al configuration with oxide layer 100 - 200A thick) an emission current density up to 10^{-3}A/cm^2 was obtained into vacuum[65]. These electrodes are capable of supplying over 10^{-7}A/cm^2 into organic liquids such as cyclohexane and benzene. Space charge limitation at room temperature sets in at about 10^{-11}A/cm^2 for an electrode spacing of a few millimetres, and a field strength of 100 V/cm. The carrier mobilities derived from the steady-state space charge limited current and from the transient agreed, assuming that the entire area of the tunnel junction was emitting, and both were $\simeq 2.8 \times 10^{-4}$ cm^2/volt sec in cyclohexane[66]. Besides organic liquids, electron injection from these cathodes into liquids such as Ar and He has also been successfully used[67].

Charge injection by high energy radiation of an electrode, although giving rise to high conduction currents, also causes ionisation of the liquid as a result of the direct action of primary radiation passing through the cathode and the energetic photoelectrons escaping from it. Due to bulk ionisation and the consequent deterioration of the liquid, the method is considered unsuitable from the viewpoint of research on the true conduction mechanism in pure hexane and hence it was not used here. Electron injection through the free surface of liquids, as has been mentioned, requires pressure down to 10^{-4} torr above the liquid surface and it has been used for liquids of very low vapour pressure. Hexane, because of its high vapour pressure, cannot be used as an experimental liquid for such carrier injection, and it was not considered further for this work.

At the beginning of the work, electron-injection from a tunnel cathode into hexane was seriously considered as a method of increasing the conduction. As a preliminary step some properties of these cathodes have been investigated in this laboratory by Green[65] in his M.Sc. dissertation. The emission current density from such cathodes, although reaching as high as 10^{-3} A/cm^2 in vacuum, was found to fluctuate violently and hence these cathodes could not be used for electron injection into hexane.

In this work conduction processes due to photo- and high-field injection have therefore been investigated.

CHAPTER III

THEORETICAL ASPECTS OF CONDUCTION AND INJECTION

Although a number of workers have attempted to develop theories of electrical conduction in insulating liquids (such as hexane), a unified theory is yet to come. This Chapter deals briefly with some of the possible conduction mechanisms in liquid hexane. Unless electrons are injected by some artificial means, the carriers are probably formed by field dissociation of impurity molecules or of the hexane molecules themselves. At high field strengths electron emission from the cathode may also take place.

3.1 Mechanisms of Electrical Conduction in Dielectric Liquids

In recent years a great number of measurements of electrical conduction in saturated hydrocarbon liquids have been made. This section gives a brief account of some of the mechanisms put forward by different scientists. The main ideas are grouped together in three sub-sections.

3.1.1 Ionic conduction

As has been mentioned in the previous Chapter, the intrinsic conductivity of liquids at low field strengths may be explained by the ionising effect of cosmic rays. Also the dissociation of electrolytic impurities cannot be ruled out in moderately high fields. In the high-field region carrier formation by collision ionisation may possibly become predominant. These mechanisms are characterised by the fact that they give rise to equal numbers of positive and negative charge carriers. The

carriers or ions are generally formed uniformly within the volume and impart their charges to the opposite electrodes. In the space between the electrodes the carriers disappear only by recombination with those of opposite sign. The ions which escape recombination eventually move towards the opposite electrodes and become neutralised. If the neutralization is not instantaneous as, for example, when there is aggregation of neutral molecules around an ion, a space charge region is formed near the electrodes, particularly at the lower field strengths[28]. In a steady state the rate of generation of ion-pairs will be exactly balanced by the recombination of ions in the bulk of the liquid and their collection at the electrodes.

Adamczewski[1] has put forward a general formula for electrical conduction in ionised dielectric liquids. The energy of activation for charge transfer was assumed to decrease by an amount (γ dE) for an electric field E and electrode gap d and where γ is a constant with an experimentally determined value of 10^{-6} e. Detailed analysis of the problem for constant temperature conditions leads to the formula

$$I = I_o \exp(\gamma^* dE) \qquad (4)$$

where γ^* is equal to γ/kT. For low-field strengths $\gamma^* dE$ is very much less than unity and one can write

$$I = I_o (1 + \gamma^* dE) \qquad (5)$$

which, in the most general form is

$$I = I_o + cE \qquad (6)$$

At high field strengths (> 200 KV/cm) the increase in the conduction current has been assumed to be due to an exponential growth in the number of ions by collision ionisation and the above simplification no longer

holds good. The high-field characteristics thus follow equation 4 more closely. At such field-strengths, the effects of the electrodes and of dissolved gases on the conduction currents cannot be ruled out.

3.1.2 Electron attachment theories

Various methods of electron injection into dielectric liquids have been reviewed in the previous Chapter. If the injected electrons remain as free charge carriers, they should have a high drift mobility in an applied electric field. The values of mobility measured by different workers (except those reported recently[41]) are very low for such a model. Crowe[38] sought to explain the abnormally low mobility by proposing that reversible electron trapping occurs in the liquid. This idea was later developed by Le Blanc[45] on the basis of his experimental data which indicate that electrons in liquid hexane move neither as free particles nor as negative molecular ions. According to his hypothesis, the electron travels an average distance λ as a free electron and it is then captured by a molecule, i.e. it is trapped. It remains in the trap in a bound state for a time τ and then escapes, travels another distance λ and is trapped again. The average time spent in a trap will vary exponentially with temperature and applied field strength.

The above hypothesis is similar to the original idea of electron attachment put forward by Frenkel[68]. An electron introduced into a dielectric liquid attaches itself to a molecule and forms a quasi-stable entity. As a result of thermal motion, the molecules, bound together by forces of cohesion, oscillate widely around their position of equilibrium and the electron is eventually able to separate itself from the molecule. The electron travels for a certain 'free-path' whose length is comparable

to the dimensions of the molecule and it then attaches itself to another molecule. Although the conductivity measurements at low field strengths are consistent with his mathematical formula, Frenkel failed to account for the dependence of the current on the field strength.

Another possibility is for the electron attachment to be to oxygen molecules in solution in gassy liquids. Oxygen being strongly electronegative is quite likely to act as a source of traps for electrons leaving the cathode[69].

The presence of solvated electrons in some aqueous and organic solutions can be interpreted in terms of polaron theory. Weiss[70] assumed that a polaron is relatively stable in a liquid and that it forms a trap for an electron. In the case of liquid hexane, electric conduction through polaron formation has also been considered[42].

All the mechanisms mentioned above picture some form of electron solvation in dielectric liquids and any of them can explain the low carrier mobility. These hypotheses, however, fail to explain the conduction mechanism at the high field strengths as they indicate a field-dependent mobility, whereas measurements have shown no change in the mobility of the charge carriers for fields of up to 500 KV/cm.[44] Among other explanations of the high field conduction Kahan[16] has proposed a conduction mechanism through channels of aligned or ordered molecules. These channels would be expected to be of a transitory nature, thus giving rise to the observed erratic currents at moderately high and steadier currents at very high fields.

3.1.3 Electron emission theories

Considering the conduction mechanism, particularly at high field

strengths, the phenomenon of electron emission from the cathode may not be ruled out. The extracting field reduces the magnitude of the work function barrier for electron emission, which therefore increases with field strength, and may account for the increased current in a liquid at high fields. As this is a surface phenomenon, it depends on the electrode material and its chemical nature, which should therefore influence the current.

Baker and Boltz[24] suggested a Schottky-type thermionic emission model for liquid conduction and they put forward an expression for emission current from a metal surface into the liquid. Their equation may further be modified by surface irregularities[71] and by surface layers[72]. The effect of surface layers has been shown to be the most important factor in determining the current in the range 0 - 250 KV/cm[26]. The space charge formed near the electrodes[28] also distorts the electric field and may aid electron emission from the cathode.

At high field strengths, the Schottky equation does not explain the high field current increase in liquids, even after the above modifications. A cold field emission process entirely due to electrons tunnelling through the barrier has been proposed by a number of workers[1]. They have considered the possibility of explaining the electron emission from a metal into the liquid by applying the Fowler-Nordheim theory for field strengths greater than 10^6 V/cm.

3.2 Mechanisms of Electron Injection into Dielectric Liquids

The various methods of electron injection into dielectric liquids by external means have been reviewed in Chapter II. Details of the mechanism of injection are beyond the scope of this Chapter but two new theories will be discussed in Chapters VI & VII. This section reviews some previous attempts

to explain the conduction induced in liquids by photo- and field injected electrons.

3.2.1 Conduction due to photoinjected electrons

When a photocathode, immersed in a liquid, is irradiated with ultra-violet light of frequency ν, photoelectrons leave the cathode with energies

$$E = h(\nu - \nu_o) \qquad (7)$$

where ν_o is the threshold frequency for electron emission into the liquid. For u-v radiation, these energies are of the order of few electron volts. Most of the emitted electrons suffer elastic scattering with the liquid molecules and return to the cathode. This phenomenon of back diffusion, originally put forward by Thomson[73] while studying photoemission into a gas, has recently been reconsidered for emission into liquid gases[74]. The electrons that do not return to the cathode become thermalised and may subsequently form heavy negative carriers very near to the cathode. With oxygen in solution the heavy carrier may be of a different type from that in the pure liquid so that the mobility may vary with oxygen content of the liquid and with the field strength. Measurements of carrier mobility by Bloor[3], however, showed no effect of oxygen in the liquid (down to a pressure of 10^{-6} torr) or applied field (up to 140 KV/cm).

The injected carriers take comparatively long times to cross the gap because of their low mobility, so that a large number of charge carriers remains in transit under d-c photoinjection conditions. As a result, the field distortion due to these carriers cannot be ruled out. While the photocurrents at high field strengths are found to be emission limited[2], a space charge limitation may therefore take place at lower field strengths.

In order to present a theoretical picture of photoconduction at low field strengths, the following simple assumptions are made:-

a) The photoconduction is due to a single kind of carrier, and

b) The carriers have a single mobility.

If n is the number of carriers per unit volume with μ and D their mobility and diffusion constant respectively, the current density J at a field strength E is given by

$$J = ne\,\mu E + D\frac{dn}{dx}e \qquad (8)$$

For mathematical simplicity, the diffusion term in the above equation is usually neglected. Equation (8) with the help of Poisson's equation

$$\left(\frac{dE}{dx} = \frac{ne}{K\,\varepsilon_o}\right)$$

takes the form

$$J = K\,\varepsilon_o\,\mu E\,\frac{dE}{dx} \qquad (9)$$

where ε_o is the permittivity of free space and K the dielectric constant of hexane. From equation (9) the relationship between the current density J and the applied voltage V, applying appropriate boundary conditions (see Appendix A), becomes

$$\frac{K\,\varepsilon_o\,\mu}{3J}\left[\left(\frac{2Jd}{K\,\varepsilon_o\,\mu} + E_o^{\,2}\right)^{3/2} - E_o^{\,3}\right] = V \qquad (10)$$

If it is assumed that the liquid moves away from the cathode at velocity v, due to momentum transfer from the carriers to the liquid, the relationship between the current density and the applied voltage is modified to the form[75]

$$V = \tfrac{1}{3}\frac{K\,\varepsilon_o\,\mu}{J}\left[\left\{\left(\frac{v}{\mu}\right)^2 + \frac{2Jd}{K\,\varepsilon_o\,\mu}\right\}^{3/2} - \left(\frac{v}{u}\right)^3\right] - \frac{v}{\mu}d \qquad (11)$$

At moderately high applied voltages the effect of space charge can be neglected as one passes to the emission limited region.

The use of this approach will be discussed further in Chapter VI.

3.2.2 Conduction due to field injection

Field injection experiments using stainless steel razor blades in hexane are described in Chapter V. In most of the experimental cases the hexane was dried and filtered and then doped with alcohol. The conduction mechanism in doped liquids obviously becomes complicated by field ionisation of these dopant molecules.

Considering the electrode arrangement (section 5.1) as a portion of a concentric cylindrical system, the field at the tip of the razor blade is given by[51]

$$E \simeq \frac{V}{r \log_e {}^{D}/_{r}} \qquad (12)$$

where V is the applied voltage, r is the tip radius and D is the emitter-grid distance. Thus for an electrode gap of a few millimetres and a tip radius of a few hundred Angstrom units, the field at the tip, even for a small applied voltage increases to a very high value. At such high fields strengths the carriers are created primarily by field ionisation of impurities near the tip[76]. With the blade negative, there is a high possibility of electron emission either by Schottky or Fowler-Nordheim emission due to the reduction of the barrier height by such an intense field. Any such electron injected into the liquid, is probably rapidly trapped to form a negative ion or a charge shielding complex. However, the products of molecular dissociation contribute equally to the conduction current so that any polarity effect may be taken as proof of field emission of some kind.

In pure liquids, the conduction current may be considered as emission limited in these conditions. Electrons are injected from the electrodes so that movement of the bulk will have no effect on the conduction current.

The large increase of the current in hexane containing some added impurity shows the great influence of impurities. The impurity molecules are dissociated by the high local field and they give rise to bipolar conduction in addition to the unipolar injection current. With the blade negative, the positive ions approaching it are assumed to be neutralised at the tip, while the negative ions lose their charges to the anode. If the liquid is being pumped towards the anode, the negative ions are swept away more quickly. This may enable more ions to be formed near the tip resulting in an increase in the conduction current. The current may continue to increase with liquid velocity up to the value at which the dissociation of the impurity molecules (giving rise to the current) reaches its limit for that particular field.

When the blade is made positive, there may appear an altogether different mechanism. The negative ions formed due to field dissociation approach the tip but unlike the positive ions, they may not be discharged instantaneously at the tip. As a result a negative space charge region will be formed around the tip. By pumping the bulk of the liquid away from the point, most of the positive ions will reach the opposite electrode (i.e. the cathode) and give up their charges. This will result in an increase in the negative space charge density around the tip. The effect of such a layer is to reduce the field strength at the tip and so decrease the dissociation.

The current due to impurity ionisation is expected to vary as $\sqrt{C\ K(E)}$ [77], C is the impurity concentration and K(E) is the field dependent dissociation constant (See Appendix B). Based on the earlier theory of Onsager[79], Coehlo[76] calculated K(E) of a weak electrolyte in hexane and the dependence of current on field strength was shown to be

$$i \propto E^{\frac{5}{8}}.10^{4.6\times10^{-3}\sqrt{E}}.\ C^{\frac{1}{2}} \qquad (13)$$

The application of this to the present work will be discussed in Chapter VII.

CHAPTER IV

PHOTOINJECTION EXPERIMENTS

4.1 Introduction

As explained in Chapter I, the original aim of the present work was to increase the conduction current in hexane by methods that do not give bulk ionisation of either the liquid itself or of impurities. This can be achieved by increasing the cathode injection in of the following ways:-

a) Photoinjection

b) High field injection

The experiments and the results on photoinjection are described in this Chapter. The work is an extension of that of Pugh[2] and Bloor[3] in this laboratory. Pugh found that true photoinjection is only possible with the following conditions:-

a) Liquid to be highly pure - not absorbing in the far u.v. range

b) Liquid to be highly degassed

c) Photocathode to be freshly prepared

d) The use of u.v. radiation of the correct wavelength;

These conditions lead to the following requirements for experiments on photoinjection:-

1. A high vacuum test cell that can be filled with degassed hexane and sealed off
2. A strong u.v. source of the required wavelength range
3. A method of preparing a fresh semi-transparent cathode surface by

vacuum evaporation in the test cell before filling with liquid.

4. A silica window on the cell to enable u.v, to reach the back of the cathode
5. A method of removing the unsaturated hydrocarbons from hexane to make it completely transparent to u.v. radiation in the wavelength range 2700-4000 Å.
6. The usual methods for measuring small currents and applying the highest possible voltage to the test cell. Fields of only a few KV/cm are required to study photoinjection.

The two most important results of earlier work on photoinjection are shown in Fig. 4.1, where (a) is a typical result obtained by Pugh and (b) a typical result of Bloor's work. Pugh measured d.c. photoinjection characteristics and he concentrated in establishing the correct conditions of photoinjection. Bloor used these conditions to measure the mobility of the carriers formed in the liquid by the action of a pulse of u.v. radiation on the cathode. He was also interested in the magnitude of the injected charge.

Pugh obtained the approximately linear photocurrent-voltage characteristics for photoinjection, shown in Fig 4.1(a), although some of his results suggest that the curve bends up slightly. Bloor found that the injected charge is also approximately a linear function of applied voltage (Fig. 4.1(b)). These measurements of photocurrent and of photoinjected charge were, however, carried out at completely different times, in different test cells and with different liquid samples. Consideration of the possible mechanisms of charge injection and transport in these conditions (discussed in Chapter VI) showed the desirability of measuring

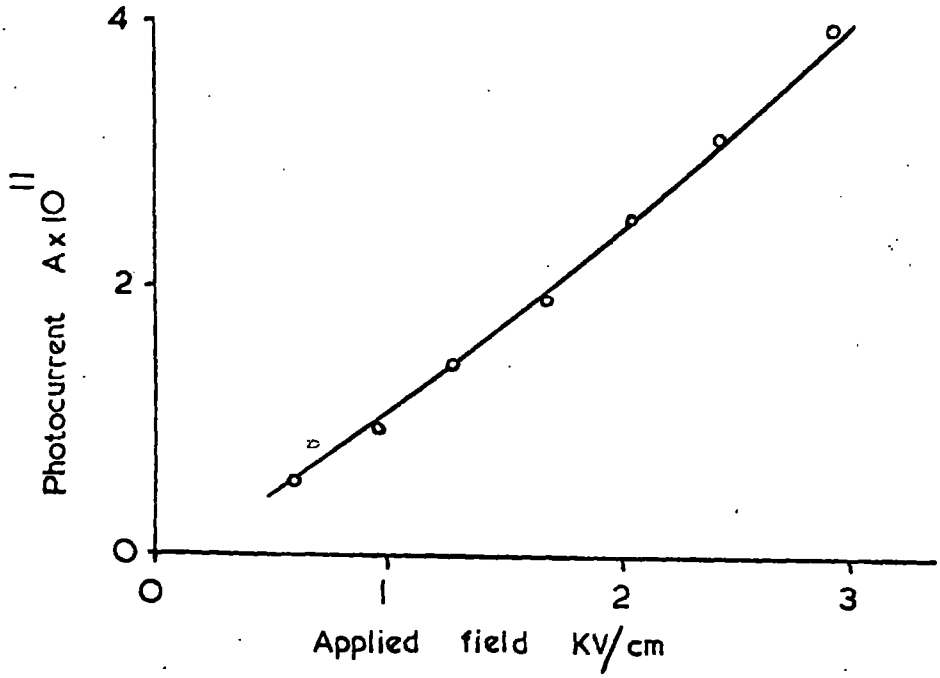

(a) Variation of photocurrent with applied field (Ref. 2)

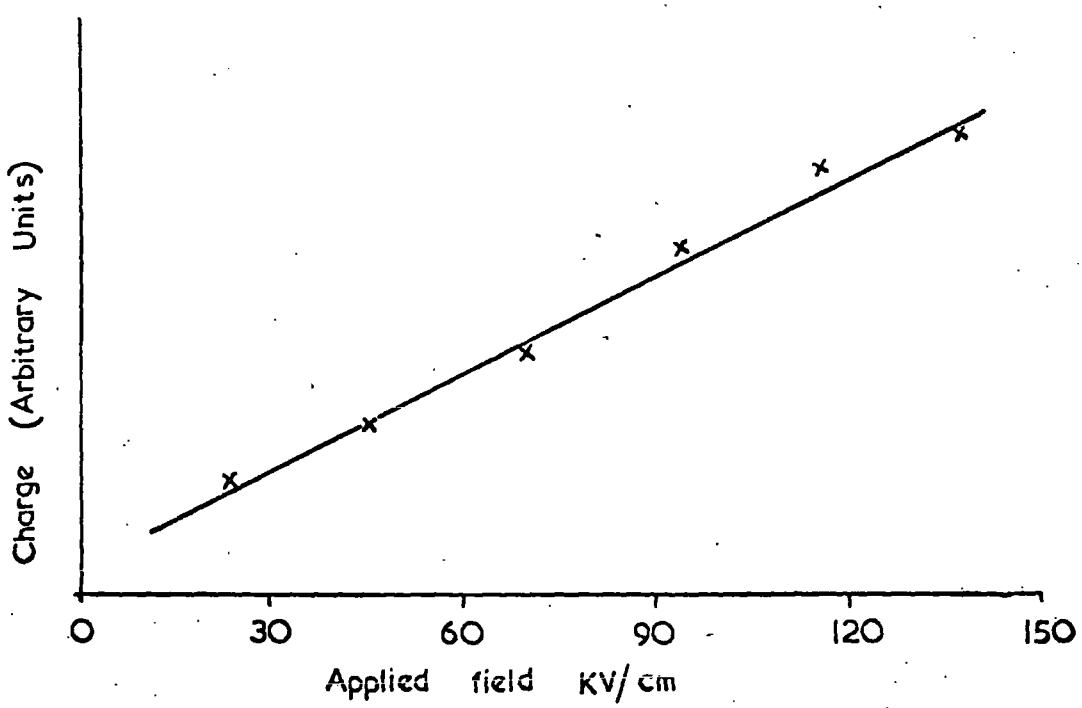

(b) Variation of photocharge with applied field (Ref. 3)

Figure 4.1

both the d.c. photoinjected current and the pulse photoinjected charge simultaneously for one sample of liquid. This therefore became the main aim of the present work on photoinjection. The subsidiary aims were to independently confirm the results of both Pugh and Bloor and to attempt to obtain larger photoinjected currents than in the previous work by careful preparation of the photocathode and thorough degassing of the liquid.

A description of the test cell used and of the techniques of liquid analysis, purification and degassing, the preparation of the photocathode and experimental technique are dealt with in Section 4.2. Section 4.3. gives an account of the results obtained in these photoinjection experiments. A comparison of the important results with those of previous workers in this laboratory is given in Section 4.4.

4.2 Experimental Apparatus and Techniques

4.2.1 The test cell

The test cell built for this work was developed from those used earlier. The cathode was to be a semi-transparent layer of aluminium formed on the inside of a silica window. Ultraviolet radiation from below was passed through the window and was absorbed in the aluminium from which electrons were injected into the liquid. The photocathode had to be freshly prepared by vacuum evaporation from a suitable filament just before filling with hexane so that independent heater connections were required for this. The anode had to be mounted accurately parallel to the cathode and to have a lead in to the cell which would withstand a few thousand volts. The cathode connection was via a thick film of aluminium covering the whole top surface of the silica window except for the central cathode region. The film was sandwiched between the silica and the cell wall for the external connection.

A diagram of the cell, with its different parts, is shown in Fig. 4.2. The cell was constructed from a Pyrex tube, 3.5 cm internal diameter and 10 cm long with one end ground flat. The other end was tapered, for making a 2 mm diameter tungsten rod seal to support the anode. A brass rod 6.2 mm diameter and 1.7 cm long, was connected to the tungsten rod. Another brass rod of the same diameter and 1.9 cm long, with a 1.55 cm diameter and 3.5 mm thick boss at one end, was screwed to the brass rod. A 1.55 cm diameter and 3 mm thick aluminium alloy disc was fixed onto the boss by three 10 BA grub screws and it forms the anode. The arrangement was devised for easy removal of the anode fixed to the boss, for cleaning, while leaving the tungsten-brass joint intact.

Two other tungsten seals of 2 mm diameter were made facing each other, at a distance of 2.5 cm from the flat end of the tube. These seals served to hold the filament in position and also to connect it with the transformer used for heating. The filament was made by twisting fine tungsten wire (having a diameter of 0.3 mm) into a circular ring (about 2.5 cm diameter) with a couple of legs 2 cm long. Aluminium was chosen as evaporant for the photocathode because of its high photosensitivity.[2,43] U shaped strips of pure aluminium cut to 3 - 4 mm long, were placed on the ring and melted in to the filament by heating the ring to about 660^{o}C at a pressure of 10^{-4} torr inside an Edwards 6E4 vacuum evaporator.

The filament, covered with the shiny aluminium layer, was mounted in the test cell on the two tungsten rods by brass connectors. Aluminium forms a low melting point alloy with tungsten, containing 22% of tungsten by weight, i.e. 3% by volume.[80] With this solubility the filament diameter will be reduced by the alloying reaction unless the filament diameter is

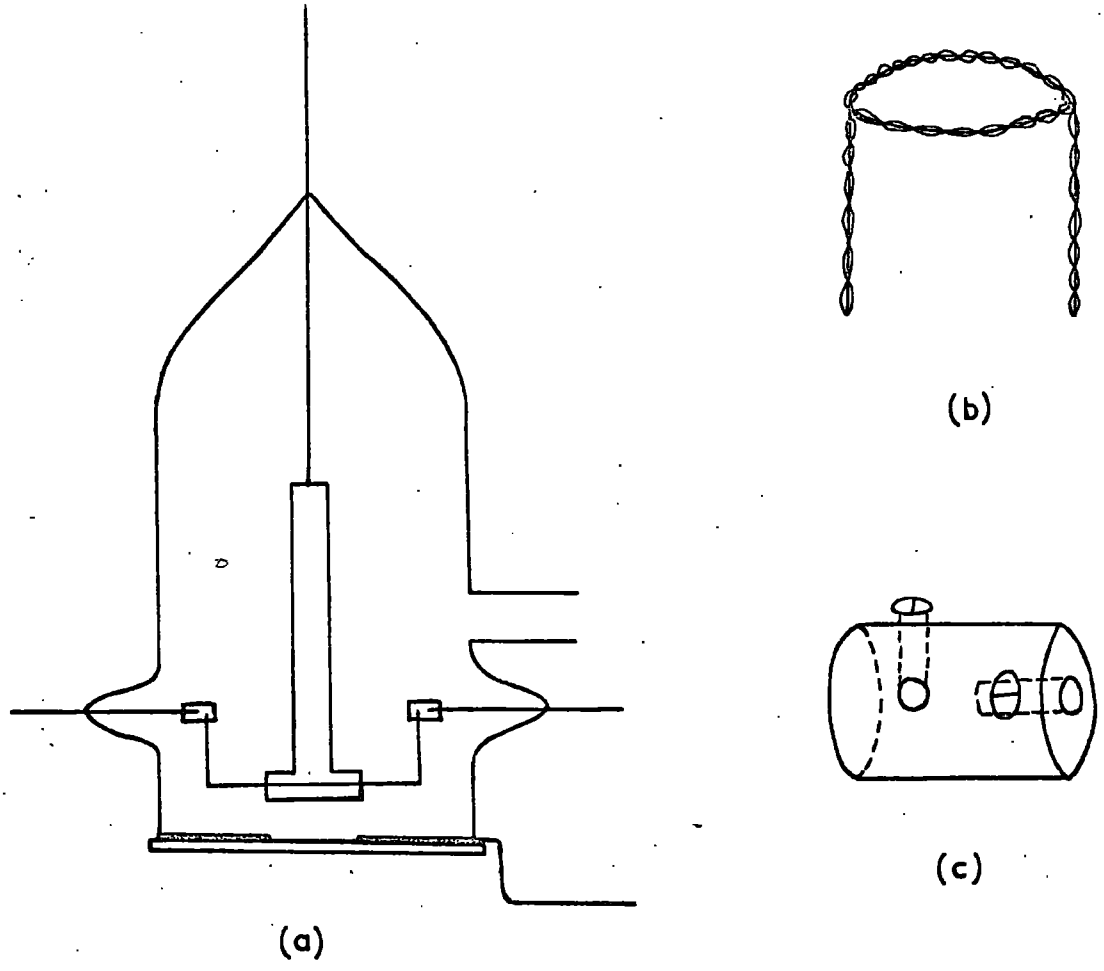

Figure 4.2

(a) The cell assembly (b) The twisted tungsten filament
(c) The brass connector

made sufficiently large in proportion to the evaporant mass. To reduce the likelihood of the filament breaking, great care was therefore taken in mounting the filament. The end window of the cell was 40 mm diameter and 3 mm thick optically polished silica disc. A thick aluminium film was deposited on the top face to form the cathode connection. To do this the disc was first thoroughly cleaned. It was washed with detergent (Teepol) and water, soaked in 10% potassium bichromate solution, rinsed with distilled water and finally washed with alcohol. It was then dried and placed on the platform of the vacuum coating unit (also cleaned thoroughly). Backing pressure was established and the disc was subjected to ion bombardment cleaning for a few minutes to provide a surface to which aluminium would adhere strongly. Air was admitted to the chamber and a thin brass disc of 1.5 cm diameter was placed in the centre of the disc to act as a mask. A multi-strand v-shaped tungsten wire was used as a filament heater for the evaporation of aluminium. The v-shaped portion was placed above the metal disc which protected the exposed part of disc from occasional molten Al droplets from the filament. With a current of a few amperes, at a pressure of 10^{-4} torr or below, the aluminium evaporated rapidly (1200 - 1400^{o}C) to form a thick layer on the disc. The central masked portion remained free from evaporant. If the heater was placed very near to the disc, the film had a hazy appearance. This was due[81] either to the large angle of incidence of the vapour or to too much metal deposition. By placing the heater further away this haziness could be overcome.

The disc with the evaporated film was fixed to the flat end of the cell with hot setting Araldite. A fine wire, connected to the Al-layer by 'silver dag', acted as the electrical lead for the cathode.

A glass reservoir, permanently joined to the side-tube of the cell, was used for freezing out the hexane in the cell for the preparation of a fresh photocathode. The cell was connected to the hexane degassing system via a narrow bore constriction, which could be easily sealed off to remove the cell for electrical measurements. After preparation the cell was washed out with clean hexane, dried and joined on to the degassing system.

The same cell was used for all the measurements to be described, but a fresh photocathode was needed for each test. The window was therefore removed each time, the cell cleaned and a fresh evaporating filament and cathode connection were made before sealing on a new window.

4.2.2 Analysis and purification of hexane

The analysis of different grades of hexane has been done previously in the Department by Kahan[16] and Pugh[2], using both vapour phase chromatography and u.v. spectrophotometry methods. In the present analysis only the latter method was used.

It has been shown by Evans[82] and others[83] that the u.v. absorption in a variety of organic solvents is due to oxygen in solution. The absorption is directly proportional to the partial pressure of oxygen above the solution and it is completely removed by boiling, or by bubbling nitrogen or other gases through the solvent, provided that it is chemically pure. For saturated hydrocarbons, the absorption is unlikely to be due to the formation of complexes with oxygen and is more likely to be due to the oxygen itself, possibly as a result of charge transfer. For saturated hydrocarbons absorption begins at around 2500 Å, with a maximum at about 2000 Å. Unsaturated hydrocarbons, on the other hand, absorb in the wavelength range 2000 - 4000 Å. A very small amount of an unsaturated compound can thus be

detected as an impurity in hexane by the use of a u.v. spectrophotometer.

A double beam u.v. spectrophotometer, Unicam SP 800, which covers a wavelength range 1900 - 7000 Å was used for analysis of the liquid by courtesy of the Chemistry Department. Absorption spectra were taken up to a wavelength of 4500 Å. The pen recorder trace gave the transmission of 1.0 - 100% on a logarithmic scale. The final purified samples were analysed on a CF4DR spectrophotometer (Optica Ltd.), having a linear scale for transmission and covering a wavelength range 1850 - 10,000 Å. In this case also, the measurement was limited to a wavelength of 4500 Å.

The liquid samples were contained in a 10 cm long stoppered silica cell (Suprasil), with optically polished end windows. The recorder trace with an empty cell gave the zero line in the absorption scale. The absorption due to the cell windows was negligible throughout the region of wavelength under consideration. The cell was cleaned and rinsed with clean hexane before each test. Care was taken not to touch the windows except with a clean Selvyt cloth.

Hopkin & Williams 'Spectrosol' grade hexane was used for the first exploratory measurements. Although this has a high isomer content of hexane, it has the lowest u.v. absorption of any of the various grades used. The absorption curve (Fig. 4.3) shows that it is already sufficiently transparent for photoinjection work and no further purification was done with this grade.

The best known n-hexane, with the least isomer content, is the 'Puriss' grade from Koch-light Laboratories. A vapour phase chromatography analysis showed that it contains 99.7% of n-hexane, with only small quantities of other compounds, which are mainly isomers with a very little disubstituted

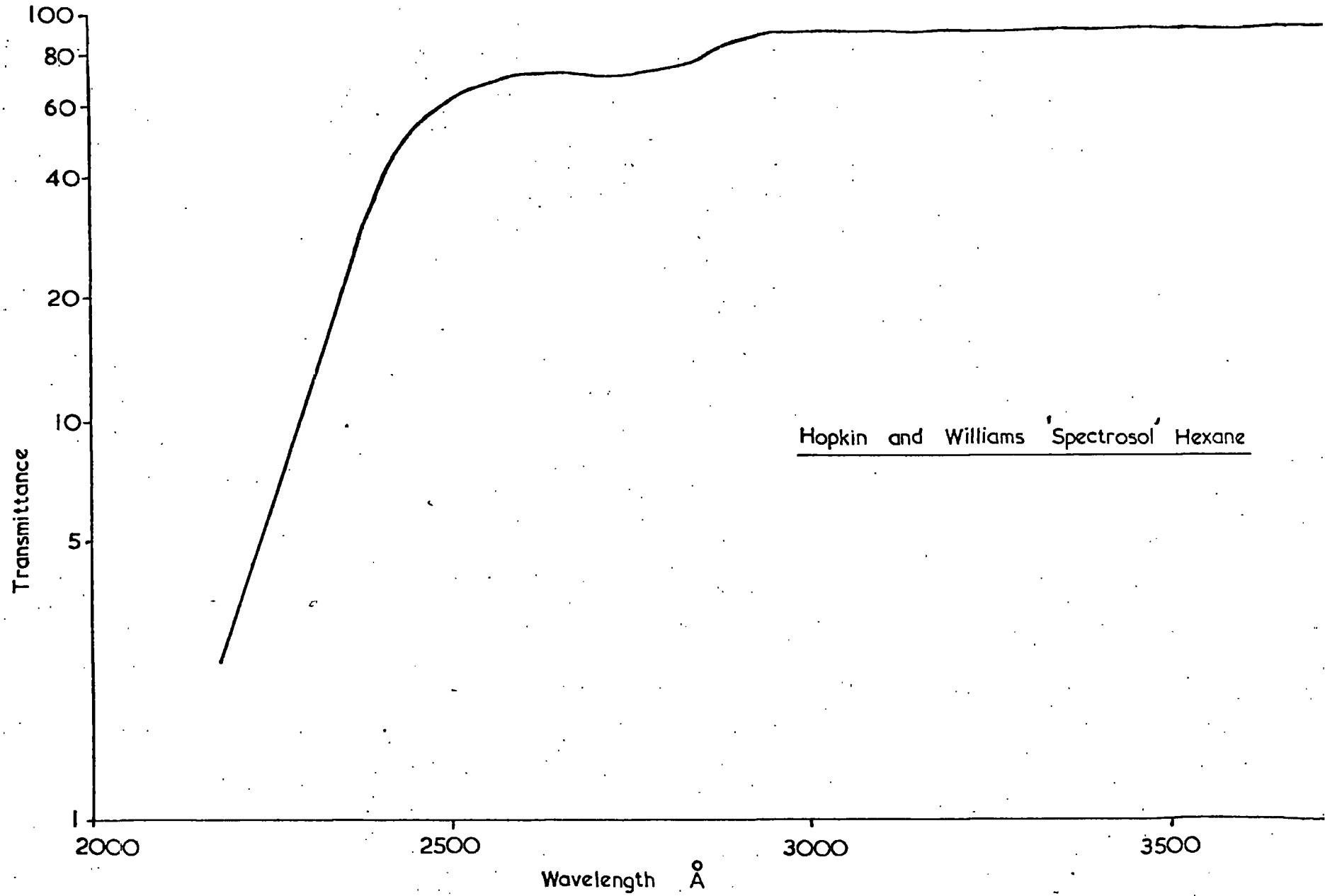

Figure 4.3. The optical absorption of Hopkin and Williams' 'spectrosol' hexane. Optical path length: 10 cm, Reference cell: air.

napthylamine, giving it a slightly yellowish colour. As these unsaturated impurities absorb strongly in the wavelength range used for photoinjection (2500 - 4000 Å), it was necessary to further purify this grade of hexane to remove the last possible trace of them.

The purification process employed was percolation through silica gel. This method was originally used by Potts[84] for purifying hydrocarbons for use as solvents in far u.v. spectroscopy. He found that treatment with silica gel had a reduced effect unless the hydrocarbons and the gel were absolutely dry. With prolonged vacuum treatment at a temperature not above 150°C, Kiselev[85] was able to produce silica gel surfaces free from absorbed water but not from a dense coating of hydroxyl groups. The presence of such a coating results in strong absorption of any molecules capable of forming hydrogen bonds with the silicic acid hydroxyl groups. Evacuation at a temperature of 200°C gives surfaces free of the hydroxyl groups.[2] Further increase of the temperature to more than 350°C, however, destroys the crystal structures of silica gel. To adsorb unsaturated hydrocarbons, it is therefore necessary to first activate the silica gel under vacuum at a temperature between 200 - 350°C, and to cool it in a moisture-free atmosphere.

About 400 gms of coarse silica crystals (B.D.H.) from a newly opened bottle was required for each percolation. The crystals were wrapped in several thicknesses of 32 cm diameter filter paper (Whatman 115) to avoid absorption of water from the atmosphere, and they were crushed to a fine powder by hammering. A Pyrex-tube 100 cm long and 3 cm diameter, with one end tapered and fitted with a sintered glass disc (No. 4 porosity with maximum pore diameter of 1 μm) was used as the percolating column. The tube was cleaned, dried, rinsed with hexane and then almost filled with freshly

crushed silica gel. It was then heated for about six hours in a furnace at a temperature of 250^{o}C and under backing pump pressure (Fig. 4.4). A stream of argon was passed over the gel while it was cooling, after which the inlet and outlet of the column, which were fitted with rubber tubing, were closed with Bunsen clips. After removal from the furnace, the column was supported vertically, the rubber tubing removed and the hexane poured in the top. With a little hexane running from the outlet, the cleaned and dried container was rinsed before collecting hexane in it. The flow rate of the liquid depends on the fineness of the gell; it took about six hours to percolate 400 gms of hexane through very fine gel. The cleaned liquid was stored under argon in a coloured bottle to avoid photochemical reaction.

The u.v. absorption, before and after percolation of this grade of hexane, are shown in the Fig. 4.5. A second percolation with freshly powdered, activated gel gave no remarkable improvement in the u.v. transmission.

A yellow colouration at the top of the silica gel column was observed during the first percolation. This was identified[2] as being due to the disubstituted napthylamine present in the hexane.

4.2.3 Experimental techniques

Besides giving an absorption band in the u.v. range, dissolved oxygen has a considerable effect on the charge injection and conduction mechanism of saturated hydrocarbons. To remove the dissolved gases the liquid was purified in a special, vacuum degassing, apparatus. This removed the gas in a series of stages initially at backing pump pressure and finally by a slow distillation at a pressure of about 10^{-6} torr, established by a mercury diffusion pump (G.E.C.).

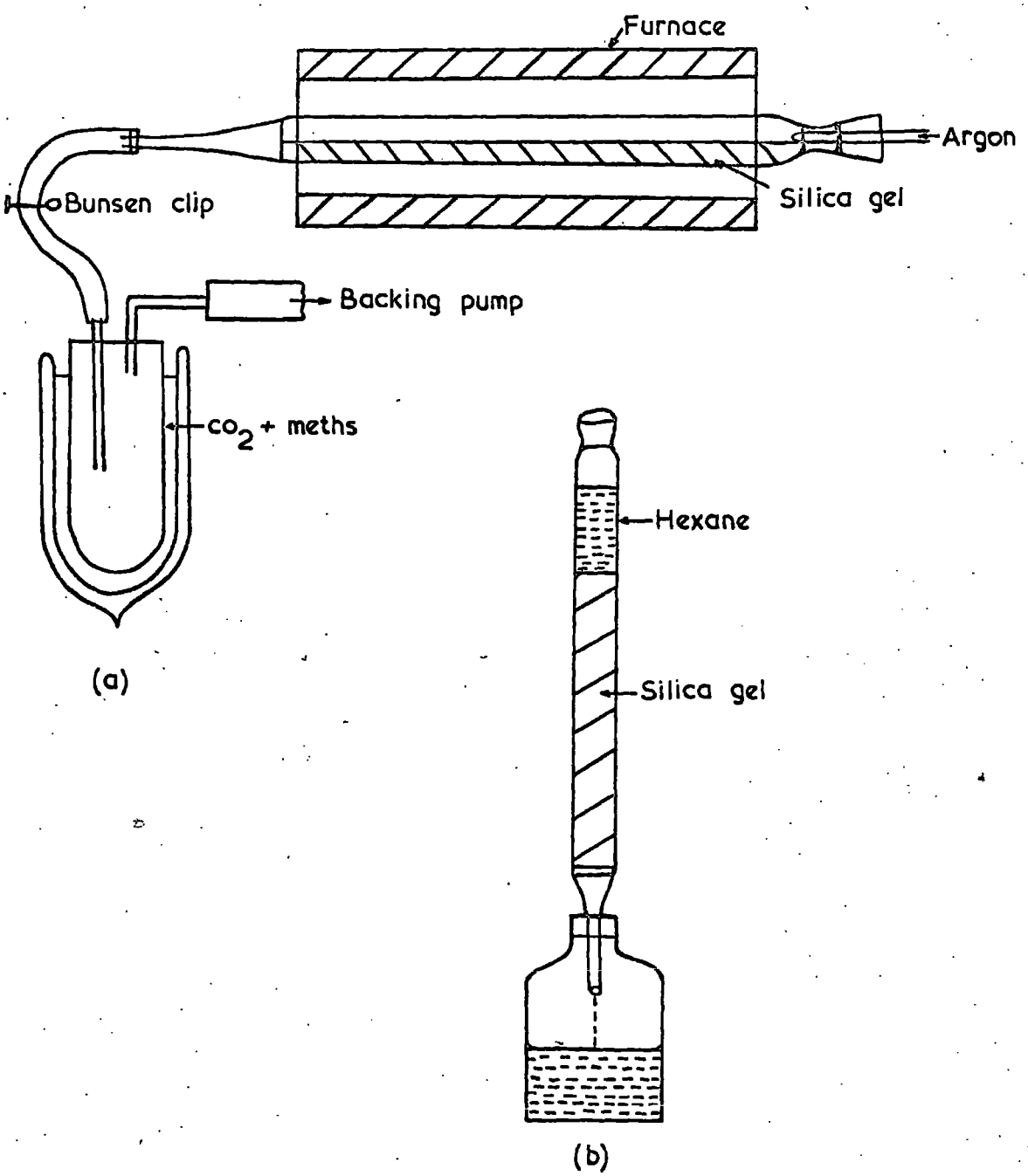

Figure 4.4 (a) Activation of silica gel
(b) Percolation of hexane through activated silica gel

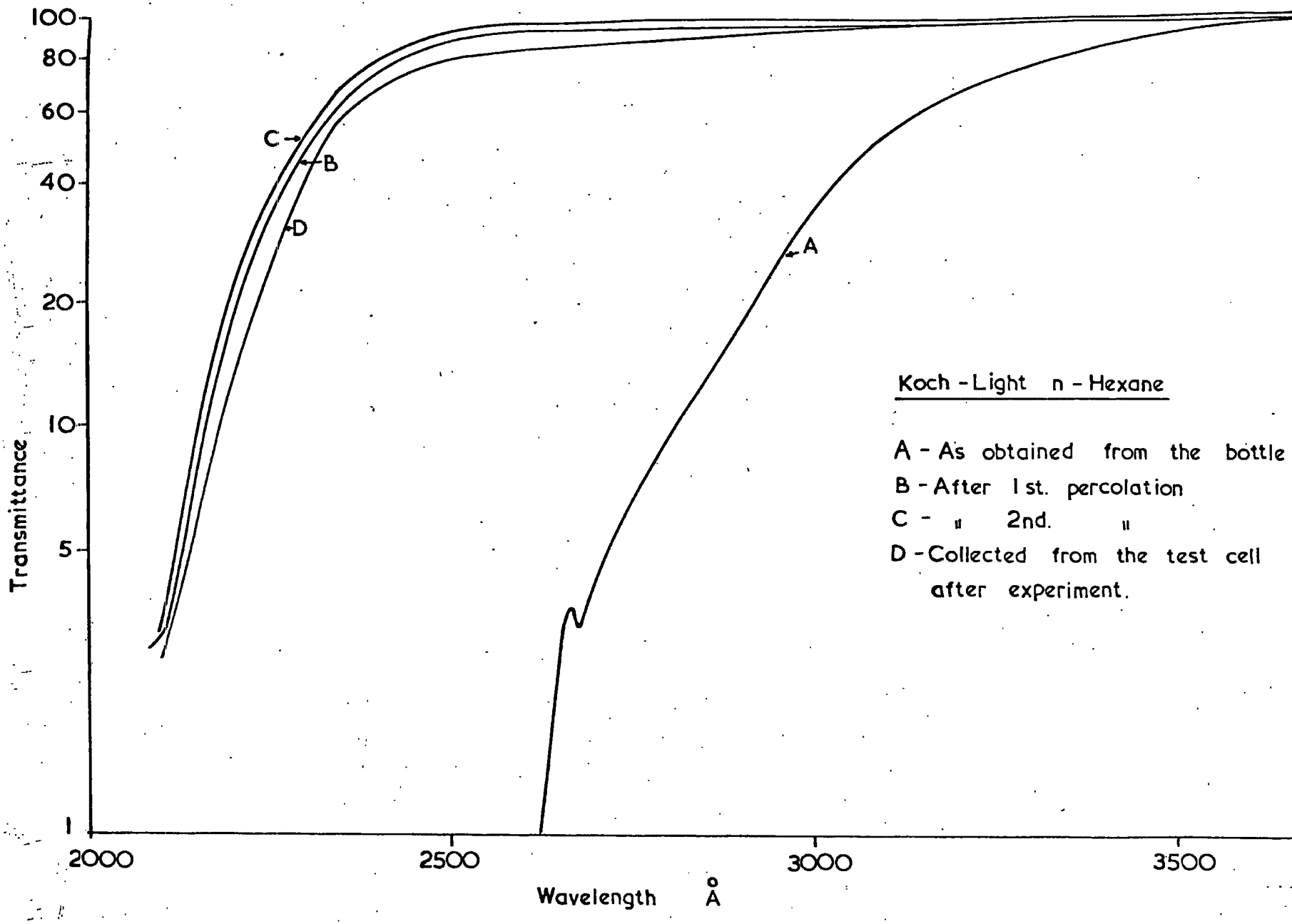

Figure 4.5 The optical absorption of Koch-light n-hexane. Optical path: 10cm, Reference cell: air.

A detailed description of the degassing apparatus was given by Pugh.[2] The apparatus, built originally by Morant and slightly modified since, is essentially a three-stage distillation system (Fig. 4.6) constructed from Pyrex-glass. Greaseless taps (G. Sprinham & Co.) with Viton A inserts as the sealing material, were used at only two points to avoid contamination of the hexane. The only greased tap in the apparatus was well isolated from the liquid by a liquid nitrogen trap.

At the beginning of every run the system, with the test cell already sealed on, was pumped down to a pressure of 10^{-6} torr and tested for degassing. The pumping was continued for several days until the total leak and degassing rate was less than 10^{-7} lusec (measured by timing the rise in pressure in the system, isolated from the pumps, with a Pirani gauge).

To get the liquid into the system, the tap J was first closed and G opened, thus maintaining backing pressure in the section X. The inlet spiral with glass filter B and reservoir D, were surrounded by cooling mixture (a slurry of solid CO_2 and methylated spirit at $-79^{o}C$). The inlet pipe was immersed in the hexane container A and tap C was opened so that hexane flowed slowly into D. Backstreaming of oil from the rotary pump into the system was prevented by filling trap H with cooling mixture. After collecting about 100 cc of hexane in D, tap C was closed. Traps E and F were filled, and reservoir I was surrounded by cooling mixture. With the removal of the cooling mixture from around D, hexane evaporated, condensed on the cold surfaces of E and F, and finally collected in I. The transfer of hexane from D to I took more than two hours, the vapour being pumped continuously. The tap G was then closed and the liquid, well surrounded by cooling mixture, was left in I overnight.

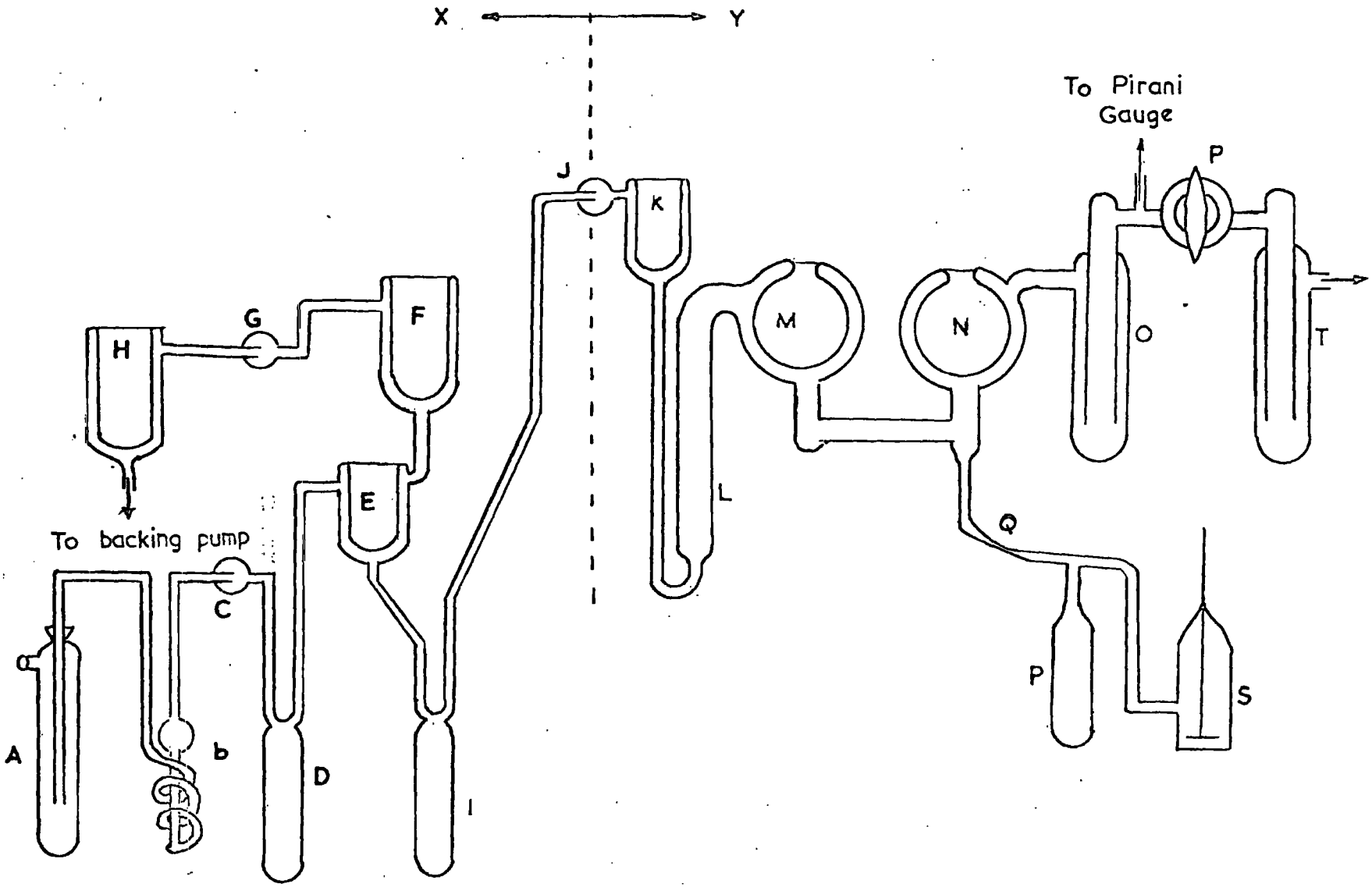

Figure: 4.6. Degassing apparatus.

On the following morning, degassing was started in section Y at a pressure of approximately 10^{-6} torr. With I surrounded by cooling mixture, and with some in M, a little liquid nitrogen was placed in trap K and the tap J was opened. By partially removing the cooling mixture from around I, the hexane evaporated slowly and formed a solid layer on the surface of K. The distillation rate could be easily controlled by varying the amount of cooling mixture at I. The level of liquid nitrogen in K was gradually raised and a thick solid layer of hexane formed around K. When there were only a few drops of hexane left in I, taps J and P were closed. The liquid nitrogen trap was removed from O and, as the liquid nitrogen evaporated from K, the hexane melted and collected in L which was surrounded by cooling mixture.

Distillation from L to M was done by slowly adding liquid nitrogen to M. Trap N was almost filled with cooling mixture, trap O surround by liquid nitrogen and tap P opened, The slow evaporation of hexane from L ensured thorough degassing at a gas pressure of about 10^{-6} torr and a thick layer of hexane gradually formed around the trap M. The cell reservoir was then surrounded by liquid nitrogen and the trap M was emptied. Hexane from around M melted and flowed into the cell reservoir. The transfer from around M to the cell reservoir was so quick that some hexane also found its way to trap O. The liquid nitrogen trap T stops any mercury vapour from entering the degassing system.

The cooling mixture was replaced by liquid nitrogen trap N, and the pumping continued during the preparation of the photocathode at an indicated vacuum of about 10^{-6} torr. To evaporate the aluminium for the photocathode a few amperes of current, from a step-down transformer, were passed through the test cell filament. The aluminium evaporated onto the silica disc and

parts of the inside of the cell. During the evaporation of aluminium from tungsten, the tungsten dissolved in the aluminium charge is precipitated on to the filament, forming a porous sintered layer.[80] Evaporation was stopped when a film of approximately 50% optical transmission had been deposited on to the silica. This is stated to give the best photoemission into liquid n-hexane with u.v. irradiation.[46] The thickness of the film was ascertained by looking through the central portion of the disc during the evaporation. As the aluminium coated tungsten could become very fragile,[80] care was taken not to break the filament by overheating.

After the evaporation of a good cathode, the supply was switched off and the filament was allowed to cool. The constriction in the pumping line was sealed off with an oxy-coal gas flame and the cell was disconnected from the system at a pressure of about 10^{-6} torr. The liquid nitrogen Dewar was removed from around the cell reservoir. The hexane melted in a few minutes and it was transferred to the electrode compartment. The cell was then fixed inside a metal screen for electrical measurements.

The screening box (20 cm x 20 cm x 33 cm) was made from 1.6 mm thick aluminium sheet and it was fixed to a wooden table. There were two 2.9 cm diameter holes, one for the light-tube, and the other for a screening tube for the electrode/electrometer connection. A Plessey socket in the top of the box connected the power supply to the test cell. The cell itself was clamped inside the box by a 1.3 cm wide brass strip having a foam rubber lining (to stop slipping) and fitted with tightening screws.

The light-tube was essentially a brass tube 4.3 cm long, having a diameter of 2.5 cm and 0.16 cm wall, with one end closed by a brass plug. The inner end of the plug was cut at an angle of 45^{o}. A 2.5 cm diameter

glass disc with an aluminium film evaporated on the surface was placed on the angled face and held in position with plasticine. A small hole was made in the tube, just above the centre of the inclined disc. Light entering the tube was reflected by the disc on to the centre of the cell window. The reflectivity of such a mirror is much higher than for a silvered mirror[80] for u.v. radiation and it did not tarnish in six months.

A 125 watt medium pressure, mercury vapour lamp (Type 6721A/T, Hanovia Ltd.) was used for d.c. photoinjection. A quartz lens focussed the light on to the reflecting disc. The intensity of the lamp could be controlled by adjusting an iris diaphragm and the light could be interrupted when necessary with a shutter. The brightness of the lamp remained constant after a warming up period of about 15 minutes. A bandpass filter (Chance-Pilkington Ox-7), in combination with this lamp, gave the required wavelength range for photoinjection.

For pulse photoinjection, the mercury lamp was replaced by an FA.41 quartz flash-tube, manufactured by AEI Lamp & Lighting Co. Ltd. The tube was 9 cm long and 8 mm diameter with arc length of about 5 cm. The flash-tube supply was the same as that used by Bloor.[3] The flash duration was 0.5 millisec, covering a wavelength range 2000 - 4000 Å. The tube fitted with flexible leads, was enclosed in a small box (18 cm x 16 cm x 4 cm) made from 3 mm thick aluminium alloy sheet. Connections to the voltage supply and triggering circuit were made through two sockets fitted at the back of the box. A 2.5 cm diameter hole was made in the front of the box for the radiation exit. A 2 cm brass tube of 2.5 cm O.D. was fitted to the hole with the other end pushed well into the light-tube.

After completing a set of measurements, air was let in to the cell by breaking off the sealing-off tip. The cell was emptied and the lower part

immersed in Stripalene, covered with a layer of water (to stop harmful vapours). This slowly dissolved the Araldite seal and the silica window became separated from the cell in a few hours. The cell and the silica disc were thoroughly washed with water before cleaning and preparing for the next run.

4.2.4 Measuring apparatus

A diagram of the measuring apparatus is shown in Fig. 4.7.

For both d.c. and pulse photoinjection, a highly stabilised power supply (Type N103, Dynatron Radio Ltd.) was used. This supplied calibrated voltages from 300 to 3,300 V (of either polarity) to the test cell via a special low-noise coaxial cable. Lower voltages were obtained from a laboratory power supply. The low voltage electrode was connected by a screened connector to the input of the head unit (Model B33C) of a Model 33C Vibron electrometer. The unit has a switched range of measuring resistors (10^5 - 10^{12} ohms) between input and earth and the electrometer has ranges of 10, 30, 100, 300 and 1000 mV (full scale) enabling currents as low as 10^{-15} A to be measured. The intrinsic speed of response of the instrument is 0.7 sec to reach 90% of the final reading (this does not follow an exponential law). A pen recorder, with a sensitivity of 1 mA full scale into 1500 ohms, was used to record the current from the Vibron output.

For pulse photoinjection measurements, the converter unit and electrometer were replaced by a cathode follower, an amplifier and oscilloscope, as used by Bloor[3] who gives their full specifications. A high quality capacitor of a few pF was connected across the input of the cathode follower and was used to integrate the transient current and give a voltage output

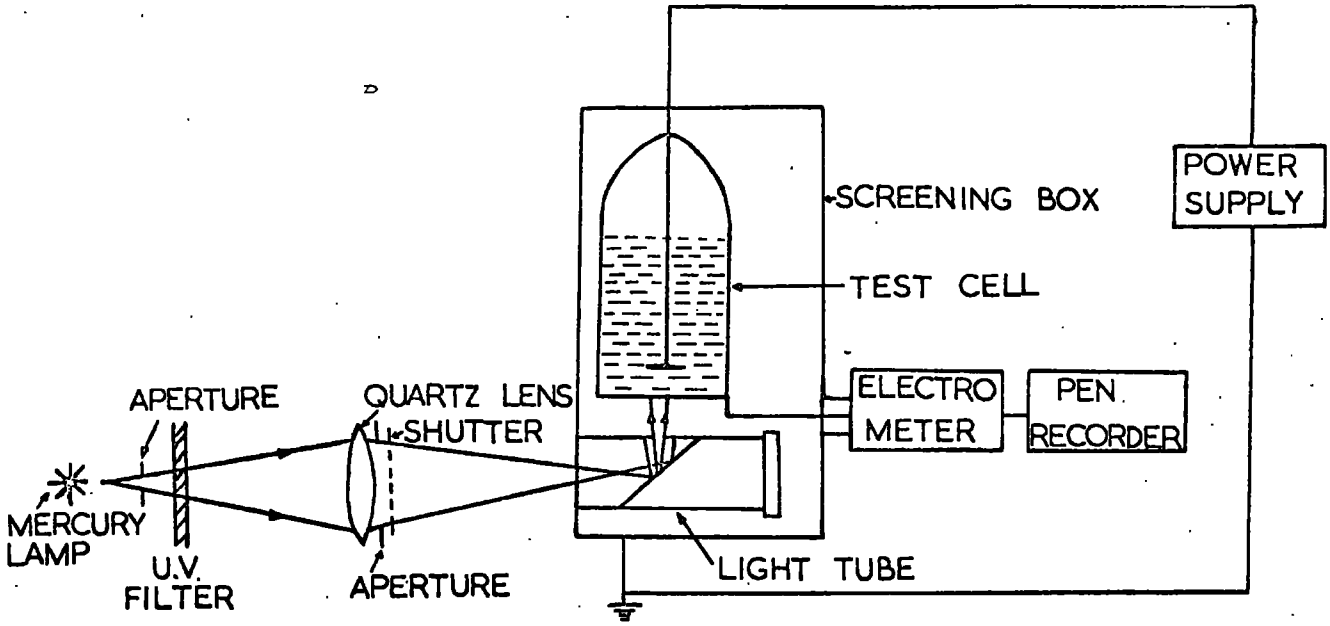

(a)

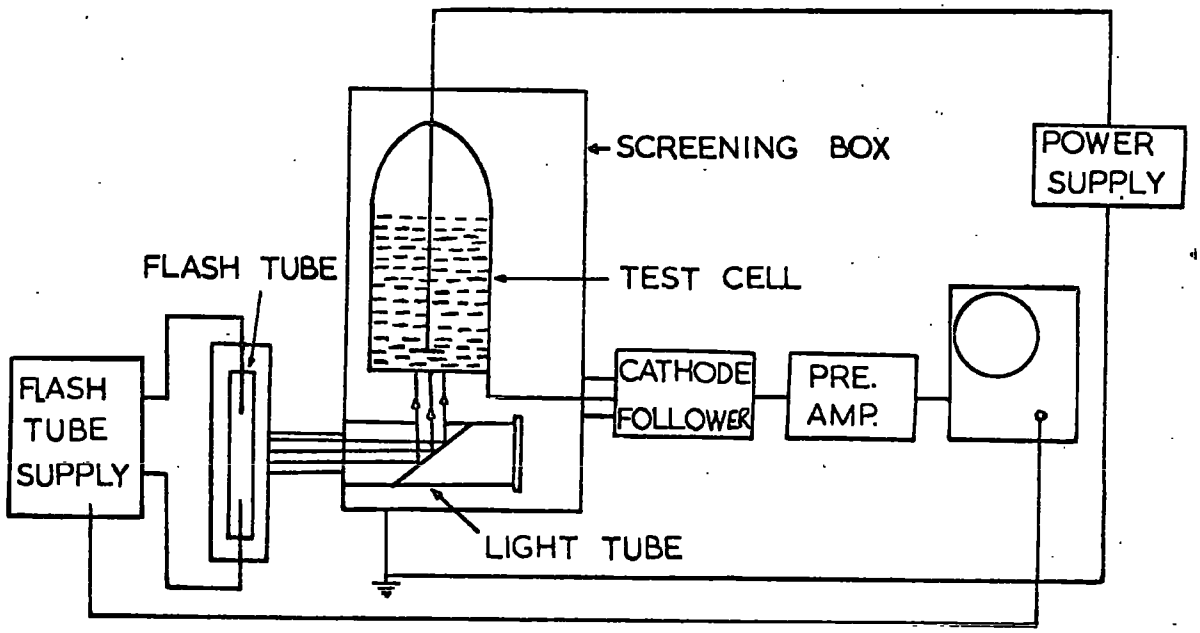

(b)

Figure 4.7 Experimental arrangements for (a) d.c. and (b) flash measurements.

proportional to the charge transfer in the cell. The high input impedance of the cathode follower enabled the signal to be fed to a Tektronix 1121 wide band pre-amplifier with an input impedance of 10^6 ohms, to a Tektronix Type 545A oscilloscope triggered from the flash-tube supply.

All the connections were made with coaxial cables. To overcome direct pick-up from the flash unit and to minimise the noise level, particular care was taken with earthing. The earth terminals of the cathode follower, flash-tube circuit and oscilloscope, were all connected together by copper braiding. Connection to the main earth point in the laboratory was made by a copper strip. The oscilloscope traces were photographed using fast Polaroid film.

4.3 Results

All measurements were carried out in the same test cell (Sec.4.2.1) The first two runs were done using Hopkin and Williams 'spectroscopic grade' hexane without any purification, Later experiments used n-hexane from Koch-light Laboratories (Puriss grade) further purified as described in section 4.2.2. The ultraviolet absorption spectrum at each purified sample was measured before degassing. All the pulse measurements were for this liquid. In all cases, the hexane was degassed at a pressure of about 10^{-6} torr and sealed off at this pressure in the test cell which had a degassing rate of about 10^{-7} lusec.

All the experiments used a fixed electrode gap of 1.2 cm and room temperature. In most cases the u.v. radiation was filtered by a band-pass filter (OX-7) to prevent photochemical reactions and it was directed only onto the photocathode. Photocurrents were recorded on the pen recorder as a superposition of dark and photocurrents. 'Reverse' polarity measurements

were made with the evaporated film electrode positive and solid metal (upper) electrode negative.

After the evaporation of a good photocathode, it took about half an hour to seal off the test cell, transfer the hexane and make the electrical connections before starting the photoinjection measurements. Elapsed time was recorded from the deposition of the aluminium photocathode in the test cell.

The results are presented in chronological order. Graphs are presented as I_p-V and Q-V characteristics, where I_p is the d.c. photocurrent, V the applied voltage and Q the pulse injected charge. The shape of charge oscillograms for the pulse measurements also gave the drift mobility of the charge carriers to confirm previous works.

4.3.1 The I_p-V characteristics of spectroscopic grade hexane

The first measurements in the first run were started half an hour after evaporating the photocathode. With a forward voltage of 300 V applied to the test cell, the recorded photocurrent was 4×10^{-13} A, the dark current being less than 10^{-14} A. The applied voltage was increased in steps of 100 V and a gradual increase of photocurrent was noted. The cathode was illuminated at least two minutes after each change of voltage, to reduce the 'hysteresis effect'[2] to a minimum. The photocurrent reached a value of 4×10^{-12} A for an applied voltage of 2.2 KV, as shown in curve A of Fig. 4.8, with no sign of saturation.

Measurements taken on the following day indicated a decrease in the photoinjection. The photocurrents again increased steadily with voltage, but they were smaller than those obtained just after the preparation of the photocathode. A forward voltage of 300 V gave a photocurrent of

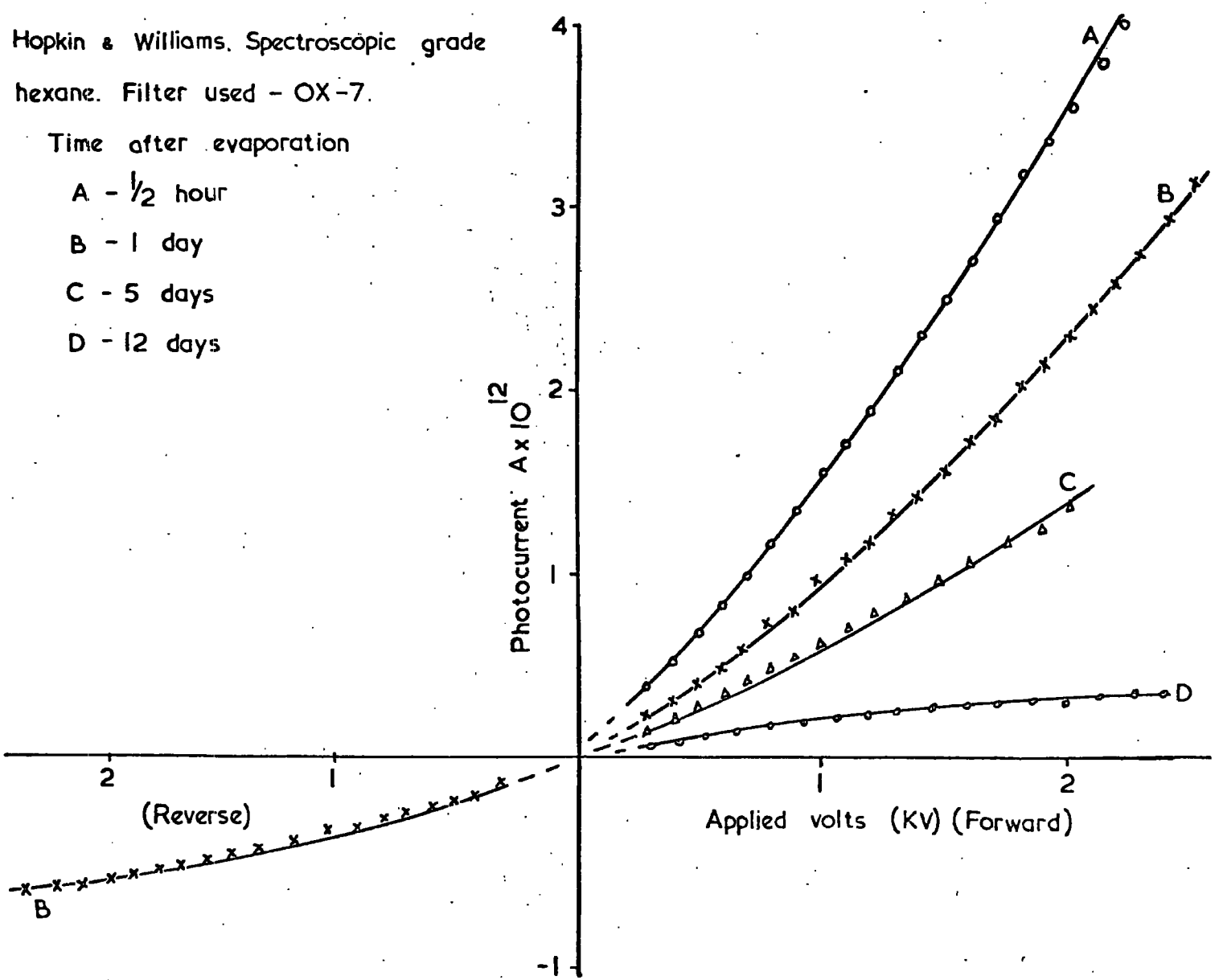

Figure 4.8 Variation of photocurrent with applied voltage.

2.4×10^{-13} A, which increased to 3.4×10^{-12} A for 2.6 KV (Fig. 4.8, curve B).

When the polarity of the applied voltage was reversed, the photocurrent was greatly reduced, being only 6.6×10^{-13} A for an applied voltage of 2.6 KV. The forward/reverse ratio of the photocurrent was therefore about 4:1. The reverse photocurrents were less sensitive to the applied voltage than the forward ones.

Measurements taken five days after evaporation gave a photocurrent of about 10^{-12} A for an applied voltage of 2 KV (Fig. 4.8, curve C). The photocurrents with the reverse polarity were very small (10^{-14}A) and they could not be easily measured because of the comparatively large dark currents (about 10^{-12} A for 2 KV) at this time. On later days the photocurrents for the normal polarity of the applied voltage continued to decrease. After thirteen days the photocurrent was about 10^{-13} A for an applied voltage of 2.4 KV (Fig. 4.8, curve D). On the other hand, the dark current continued to increase (reaching about 4×10^{-12} A for an applied voltage of 2 KV after thirteen days) and was almost independent of polarity.

Another experiment was carried out using the same grade of hexane to try to increase the photoinjection by slight improvement of technique and to measure the charge injection with a pulse of u.v. radiation. The latter was unsuccessful for a number of reasons, and because of the delay the d.c. photocurrents were not measured until the day following the cathode preparation. A series of I_p-V curves is shown in Fig. 4.9. The forward photocurrent one day after cathode preparation was 4.5×10^{-13} A for an applied voltage of 300 V rising to 4.7×10^{-12} A at 3 KV (curve A). With reverse voltages the photocurrents were comparatively small and the forward

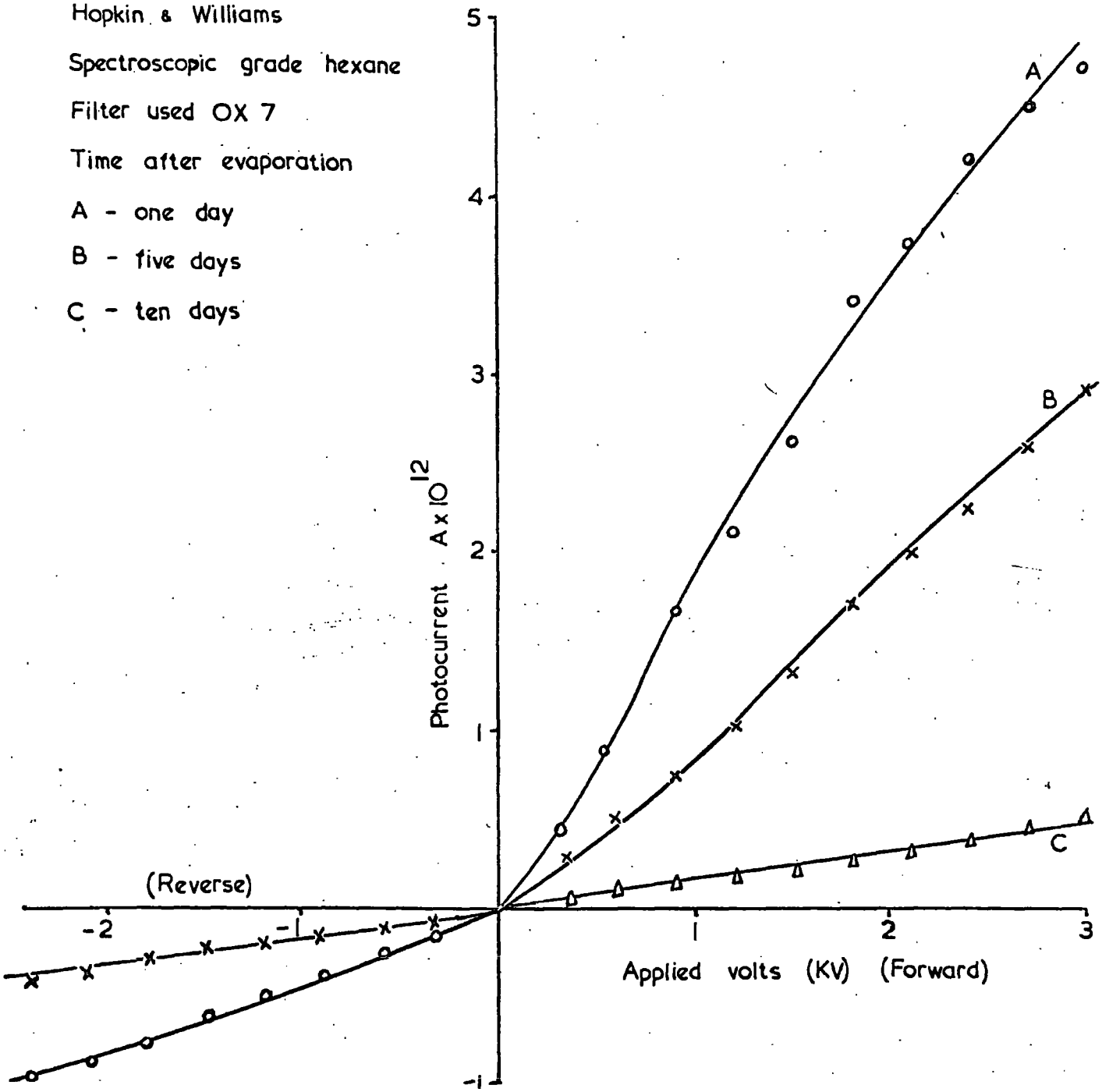

Figure 4.9. Variation of photocurrent with applied voltage.

/reverse ratio was 5:1. The dark current varied from about 10^{-13} A at 300 V up to about 10^{-12} A at 3 KV, and they were very nearly the same for both polarities.

Measurements made five and ten days after evaporation are also shown in Fig. 4.9 as curves B and C respectively. The photocurrents gradually decreased as in the previous experiment. The photocurrents for reverse applied voltages became very small after ten days of evaporation and they could not be measured. The dark current continued to increase from the day of preparation reaching a value of about 10^{-11} A for an applied voltage of 3 KV in ten days.

4.3.2 The I_p-V characteristics of Puriss grade n-hexane

Similar techniques with further slight improvements were used for measurements with the purified Puriss grade of n-hexane. A series of I_p-V curves for this liquid are shown in Fig. 4.10. The photocurrent measured half an hour after the evaporation of the photocathode was 1.6×10^{-12} A for forward voltage of 300 V increasing to 2.2×10^{-11} A for 3 KV, which was the maximum recorded photocurrent and about five times greater than the previous. The I_p-V curve, (Fig. 4.10, curve A) showed the upward trend for the entire range of applied voltage and the photocurrents with reverse voltages were very small (1.4×10^{-12} A for 3 KV). The forward/reverse ratio of the photocurrents varied between 15:1 and 10:1.

Measurements of the photocurrents taken on the following day showed a decrease for forward applied voltages, but a slight increase for reverse voltages. This decrease for the applied forward voltages continued on later days and the photocurrent was about 2.6×10^{-12} A for 3 KV after thirteen days (i.e. about an order less). On the other hand, the photo-

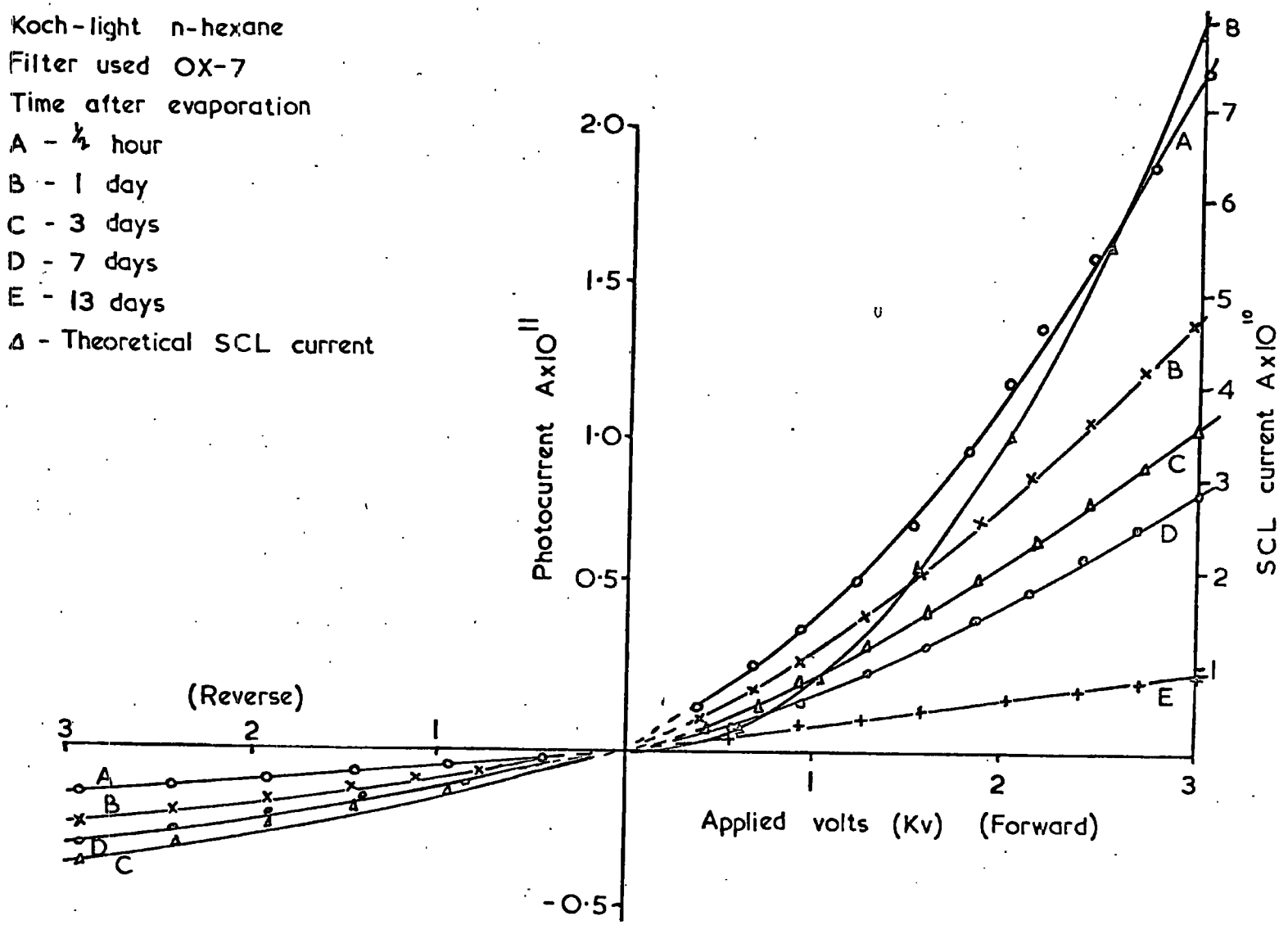

Figure 4.10 Variation of photocurrent and space charge limited current with applied voltage.

currents measured with reverse voltages showed a slight increase up to the fourth day after evaporation and then decreased again for longer times. Both the photocurrents gradually became proportional to the applied voltages after a few days. The forward/reverse ratio of the photocurrents reached a minimum of 3:1 (after 4 days) and then rose again to 7:1 (after thirteen days).

To measure photocurrents at lower voltages a Farnell E-350 power supply was used. The I_p-V curve for the voltage range up to 300 V measured thirteen days after evaporation is shown in Fig. 4.11. The variation of the photocurrent with applied forward voltage appears to be approaching saturation. For reverse voltages the photocurrents were very small, giving a forward/reverse ratio up to 30:1.

With a sealed off test cell system it is possible to produce a new photocathode by freezing the hexane into the reservoir attached and re-evaporating aluminium from the filament. This technique was used by Pugh for investigating the same decay of photocurrents as has been described here. After thirteen days the cathode was therefore re-formed by a little more aluminium evaporation so that measurements could continue on the same sample of highly purified hexane.

The subsequent measurements showed an increase of about three times in thephotocurrent. The I_p-V curves after the second evaporation, Fig. 4.12, show that the measured photocurrents were then more or less proportional to the applied voltage. With reverse polarity, the photocurrents were still less than for the forward direction; the forward/reverse ratio varied from 3:1 to 2:1. Unlike after the first evaporation, the photocurrents for both forward and reverse voltages decreased with time and the decrease was much

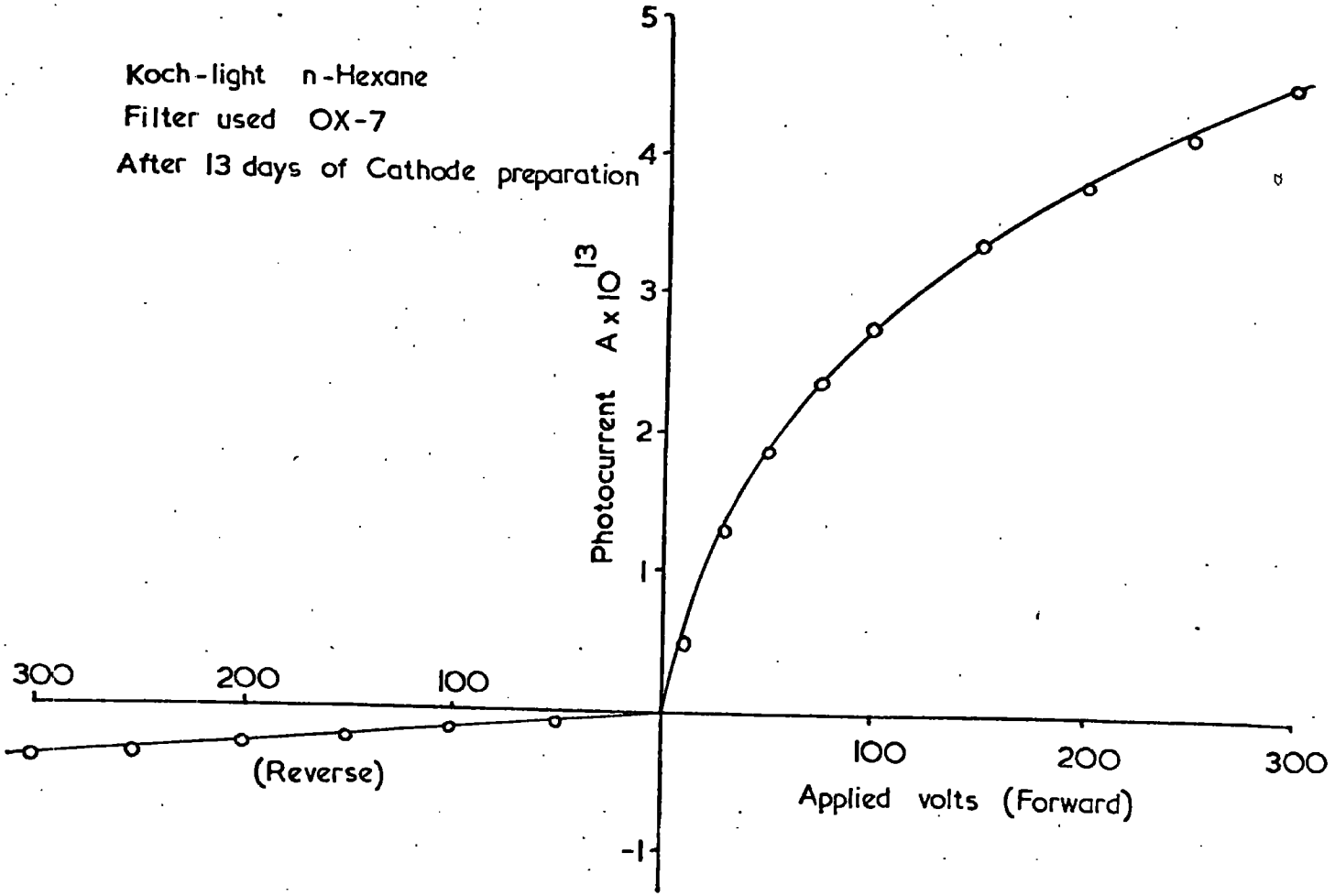

Figure 4.11 Variation of photocurrent with applied voltage

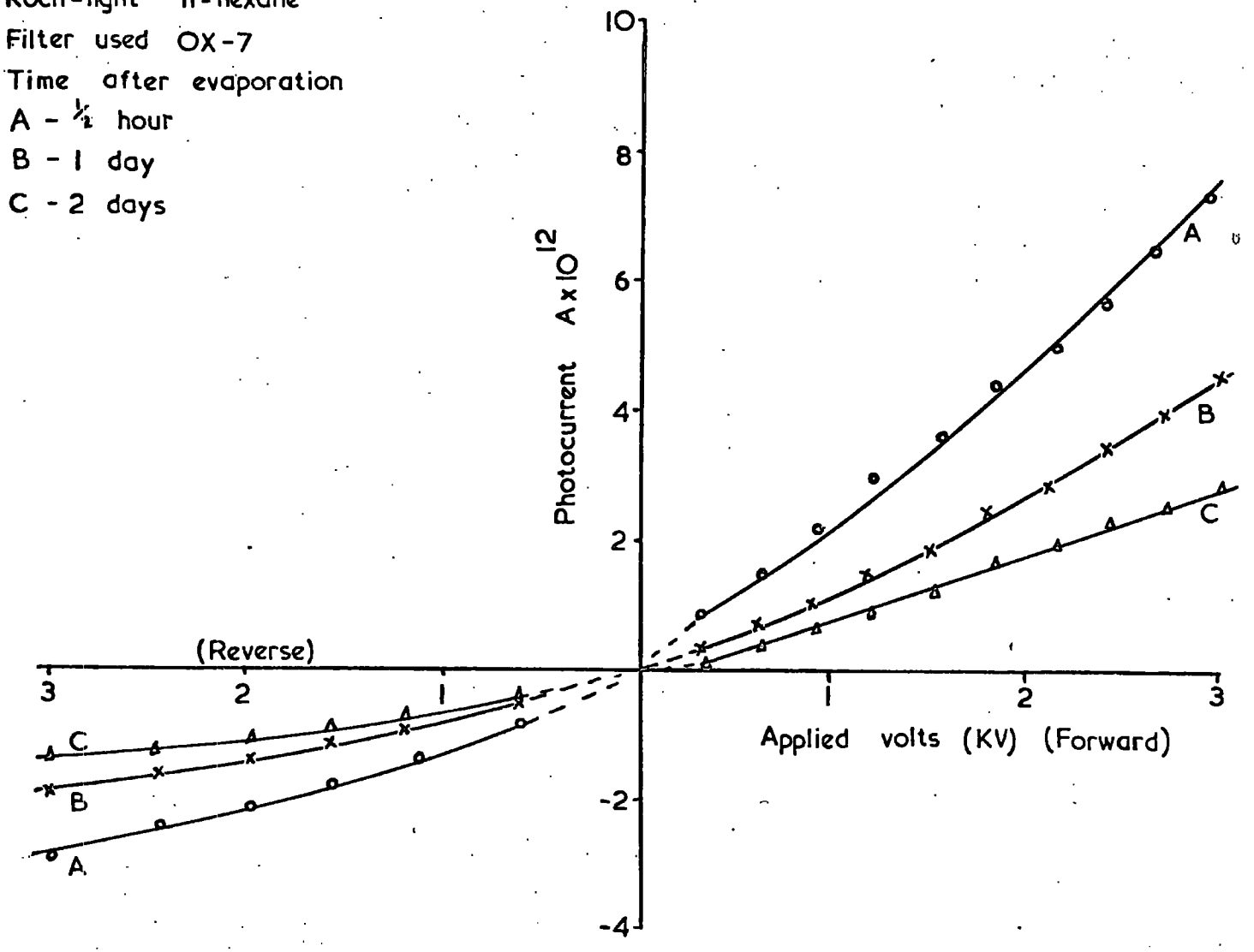

Figure 4.12 Variation of photocurrent with applied voltage

quicker in this case.(about one order of magnitude in three days.) The first pulse measurements described in Sec. 4.3.3 were made on this sample. Finally air was let in to the cell and the liquid was carefully extracted. A u.v. absorption measurement showed no appreciable change in the liquid in spite of its exposure to prolonged filtered radiation (Fig. 4.5, curve D). This also showed no chemical interaction of degassed hexane with silica, Pyrex or the metallic parts of the test cell.

Using the same grade of hexane, another experiment was undertaken, largely to compare the photocurrent with the charge injected by a pulse of u.v. radiation in more detail than in the previous test. The same cell was used again, and procedures similar to the previous were followed. The results are in Fig. 4.13. Photocurrents measured half an hour after evaporation were of about the same magnitude as in the previous experiment. With the reverse polarity they were about five times higher than the previous ones. The I_p-V curves maintained an upward trend in the first few measurements but the photocurrent gradually became proportional to the applied voltage. The photocurrent for both forward and reverse voltages decreased with time, the forward current decreasing faster. This decay of the photocurrents was in general quicker than for the previous experiment. The forward/reverse ratio varied from 9:1 to 3:1.

4.3.3 The Q-V characteristics of Puriss-grade hexane

The experimental arrangement for pulse measurements was described in Sec. 4.2.4. The pulse of u.v. light injected a thin 'disc' of electrons from the photocathode, which formed a 'disc' of low mobility carriers. The voltage between the electrodes caused these carriers to drift towards the anode producing a transient current which was integrated to give the charge

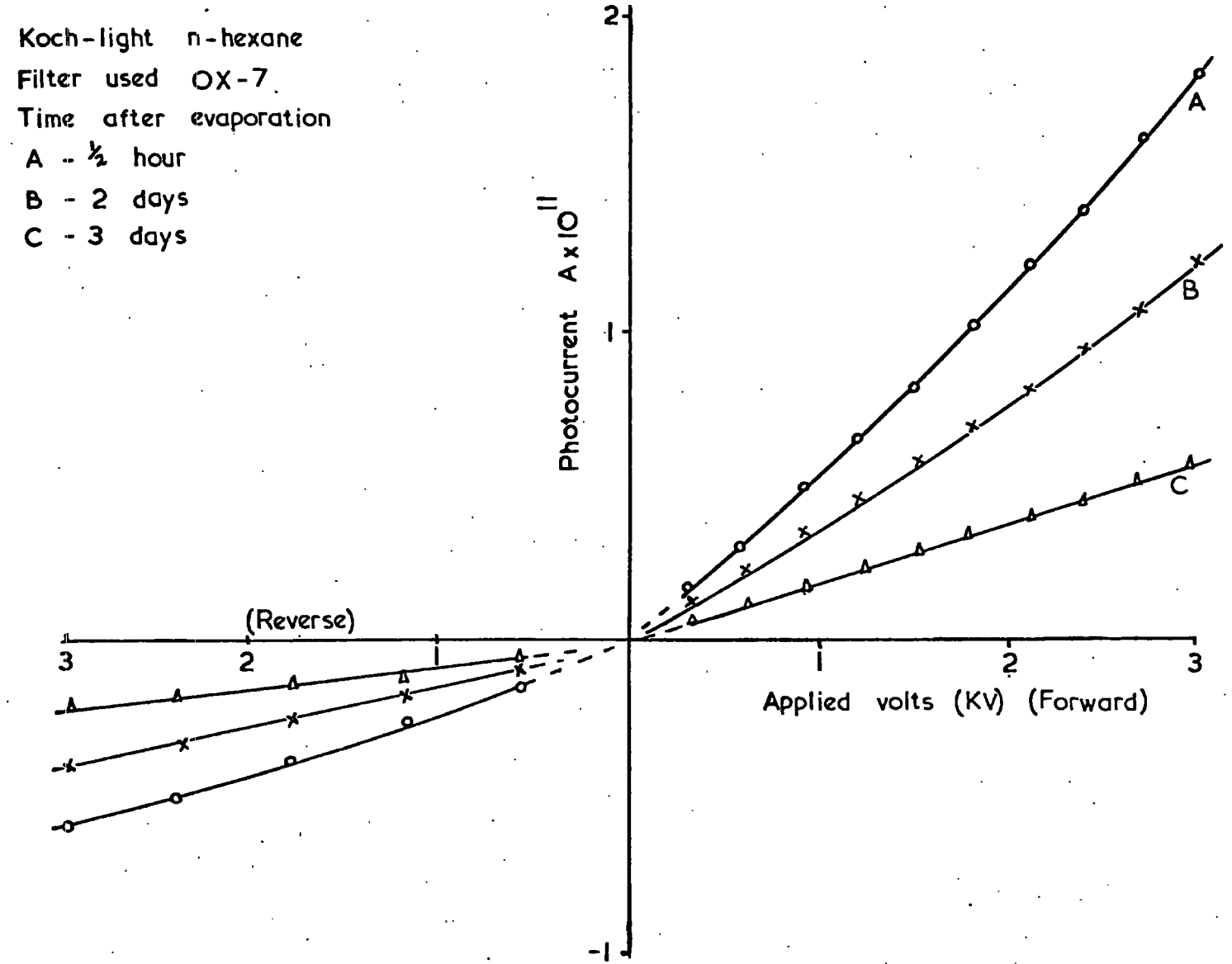

Figure 4.13 Variation of photocurrent with applied voltage

transfer as a function of time.

A 470 pF capacitor in parallel with a high resistance (10^{10} ohms) formed the integrating circuit across which the voltage was measured. The buildup of charge on the measuring capacitor due to the movement of the charge carriers in the liquid continued steadily up to the transit time. This was followed by a slow decay of charge, with the time-constant of the measuring circuit. The intensity of the u.v. flash was kept constant by taking care that the flash-tube was always fired at a constant discharge voltage of 450 V. However, it will be shown that the injected charge into hexane is, in fact, proportional to the applied voltage.

Assuming that the total charge Q generated by the pulse reached the opposite electrode, the relation between signal voltage V_s and injected charge Q at time $t = \tau$ is given by

$$V_s = Q/Cm \qquad (14)$$

where Cm in the measuring capacitance. The measurements of transit time, τ, will be described in the next sub-section.

Pulse-photoinjection measurements were first made half an hour after the second evaporation of the first d.c. run on Puriss hexane, described in Sec. 4.3.2. Fig. 4.14 shows the variation of injected charge with applied voltage measured at different intervals after the evaporation. The injected charge with a forward voltage of 3 KV was initially 7.5×10^{-12} C, and a reverse voltage of the same magnitude gave 4.2×10^{-12} C. The values obtained on the following day showed a marked decrease in charge injection (Fig. 4.14, curve B). On the third day the charge injection was too small to measure, even with an applied voltage of 3 KV of either polarity. A third evaporation did not increase the photoinjection.

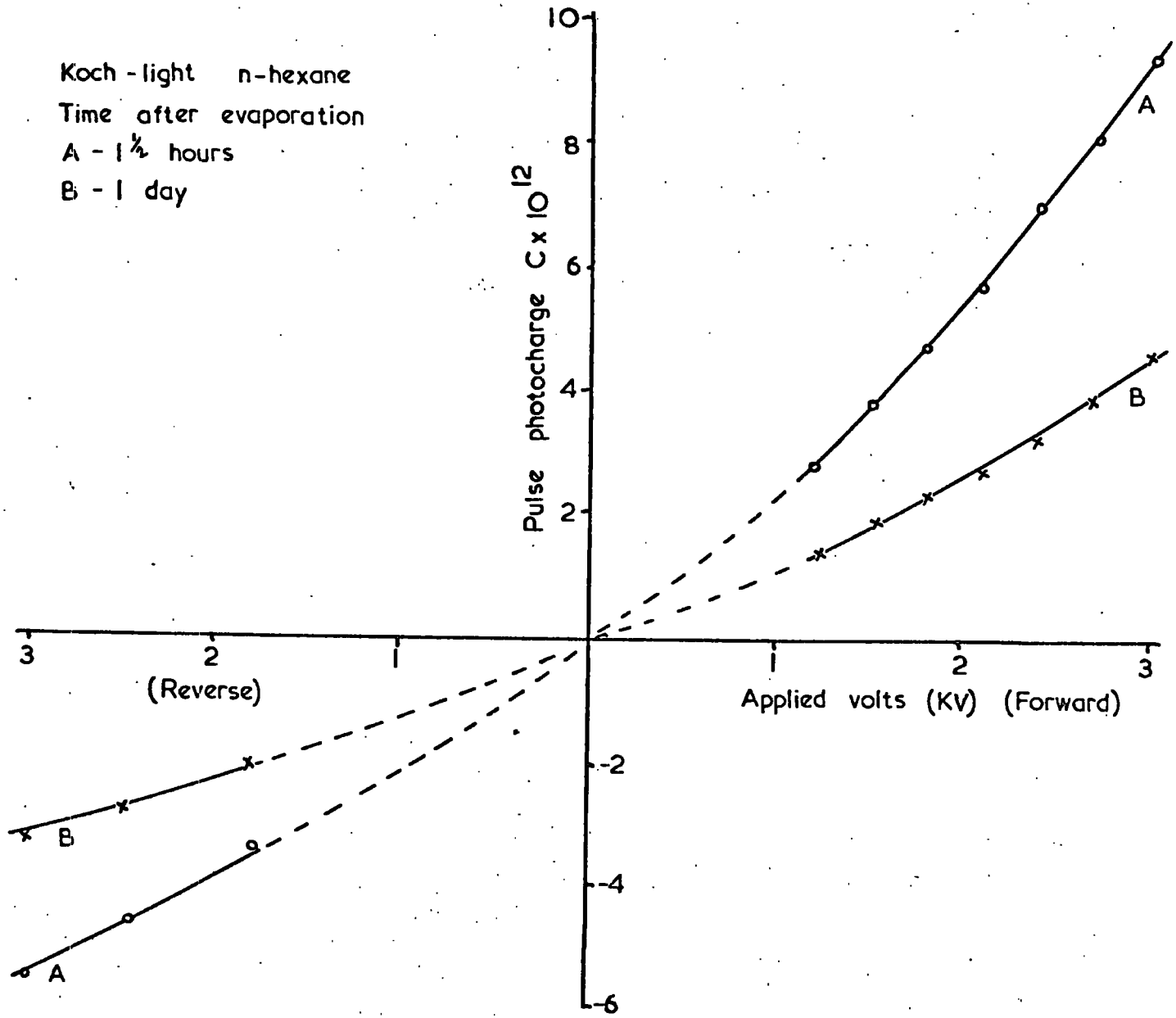

Figure 4.14 Variation of photocharge with applied voltage

Having established the method, another experiment was carried out to compare the d.c. and pulse photoinjection under similar conditions. This time a piece of OX-7 filter was placed in the aperture of the light-tube, but the other procedures remained the same.

The results given in Fig. 4.15 show that the charge injected by filtered radiation was only about a third of that with unfiltered radiation for both forward and reverse voltages. Measurements made on three consecutive days after cathode preparation showed a gradual decrease in the photoinjected charge. For example, it decreased from 5.2×10^{-12} to 2.5×10^{-12} C in three days for a forward applied voltage of 3 KV. A similar decrease was observed for the reverse voltages.

Fig. 4.16 shows the relationship between the d.c. photocurrent, I_p, and the pulse charge-injected, Q, for conditions in which only the d.c. radiation was filtered. The dots and the crosses represent two different sets of measurements. Fig. 4.17 gives more complete results for both radiations being filtered. The shaded portion represents the range of scatter. To reactivate the photocathode a second evaporation was attempted but the quantity of aluminium left on the filament after the first evaporation was too small and no further measurements were possible.

4.3.4 Carrier mobility from charge oscillograms

The drift mobility of the charge carriers was obtained by measuring the time required for them to cross the gap between the electrodes. The pulse of u.v. radiation was much shorter than the carrier transit time. The movement of the carriers up to the transit time, τ, was detected by the charge build up on the measuring capacitor. The typical shapes of transients for forward and reverse voltages applied to the test cell are

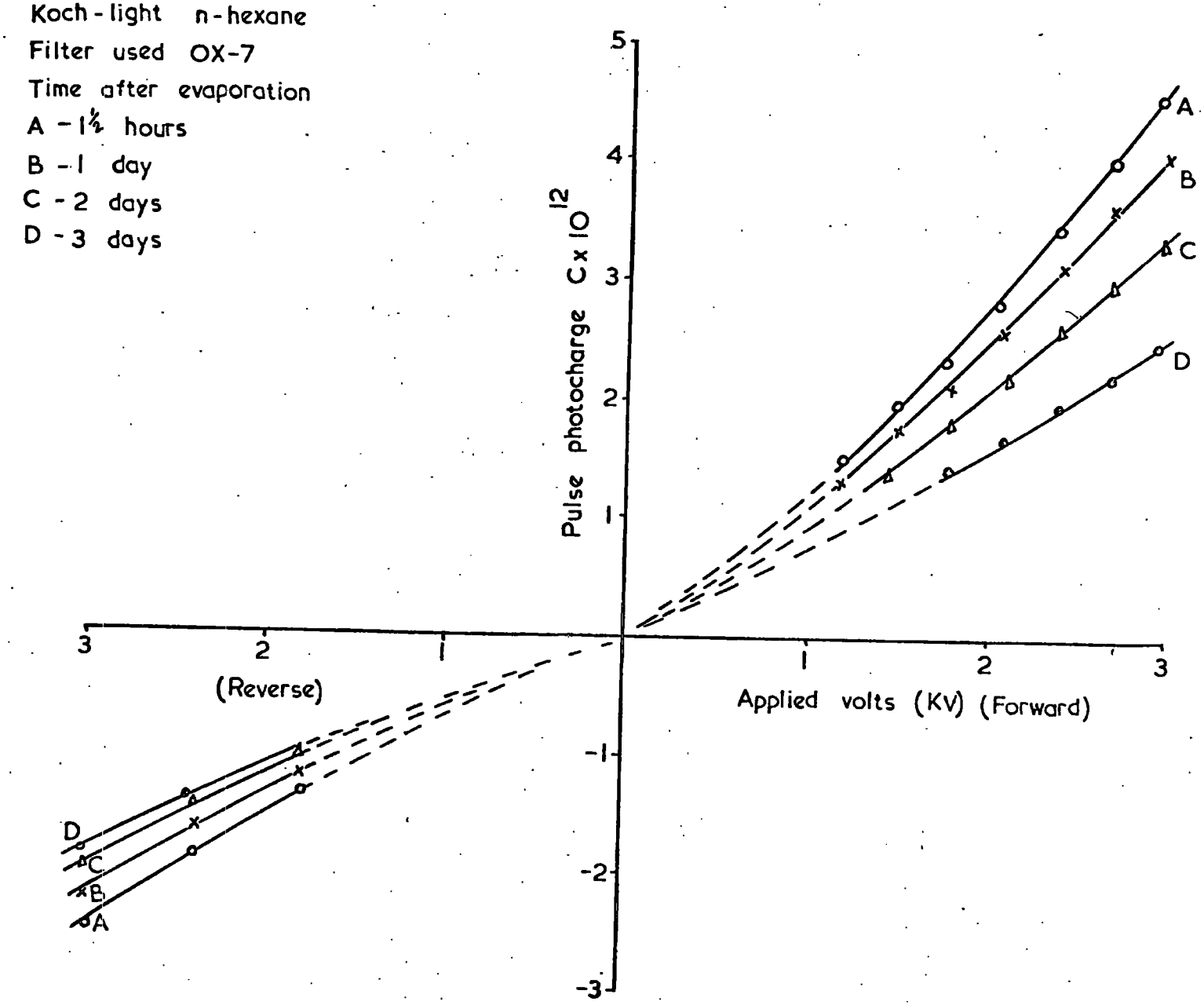

Figure 4.15 Variation of photocharge with applied voltage

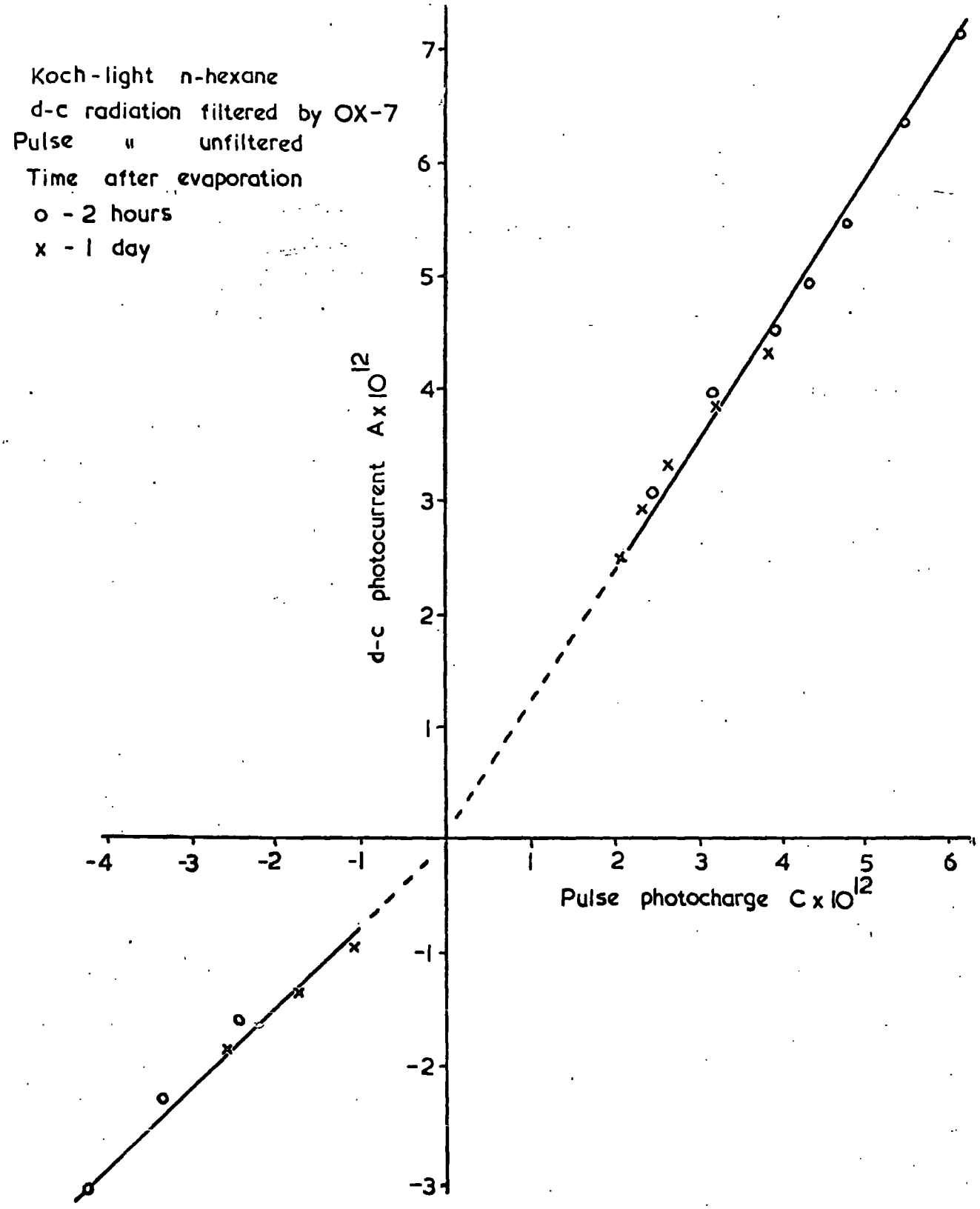

Figure 4.16 Variation of d.c. photocurrent with pulse photocharge

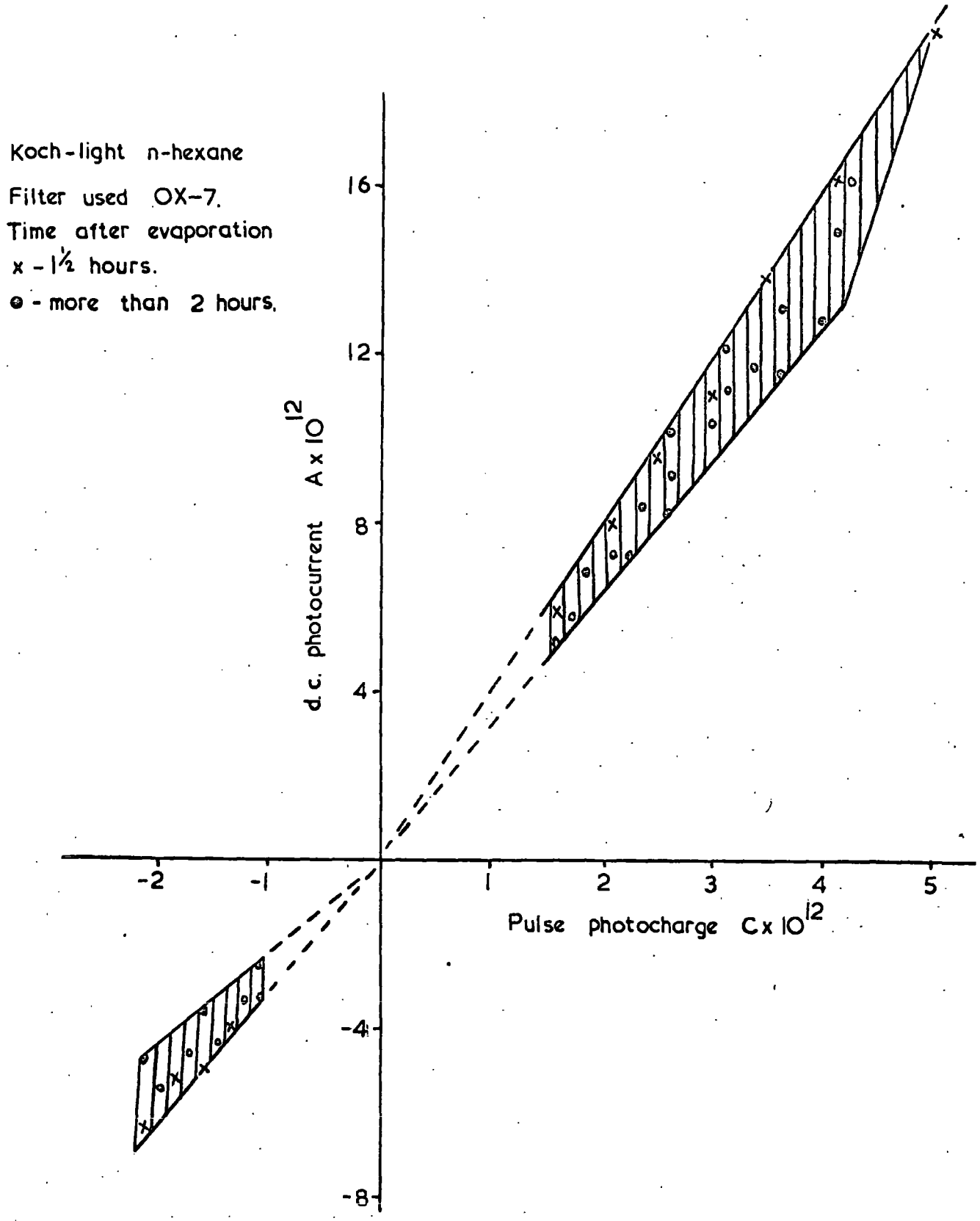

Figure 4.17 Variation of d.c. photocurrent with pulse photocharge. Shaded regions indicate the magnitude of experimental scatter.

shown in Fig. 4.18. Although the reverse transient cannot be explained by simple charge injection from the cathode, as will be discussed in Chapter VI, it will be assumed for the present that the same method of analysis applies as for the forward transient. Contrary to the predicted linear rise, the transients have curvature on the rising part and rather flat maxima. Traces obtained with forward applied voltages also showed a concave curvature on the early rising part of the transient. These shapes have been analysed in detail by Bloor[3], who showed that they may be explained by the effects of liquid movement.

Bloor's method for the determination of the transit time from such transients is shown in Fig. 4.18. Tangents are drawn to the rising and decaying parts of each oscillogram. A perpendicular drawn from the intersection of the tangents to the time base then gives the transit time of the carriers. From this the drift mobility, μ, was calculated using the formula

$$\mu = \frac{\text{Average Velocity}}{\text{Drift field}} = \frac{d/\tau}{E} = \frac{d^2}{V\tau} \qquad (15)$$

where d is the distance between the electrodes, τ the transit time and V the applied voltage. The field strength, $E = V/d$ was assumed to be uniform throughout the electrode gap.

Transit times of carriers up to applied voltages of 3 KV and of both polarities were measured. Figure 4.19 shows the variation of $\frac{1}{\tau}$ with applied voltage for unfiltered radiation. The values of μ, calculated from the gradients of these lines, were 6.3×10^{-4} cm^2/volt sec and 8.2×10^{-4} cm^2/volt sec for forward and reverse voltages respectively. Table 1 gives the individual values of drift mobility calculated from each transient using an unfiltered pulse of u.v. radiation. The values are

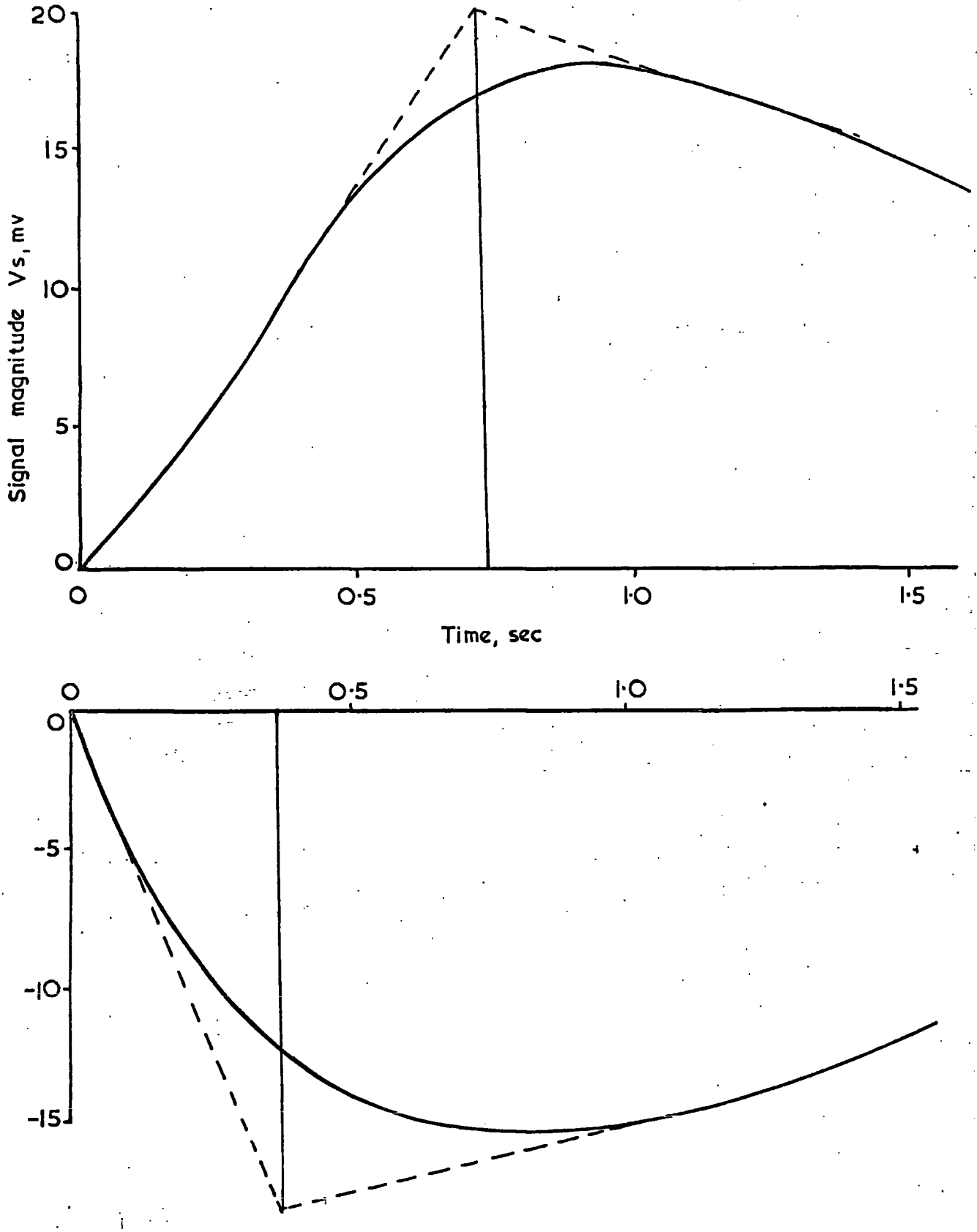

Figure 4.18 Typical shape of the charge transient: determination of transit time for forward applied voltage (upper transient) and reverse applied voltage (lower transient).

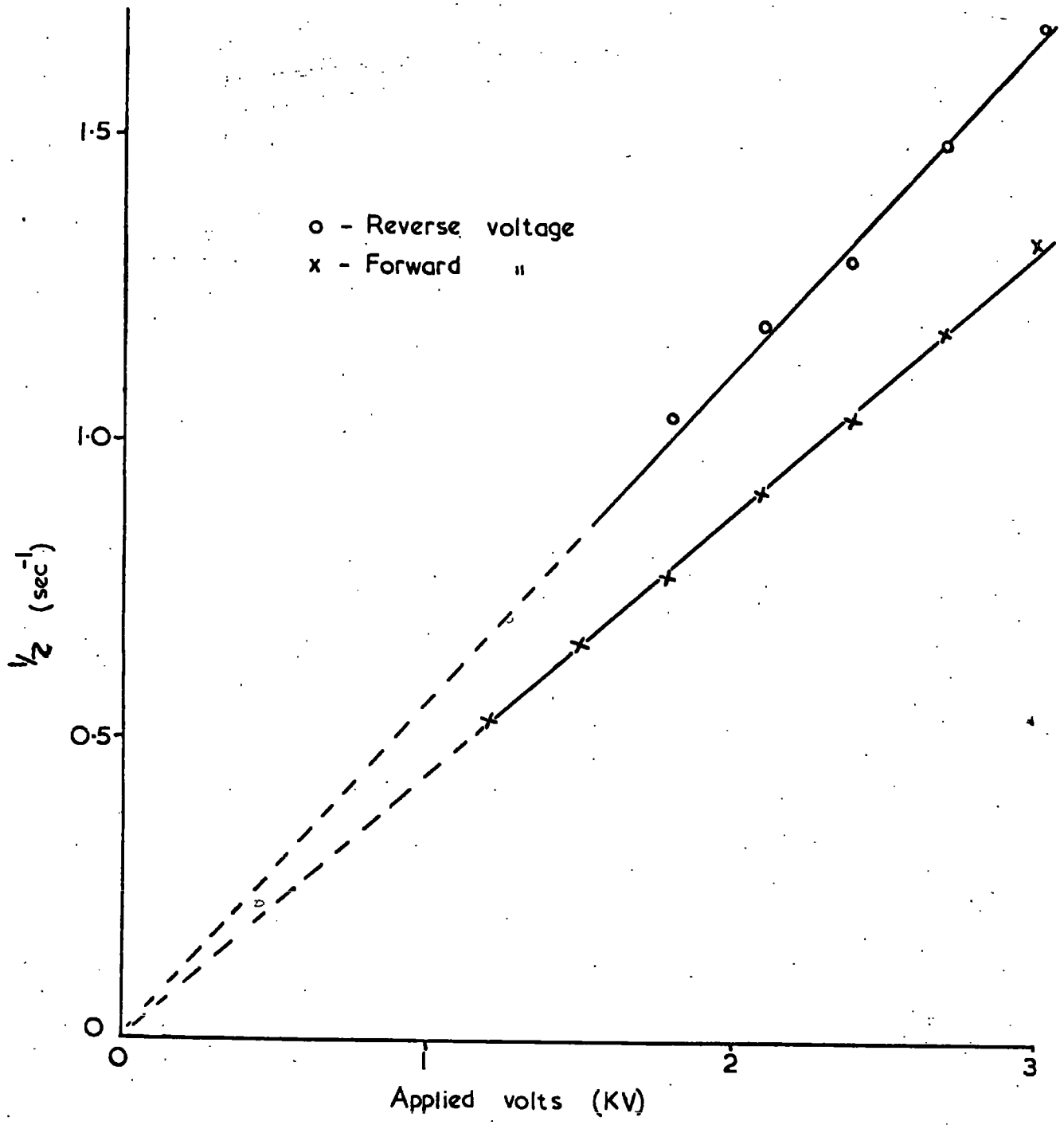

Figure 4.19 Variation of transit time with applied voltage.

independent of the field strength but dependent on the polarity of the electrodes. With the photocathode positive, the values were higher (7.5 - 8.8 x 10^{-4} cm^2/volt sec) than those obtained with the photocathode negative (6.0 - 6.9 x 10^{-4} cm^2/volt sec). For measurements on the day following evaporation, the mobility also showed no variation with field strength, but the same polarity effect was observed. The measured values were of the same magnitude as those of the previous day, in spite of a marked decrease in the charge injection. The Table also shows the photocurrents and photoinjected charges for the same set of measurements.

TABLE 1. Giving the values of the d.c. photocurrent, the pulse injected charge and the carrier mobility for different applied voltages.
Koch-light n-hexane (Puriss grade)
Filtered d.c. radiation
Unfiltered pulse radiation

Voltage applied in KV	d.c. photocurrent in 10^{-12} A		Injected charge in 10^{-12} C		Drift mobility in 10^{-4} cm^2/volt sec		Reference
	with forward V	with reverse V	with forward V	with reverse V	with forward V	with reverse V	
3.0	7.2	3.2	7.5	4.2	6.5	8.0	Measured half an hour after evaporation
2.7	6.4	-	6.1	-	6.3	-	
2.4	5.8	2.3	5.0	3.3	6.0	7.5	
2.1	5.0	-	4.2	-	6.3	-	
1.8	4.6	1.6	4.0	2.4	6.3	8.0	
1.5	4.0	-	3.3	-	6.4	-	
1.2	3.1	-	2.4	-	6.3	-	
5.0	4.4	1.9	4.5	2.5	6.9	8.8	Measured one day after evaporation
2.7	3.9	1.7	3.8	2.1	6.6	8.0	
2.4	3.4	1.4	3.1	1.8	6.4	7.5	
2.1	3.0	1.2	2.6	1.5	6.3	7.5	
1.8	2.5	1.0	2.3	1.2	6.3	-	
1.5	2.1	-	1.9	-	6.4	-	

The measured mobilities are somewhat smaller than those obtained by other workers using similar techniques. It was thought that this might have been due to the shorter wavelengths in the u.v. pulse, leading to some photoionisation of the liquid. Measurements were threfore taken with a pulse of filtered u.v. (Sec. 4.3.4). The mobility values (Table 2) did not, however, show any change. The drift mobilities were again independent of the field strength and the same polarity effect was observed. Measurements taken two days after the cathode preparation showed no change in the value. This showed that neither the state of the photocathode nor the intensity of the u.v. radiation had any effect on the transit time of charge carriers, although both effected the magnitude of the charge injected.

4.4 Comparison of Results with those of Previous Workers

The study of the conduction mechanism due to photoinjected charges has been carried out in this laboratory for the last eight years. Following the work of Morant[4], Pugh[2] made an extensive study of u.v. induced photocurrents from freshly prepared cathodes of aluminium, magnesium and gold. Later experiments by Bloor[3] were mainly concerned with the determination of the mobility of the carriers injected by a pulse of u.v. radiation from an aluminium photocathode. The present experiments were performed to correlate the d.c. photocurrent with the pulse photoinjected charge. This section compares the various results obtained here with those obtained earlier.

The variation of photocurrent with applied voltage was similar to that of the previous measurements (Fig. 4.20), the photocurrent becoming roughly proportional to voltage at the higher levels. The other characteristics also confirmed previous work in general. The main features were as follows:-

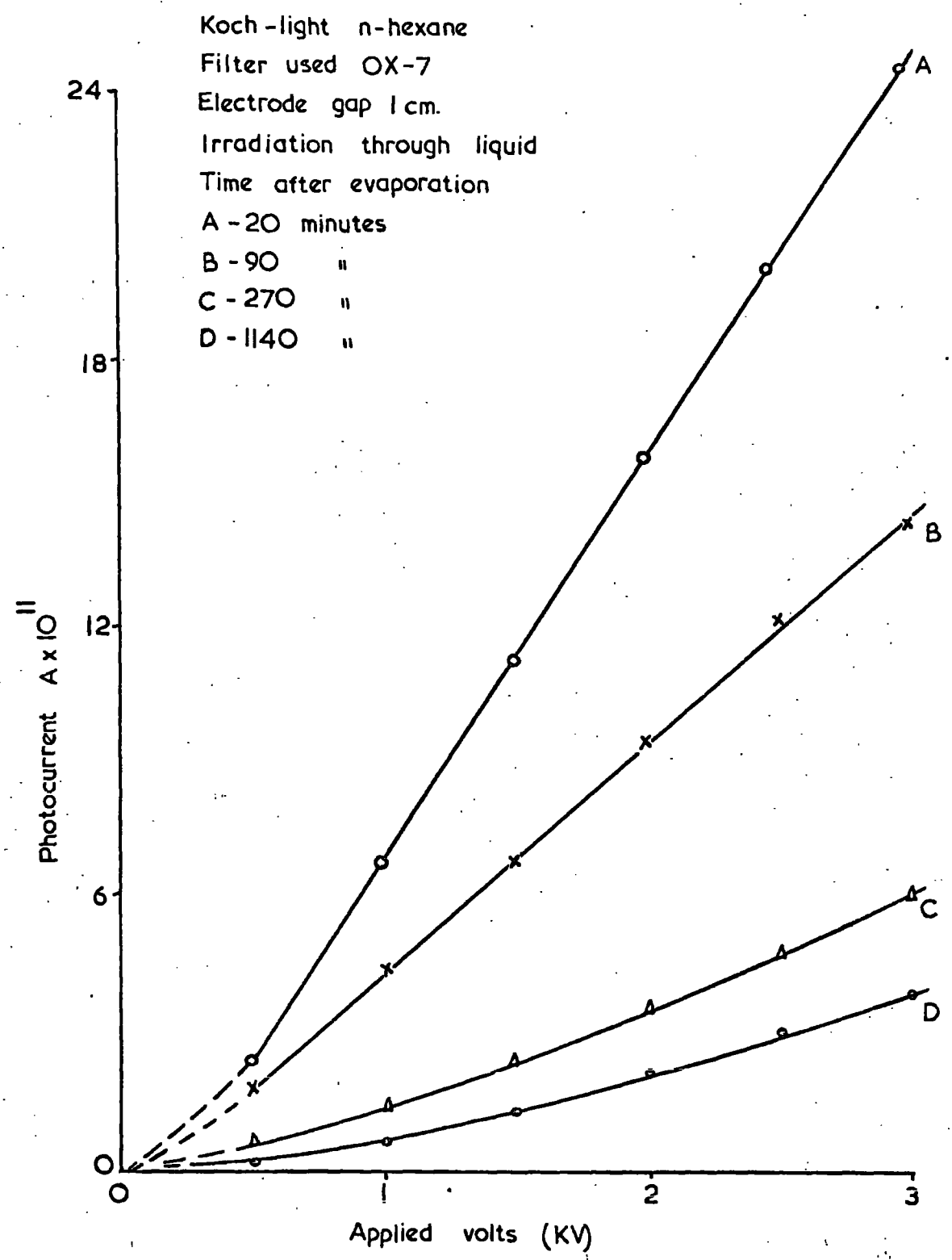

Figure 4.20 Variation of photocurrent with applied voltage (after Pugh[2])

TABLE 2. Giving the values of the d.c. photocurrent, the pulse injected charge and the carrier mobility for different applied voltages
Koch-light n-hexane (Puriss grade)
Both d.c. and pulse radiation filtered.

Voltage applied in KV	d.c. photocurrent in 10^{-12} A		Injected charge in 10^{-12} C		Drift mobility in $10^{-4}cm^2$/volt sec		Reference
	with forward V	with reverse V	with forward V	with reverse V	with forward V	with reverse V	
3.0	18.0	6.6	5.2	2.1	6.5	8.0	Measured half an hour after evaporation
2.7	16.0	5.8	4.2	1.8	6.3	8.0	
2.4	13.6	5.6	3.4	1.5	6.4	8.0	
2.1	12.0	4.2	2.8	1.3	6.3	8.5	
1.8	10.0	3.3	2.4	-	6.7	-	
1.5	8.0	-	2.0	-	6.4	-	
1.2	6.5	2.6	1.5	-	6.3	-	
3.0	15.0	6.0	4.2	2.0	6.9	8.0	Measured one day after evaporation
2.7	13.0	5.4	3.7	1.7	6.0	8.0	
2.4	11.4	5.0	3.2	1.5	6.0	8.6	
2.1	10.0	3.6	2.7	1.2	6.3	8.5	
1.8	8.3	3.0	2.3	1.0	6.3	8.8	
1.5	6.9	2.4	1.8	-	6.0	-	
1.2	5.9	2.0	1.0	-	6.0	-	
3.0	12.0	4.8	3.3	1.9	6.9	8.0	Measured two days after evaporation
2.7	10.4	4.2	3.0	1.6	6.6	7.8	
2.4	9.6	3.5	2.6	1.4	6.6	8.0	
2.1	8.4	3.0	2.2	1.0	6.3	8.1	
1.8	7.0	2.4	1.8	0.7	6.7	7.8	
1.5	6.2	2.1	1.0	-	6.4	-	
1.2	4.6	1.8	0.8	-	6.0	-	

(a) Currents measured with forward voltages were much higher than those with reverse voltages although the exact shape of the I-V curve depended on the nature of the cathode surface and the polarity. Within the voltage range up to 2.5 KV/cm, the photocurrent showed no sign of saturation.

(b) The photocurrents decreased with time after cathode preparation although the decay was retarded by maintaining a good vacuum within the test cell. A measurable photocurrent could thus be obtained with these techniques for fifteen days after the preparation of the photocathode.

(c) The dark current rose continuously in successive measurements but the u.v. absorption of the experimental liquid did not reveal any sign of contamination after prolonged exposure to filtered radiation.

Although the highest photocurrent measured in the present experiment was about an order smaller than that of Pugh, it was still considerably higher than the photocurrents obtained by other workers for the same applied field (Sec. 2.2.1). The higher value obtained by Pugh was due to (a) a smaller delay between cathode preparation and measurements, (b) higher intensity u.v. radiation with a focussed source, whereas in the present case it was a divergent beam, and (c) irradiation of the cathode through the liquid. His higher values were accompanied by a sharp decrease over a few hours as compared to a slower decrease in the present work. (E.g. comparison of the curves in Fig. 4.20 with those of Fig. 4.8 or 4.10.) The reverse photocurrents in the present work were probably due to photoemission from the metal electrode due to u.v. radiation transmitted through the photocathode and the liquid instead of originating from reflections within the cell which gave Pugh's source of reverse current.

For pulse-photoinjection, the experimental technique employed by Bloor was used. The size of the integrated voltage signal due to charge injection in the present experiments was only about a quarter of that obtained by Bloor for the same field strength. This was partly accounted for by the decrease in the radiation intensity due to use of OX-7 filters. The transients were of different shape for forward and reverse applied voltages in the present work, as shown in Fig. 4.18, and this gave rise to different values for the transit times. This indicated a value of carrier mobility about 13% higher in the latter case. A good linear relationship between the reciprocal of transit time and the applied voltage was obtained in the present measurements and also by Bloor. Values of the carrier mobility calculated from these graphs (Fig. 4.19) are in good agreement, namely 6.3×10^{-4} cm^2/volt sec for the forward polarity and 8.2×10^{-4} cm^2/volt sec for the reverse polarity, as compared to 7.6×10^{-4} cm^2/volt sec obtained by Bloor.

Some curvature of the Q-V characteristics was obtained by Bloor when the low potential electrode was irradiated as shown in Fig. 4.21, compared with Fig. 4.14 or 4.15. Irradiating the other electrode, he obtained a linear relationship between the signal voltage and the applied field strength but with a lot of scatter and none of his lines passed through the origin.

The simultaneous measurements of d.c. photocurrent and pulse photo-injected charge has not been attempted previously and the importance of the new results on this aspect will be discussed, together with a detailed model for photoinjection, in Chapter VI.

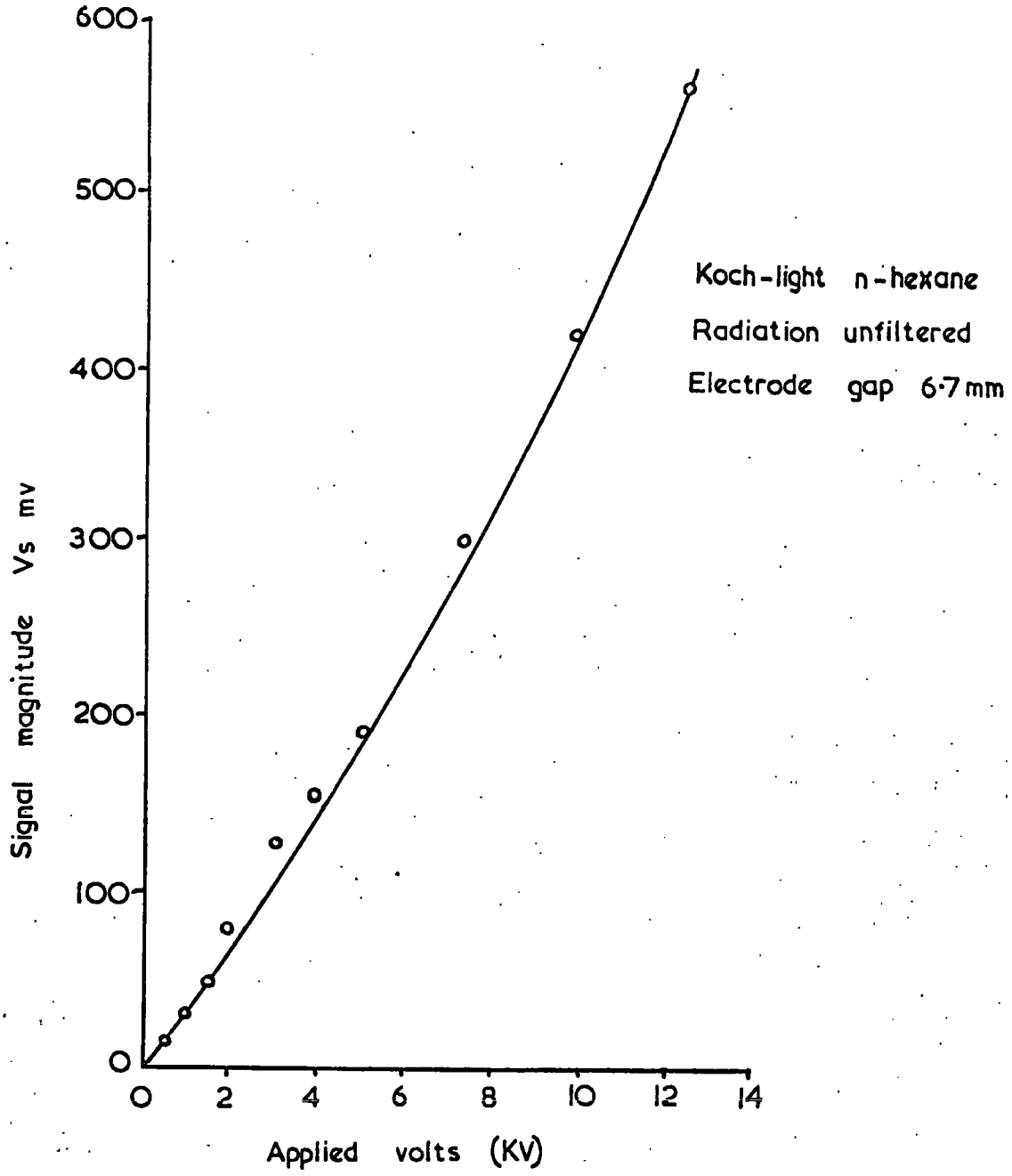

Figure 4.21 Variation of signal magnitude with applied voltage (after Bloor[3])

CHAPTER V

FIELD-INJECTION EXPERIMENTS

The experimental results of Chapter IV showed that the increase in the charge density that can be obtained by the photoinjection of carriers was still too low for ESR work. The photocurrents were of the order of 10^{-11} A for a field strength of a few KV/cm, which corresponds to a carrier density of about 10^{9} cm^{-3}. To increase the carrier density in hexane without liquid contamination, the mechanism of field emission from sharp edges, originally used by Coe et al,[51] was therefore considered. This method has the advantage over photoinjection of not being susceptible to dissolved air, and currents of up to 0.5 mA have been reported in commercial hexane with an applied voltage on the emitter of only 9.5 KV. This high injection current, as well as its possible application in high voltage machines, shows the need for more study of the mechanism of charge injection from field emitters in hexane. The considerable effects of impurities on the injection current, first observed in the present measurements and discussed later in this Chapter, led to the concentration of the present work on the study of high-field injection into different liquid samples.

This Chapter describes the various experiments and results on high-field injection. Measurements were carried out in different grades of hexane, which have been used as supplied, purified by drying and filtering, and deliberately doped with water or alcohol. Attempts have also been made to reproduce some of the recent results on high-field injection obtained else-

where[55] by using similar experimental conditions.

5.1. Experimental Details

The measurements of charge injection into hexane were carried out on three different sets of apparatus. The first measurements were exploratory in nature and were carried out with a simple apparatus housed in a PTFE beaker. The second set of apparatus was designed to measure the conduction current both in the steady-state and when the liquid in the injector region was flowing with a small velocity. In the third group of experiments, the injector and a charge collector were incorporated in a closed loop to circulate the hexane with a velocity as high as 2.6 m/sec in the injector region. The following sub-sections give brief descriptions of each set of apparatus.

5.1.1 Apparatus for preliminary measurements

All the experiments on high field injection used razor blades as one of the electrodes as in previous work.[51] Preliminary measurements of the variation of current with the voltage applied to the razor-edge were carried out on the simple apparatus shown in Fig. 5.1. The emitter was an assembly of six razor blades (Personna & Co.) each 3.6 cm long, held together by two screws (A). The blades were separated from each other by 2 mm thick copper strips. The assembly was mounted on a Plessey socket fixed to a Perspex disc (B). A thin plate of copper 4 x 1.5 cm was also fixed to the disc opposite the blade-tips to form the counter electrode (C). The spacing between the blade-tips and the plate was a few mm. The plate was well insulated from the emitter for the measurement of the collected current. It was later replaced by a grid electrode of the same dimensions.

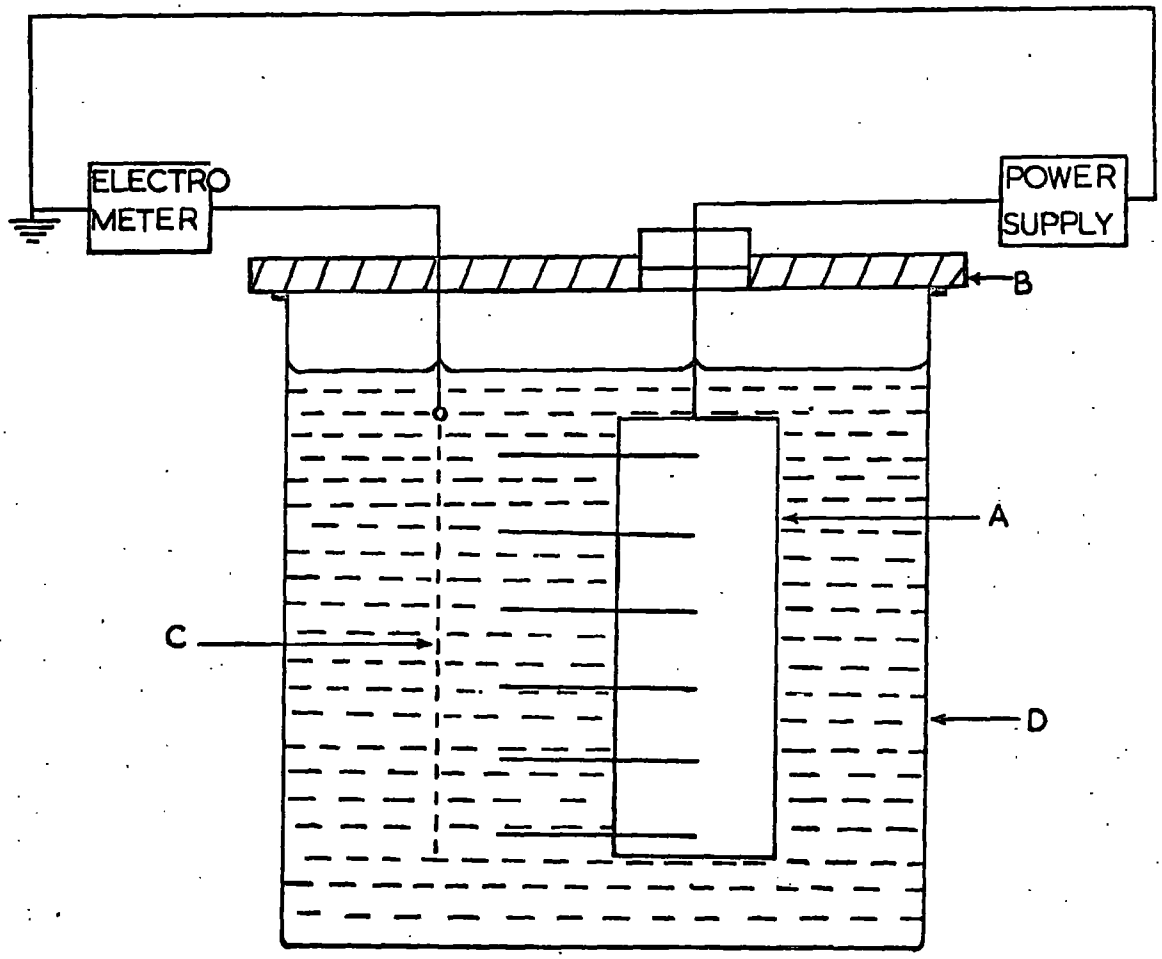

Figure 5.1 Showing the experimental arrangement for high field injection measurements. Electrode spacing 1 or 2 mm.

A PTFE beaker (D) of 100 ml capacity was used to house the electrode assembly. Hexane in the beaker completely immersed the electrode assembly. The Perspex disc reduced the evaporation of hexane during measurements. The 3 KV Dynatron power supply was connected to the emitter. For higher voltages it was replaced by a Hursant Model 50A power unit capable of supplying up to 50 KV of either polarity. Plate currents were measured with the Vibron Model 33C electrometer.

Field-injection was studied with hexane samples obtained from Koch-light laboratories and from Carless Capel & Leonard. The effect of removing the water and unsaturated compounds present in the hexane was observed by percolating the liquid through silica gel. Emitter-collector distance was also varied during the experiments.

5.1.2 Apparatus to give a low liquid flow rate

The effect of liquid motion on the charge injection, reported by earlier workers, was studied with the apparatus shown in Fig. 5.2. This apparatus was designed to give a maximum flow-rate of 20 cm/sec in the injection region. The liquid velocity was varied up to this value by changing the impedance of the flow tube.

The injector region of the apparatus is shown in Fig. 5.2(b). The emitter was an 8 mm length of razor-blade (A) (Personna & CO.). It was push-fitted into a narrow slot across a 5 cm long and 8 mm I.D. brass tube (B). The tube was made from 2.5 cm diameter brass rod, leaving a rounded shoulder in the middle into which a small hole was drilled for the H.T. connection. The inside of the tube was tapered at both ends to avoid eddy formation at the corners. The other electrode was a grid of 12 lines/cm spacing soldered on one end of a similar brass tube(C). The tubes were held together by a short

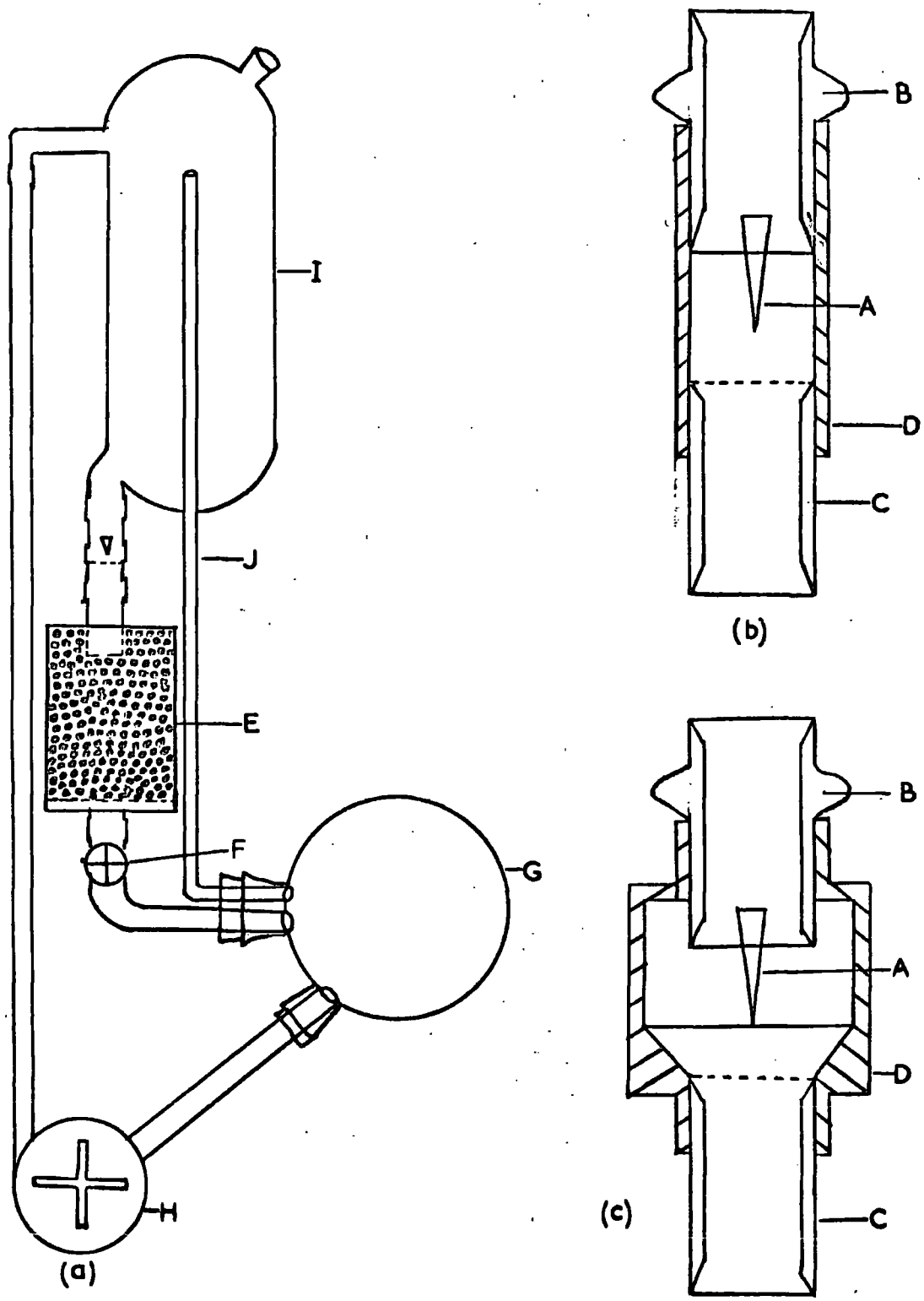

Figure 5.2 (a) Schematic diagram of the apparatus to give a low liquid flow. (b) and (c) The electrical assembly.

piece of PVC tube so that the grid faced the injecting tip (D). The emitter-grid distance could be fixed at any desired value.

The charge collector was based on the work of Hughes and Secker[86]. It was a cylindrical brass can (E) (12.5 cm Long and 5.2 cm I.D.) filled with 6 mm diameter phosphor-bronze balls. A perforated brass plate at the bottom of the can retained the balls but let the liquid through. The inlet tube was arranged to deflect the charged liquid radially outwards to come into contact with the greatest possible metallic surface acting as the charge scavenger. For efficient charge collection, the balls and the inside of the can were cleaned in acid and washed and dried before filling.

The outlet of the can was fitted with a grease free metal valve (F) which connected through a 250 ml round bottom flask (G) to the inlet nozzle of a diaphragm pump (H) (Capex MK2, Charles Austin Pumps Ltd.). To run the pump at maximum output, the flask was clamped in such a position that the inlet tube was always kept filled with hexane. Liquid from the outlet was lifted to a height of 67 cm through a copper tube into a glass reservoir (I). The reservoir had a capacity of about a litre and it was fitted with a funnel and a side tube at the top for filling. It was connected to the electrode assembly by another tube at the bottom. To give a constant volume of liquid in the reservoir, it was fitted with an overflow tube (J) directly connected to the flask (Fig. 5.2(a)). Connections to the inlet and outlet nozzles and other connections were made with short lengths of flexible PVC tube. The system was clamped to a frame with the pump fixed to the base. It was filled with hexane so that the volume in the reservoir remained steady when the liquid was flowing through the injector region at its maximum velocity. Care was taken to remove minute air bubbles trapped inside the collector before applying voltage to the emitter.

The flow-rate in the injector region was determined by measuring the outflow of liquid while establishing a continuous supply of hexane to the reservoir. The velocity remained constant when the level of hexane in the reservoir was kept to its maximum value by continuous pumping. The liquid velocity was decreased either by (a) setting the valve at a different position or (b) increasing the impedance of the flow tube by inserting brass spacers of reduced bore.

The conduction currents measured with the electrode assembly described above were relatively small. This was thought to be due to charge build-up on the walls of the PVC tube connecting the emitter and grid, which may have affected the electron emission. Moreover, after a few hours of use the PVC appeared to shrink with a gradual loss of its flexibility and change in colour. The contraction resulted in a reduction of the flow-rate in the injector region. To overcome this difficulty, the PVC tube connecting the emitter and grid holders was replaced by a simple coupling made from a 4 cm long, 2.5 cm diameter rod of PTFE (Fig. 5.1(c)). This was machined to give a large cavity around the electrodes which were fitted from each end. Thus the blade tip was well away from the cell walls and entirely surrounded with hexane. The end of the cavity in the PTFE near the grid was tapered to avoid eddy-formation from the corner. It was difficult to make leak-proof joints to the emitter and grid electrodes with the PTFE cell but this was overcome by cementing them with Araldite.

Negative voltages from a stabilized power supply were applied to the emitter. Grid currents were measured with the collector earthed and the total injected current was measured with the grid and collector connected together. Charge carriers not neutralized by the collector, transferred their charge to the metal tube at the pump outlet which was also connected

to the collector.

5.1.3. Apparatus to give a high liquid flow rate

Although the effect of liquid velocity on charge injection were observed in the above apparatus, the maximum velocity of only 20 cm/sec was not sufficient to reach any definite conclusion on saturation. A new apparatus capable of maintaining a liquid velocity of more than 2 m/sec in emitter-grid region was therefore devised with the liquid circulated by a centrifugal pump rather than flowing under gravity. It was essentially a closed loop made of 2 cm bore copper tube containing the electrode assembly charge collector, venturi-meter and pump.

The test cell part of the circuit is shown in Fig. 5.3. The emitter electrode was an 8 mm length of blade (A) spaced at a distance of 3 mm from a grid (B). As in the previous apparatus the blade was a push-fit in a brass tube 3 mm long (C). The grid (12 lines/cm) was soldered at one end of another brass tube of the same internal diameter (8 mm). The PTFE housing gave a uniform 8 mm bore with the blade and grid holders fitted at each end (E). The emitter-grid spacing was 3 mm. The ends of the PTFE housing were bored out to take neoprene O-rings to prevent leakage at the joints with the nozzles.

The test cell formed a constriction to give a fluid velocity four times greater in the injector region than in the main circulating system. The inlet (G) and outlet (H) nozzles of the cell were made from PTFE rod. The inlet nozzle was 4.4 cm long and tapered inside at an angle of 10^{o} to couple the 2 cm bore copper inlet tube to the blade holder of 1 cm bore. The outlet nozzle, about 7 cm long, similarly coupled the grid-holder to the outlet tube.

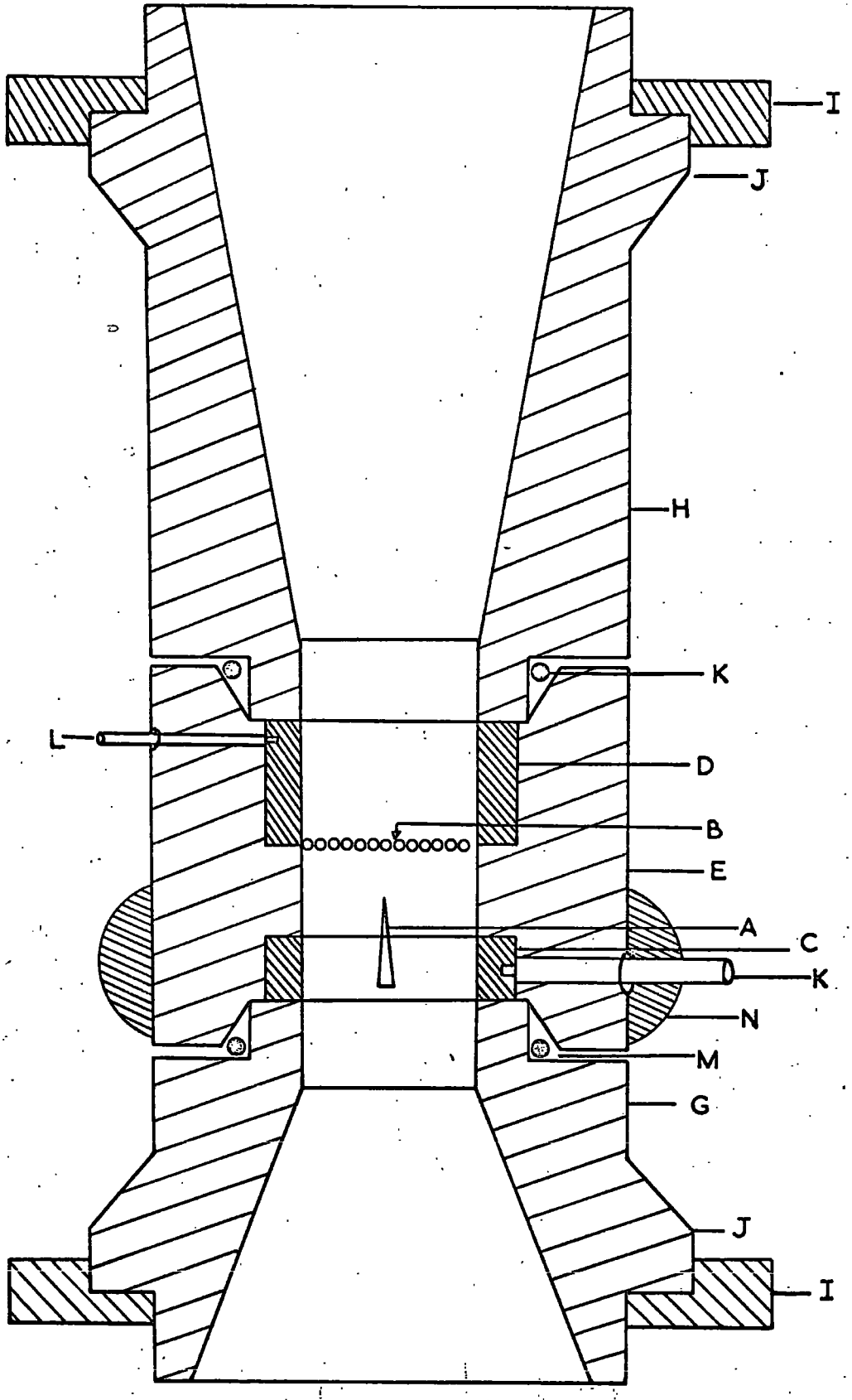

Figure 5.3 Flow Cell Assembly

To overcome the boundary effect[87] the inside taper of the outlet nozzle was made comparatively shallow, at an angle of 5^{o}. The nozzles, with the emitter-grid assembly in the middle, were held in position by Tufnol rings (I) against the nozzle shoulders (J) and screwed together with Tufnol rods. The ends of the cell were connected to the copper tubes by standard O-ring couplings.

Electrical connections to the emitter and grid holders were made by two small brass rods (K & L) screwed radially through the PTFE tube. Leakage of hexane through these connections was prevented with O-rings(M). The application of a high voltage to the emitter necessitated the use of a stress-distributing surface around the connector. This was a 1 cm wide brass ring (N) with rounded corners, fitted over the PTFE tube. The high-voltage connection to the emitter passed through the ring.

The charge collector was a brass can (12 cm long and 7 cm I.D.) filled with 6 mm diameter phosphor-bronze balls retained by a perforated plate. The can was tapered at both ends and Yorkshire bends of 2.5 cm and 1.9 cm were soldered to the inlet and outlet respectively. The inlet bend was soldered to the copper circulating system through a brass reducing section, while the outlet bend was connected to the inlet pipe of the circulating pump by a short length of plastic tube.

The complete system is shown in Fig. 5.4. A centrifugal pump (C.25, Charles Austin Pumps Ltd.) was used to circulate the liquid round the loop. The pump was driven by a variable speed motor. With the motor running to its maximum speed, the hexane reached a velocity of 3 m/sec in the emitter-grid region. The polypropylene impeller supplied with the pump was found to be unsuitable for pumping hexane and it was replaced by a brass one of the same

(a)

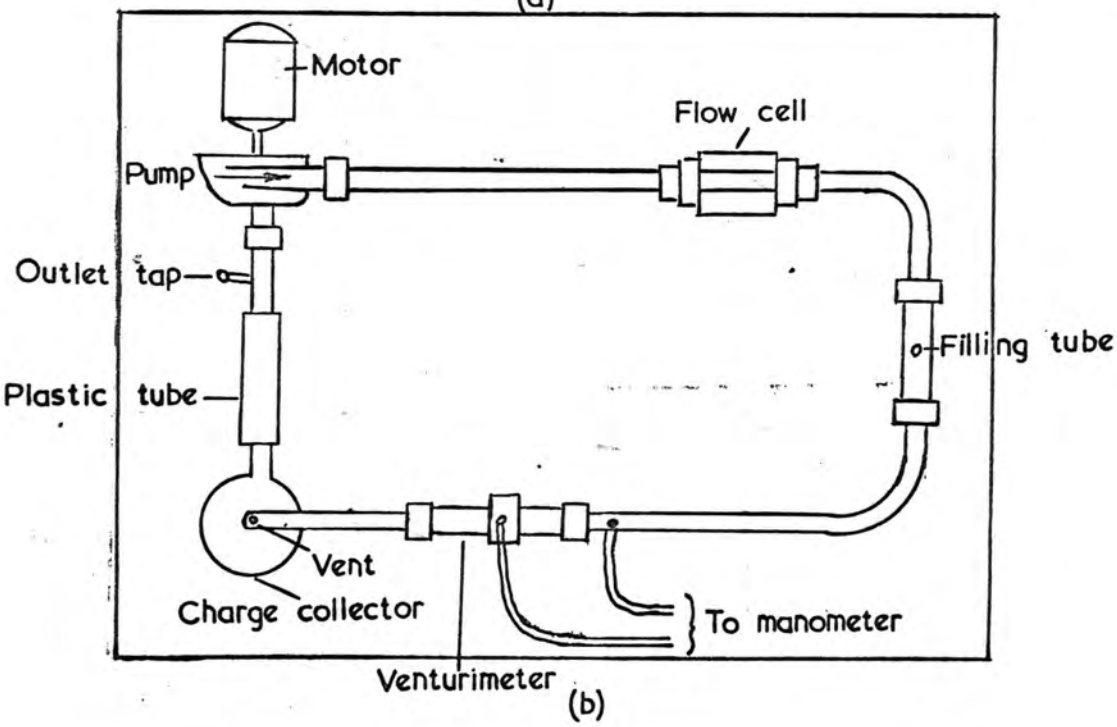

(b)

Figure 5.4 (a) The Photograph of the apparatus to give a high liquid flow
(b) Schematic diagram of the same

geometry. Connections to the pump were made with O-ring couplings.

To measure the liquid flow rate in the loop, a Venturimeter was placed in the system between the test cell and the charge collector. The Venturimeter was made from an 11.5 cm long, 3.5 cm diameter brass rod. The internal diameter was tapered from 2 cm diameter at the inlet to 1 cm at the throat, with an inclination of 10^{o}. A 1 cm long parallel section was followed by a gradual expansion to 2 cm diameter again, but with an angle of inclination of 5^{o} at this end. Glass manometer tubes with a moveable scale were connected separately to the inlet and throat of the Venturimeter by flexible plastic tubes. The difference in pressure between these two points was measured as the difference in the liquid levels in the two tubes. The liquid velocity (U) at the throat of the Venturimeter was calculated from[87]

$$U = \sqrt{\frac{2\,g\,dh}{\left(a^2/A^2 - 1\right)}} \qquad (16)$$

where dh is the difference between the meniscus levels and a and A are the cross-sectional areas at the throat and inlet of the Venturimeter respectively, g is the acceleration due to gravity.

A short length of glass tube was also included in the loop. Any gas bubbles in the liquid or cavitation resulting from a high flow rate within the system could easily be seen in this region. The system was filled through a small funnel connected to the glass tube. As this was at the highest point of the loop, it also acted as an effective exit for air bubbles.

Pressure build-up within the system was avoided by a small copper vent tube fitted to the collector. Streamline flow was achieved in the injector region by placing the test cell at a considerable distance from the pump outlet.

A tap was fitted at the lowest point of the loop to drain off the liquid after experiments. The capacity of the system was about 800 cc. The small loss of hexane due to vaporization from the vent and from the manometer was compensated by adding a few drops of hexane every half-hour.

All metallic parts of the loop were connected to the collector. Emitter, grid and total currents were measured. For the latter, the grid was also connected to the collector. A photograph of the apparatus is shown in Fig. 5.4.

5.1.4 Liquid treatment

The grades of hexane used in the field-injection measurements were (a) Puriss grade n-hexane obtained from Koch-Light Laboratories (Koch-Light n-hexane) (b) Laboratory reagent hexane obtained from Carless Capel & Leonard (CCL hexane) (c) hexane 'Special for Spectroscopy' obtained from British Drug Houses Ltd. (BDH hexane) and (d) General Purpose reagent hexane obtained from Hopkin and Williams Ltd. (HWL hexane). Solid particles of down to a micron size in these liquids were removed by filtering through a sintered glass disc fitted into a Pyrex tube (see Sec. 4.2.). Some field-injection measurements were carried out in the samples with no further treatment, but to find the effect on the conduction current of unsaturated compounds, including water, some of the hexane was passed through a column of silica gel (Sec. 4.2).

Laboratory grade hexane contains a large number of impurities including water vapour absorbed from the atmosphere. The effect of water on the conduction current was thought to be due to ionisation of the water molecules. It was therefore considered necessary to dehydrate most of the samples before carrying out any measurements, and this was done with metallic sodium.

Chips of sodium cut from a rod were put into a clean and dry bottle before filling it with hexane. After a few hours the dried liquid from the bottle was decanted and small pieces of sodium hydroxide were removed by filtration. As will be shown in Sec. 5.2, the conduction measurements with this liquid showed no effect of liquid velocity. To confirm that only the ionic component of the conduction current was dependent on liquid motion, a few drops of water was added to dehydrated hexane. The water solubility in hexane is only 100 ppm at room temperature[12] and the rate of solution was enhanced by stirring the mixture for a few hours with a magnetic stirrer. The water-saturated sample was decanted from the top of the mixing bottle. It gave a fluctuating conduction current which was thought to be due to minute droplets of water. The fluctuations were partly overcome by filtration of the liquid.

Alcohol served as an effective dopant[14] for hexane as it is miscible with hexane in all proportions. The hexane obtained from the supplier was first dehydrated as mentioned above. It was then filtered and ethyl alcohol (BDH 99-100% Alcohol) was added to obtain the desired concentration. The dried and doped hexane was kept in a well stoppered bottle before use. The low field conductivity of the doped samples was measured with a Mullard parallel plate conduction cell.

5.1.5 Charge collection

Charge carriers in a liquid in contact with a metallic surface might be expected to transfer their charge to the metal, provided that the electron energy in the carrier is greater than the Fermi energy of the metal. In practice, however, charge transfer is inhibited by the naturally occurring oxide films on metal surfaces which act as blocking layers, and it is found

that it is extremely difficult to remove charges from a flowing stream of insulating liquid.[86] Collection of charges from a flowing liquid is aided by decreasing the liquid flow velocity within the collecting region, so that the carriers are brought into close contact with the metal surfaces for longer periods of time. For a high collection efficiency, the collector metal must also be clean and of large surface area.

In the present experiments 6 mm diameter phosphor-bronze balls were used for charge collection. A cylindrical brass can filled with 1400 clean balls provided a large surface area. The can was seven times the diameter of the injection region so that a considerable decrease in the fluid velocity was achieved within the collector. The tortuous path for liquid flow between the balls also gave the charge carriers the greatest possible chance of coming into contact with the metal surfaces for the transfer of their charges. The various pieces of copper tube forming the circulating loop were also connected to the can and provided more surface area for charge scavenging. A charge collection efficiency of up to 100% was achieved with this arrangement.

5.2 Results

This section describes the conduction measurements made with razor-blade edges as high-field emitters. The experimental arrangements usually required a large quantity of hexane and a comparatively cheap grade was used except in the preliminary experiments which used Koch-light hexane. CCL hexane used in earlier measurements was considered unsuitable as an experimental liquid because of its high impurity content and it was substituted by HWL hexane. Measurements with BDH hexane showed very little difference in the current magnitudes, compared with those of HWL hexane and most of the later measurements were therefore undertaken using the latter. The liquid was

generally dried with sodium and was, in most cases, doped with alcohol for the conduction measurements. Water was used as a dopant for some measurements but was not ideal as it gave rise to current fluctuations.

The most important results obtained with the different sets of apparatus are presented in chronological order. The following measurements were taken:-

(a) The emitter current with both grid and collector connected together.

(b) The grid current with collector earthed.

(c) The flow current as the increase or decrease in the emitter current due to liquid flow in the injector region.

5.2.1 The I-V curves for high-field injection

Preliminary field-injection measurements were made with the simple six-blade assembly described in Section 5.1.1. The spacing between the blade tips and the plate electrode was one or two mm. The variation of the plate current with emitter voltage for Koch-light hexane is shown in Fig. 5.5. With an electrode spacing of 2 mm the conduction current in an untreated sample reached 3.5×10^{-8} A for an applied voltage of 3.3 KV (curve A).

To find the effect of water in the hexane, the sample was dried by one pass through a column of silica gel (Sec. 4.2.2) and curve B shows the result which was a reduction in the conduction current to one third of its previous value. This current was increased by a factor of four on decreasing the emitter-plate distance to 1 mm (curve C). A polarity reversal experiment showed a slight decrease in the conduction current for a positive voltage on the blades (Fig. 5.6).

The next measurements used higher applied voltages and the plate electrode was replaced by a grid of 12 lines/cm mesh size. A large increase in the current was observed although it is not possible to show comparative

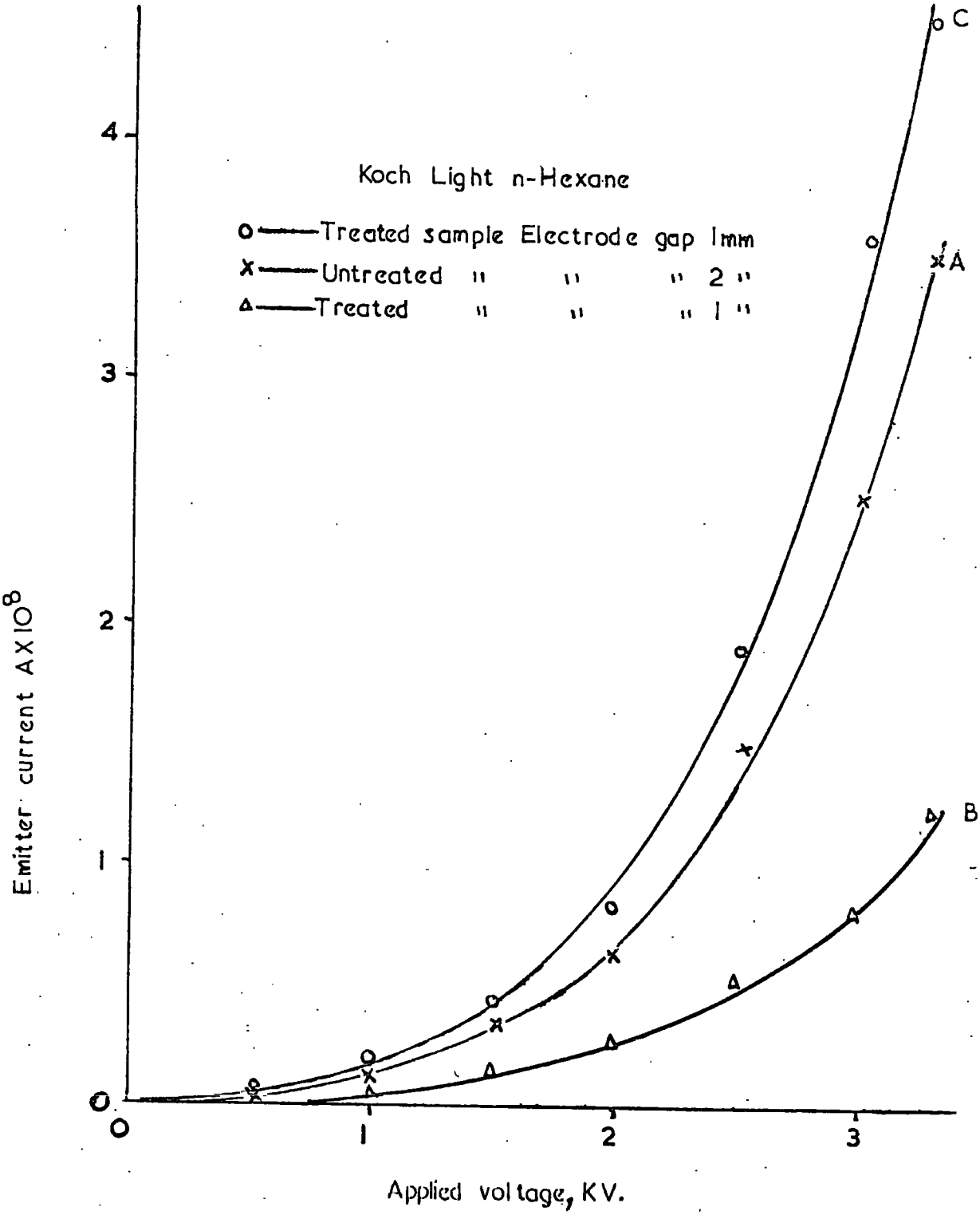

Figure 5.5 Variation of emitter current with applied voltage for an array of six blades in Koch-light n-hexane. Blades are cathode.

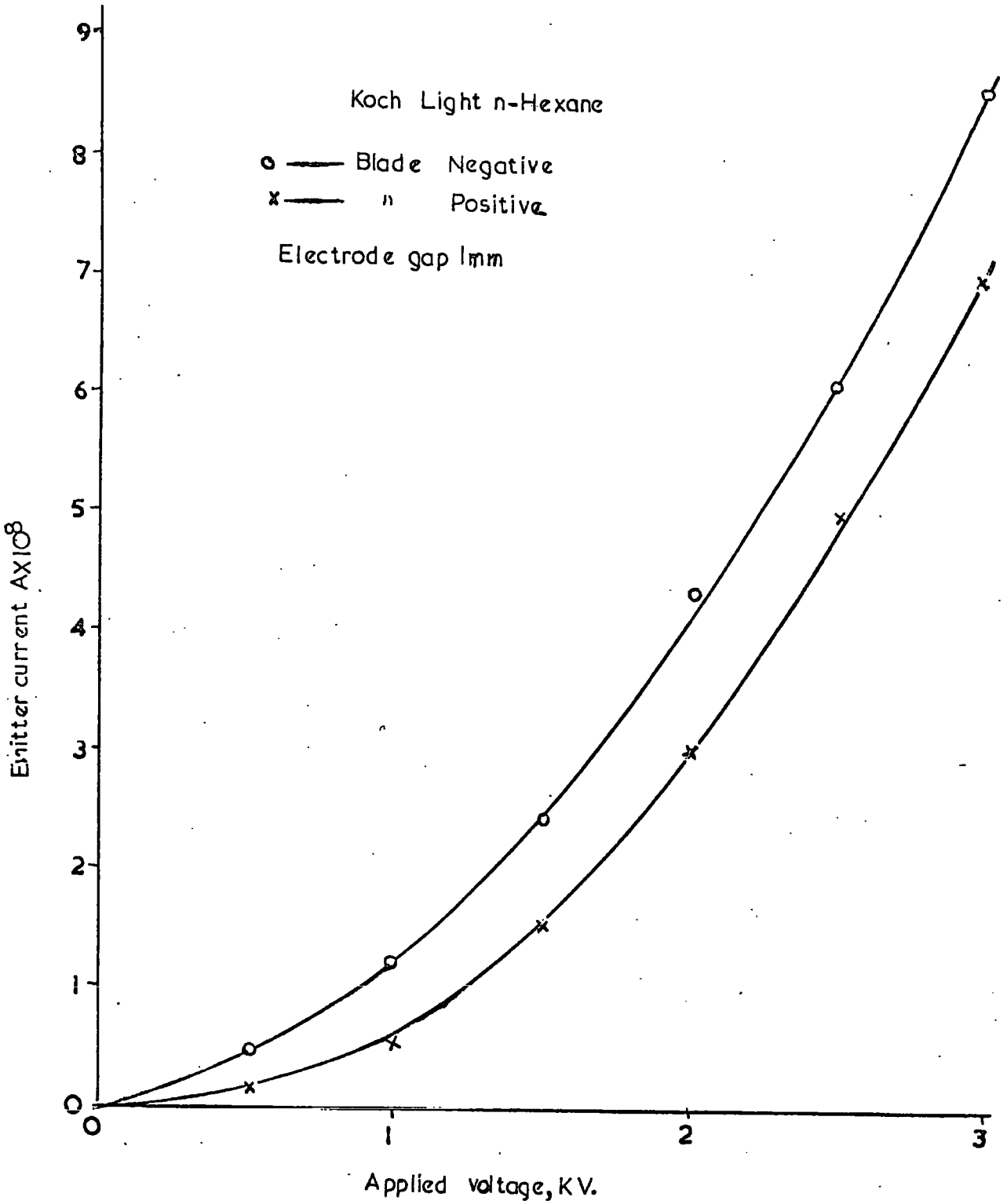

Figure 5.6 Showing the effect of polarity on emitter current from six blades to a plate electrode.

points on the graphs (Fig. 5.7 compared with Fig. 5.6). The current was of the order of microamps for an applied voltage of 6 KV and it reached 22 microamps at 10 KV for an emitter-grid distance of 1 mm (Fig. 5.7, curve A). The current decreased on drying the liquid as shown in Fig. 5.7, curve B, which agrees with the earlier measurements using a plate anode. CCL hexane gave a higher conduction current, curve C, probably because of its higher impurity content. A current of a microamp was obtained for only 2 KV and this increased to 30 μA at 10 KV.

The increase in the conduction current with voltage in all these cases showed an upward trend throughout the range of applied voltage. Beyond a certain threshold voltage the current increased at between the third and fourth powers of the applied voltage. Fluctuations in the conduction currents were well within 10% of the measured values, being less in the Koch-light than in the CCL hexane.

5.2.2 Effect of slow liquid flow on conduction current

The large increase of the conduction current with the grid anode suggested that the liquid flow might greatly affect the charge injection. To investigate this further, the first flow apparatus described in Sec. 5.1.2 was built. The emitter was now a single piece of razor-blade with a spacing of the order of a few mm to a grid electrode, beyond which was a charge collector. Negative voltages of up to 20 KV were applied to the emitter.

The variation of grid current with applied voltage in the steady liquid is shown in Fig. 5.8. This curve is similar to the previous measurements except that the magnitude of the current is almost two orders less than was obtained with the assembly of six blades.

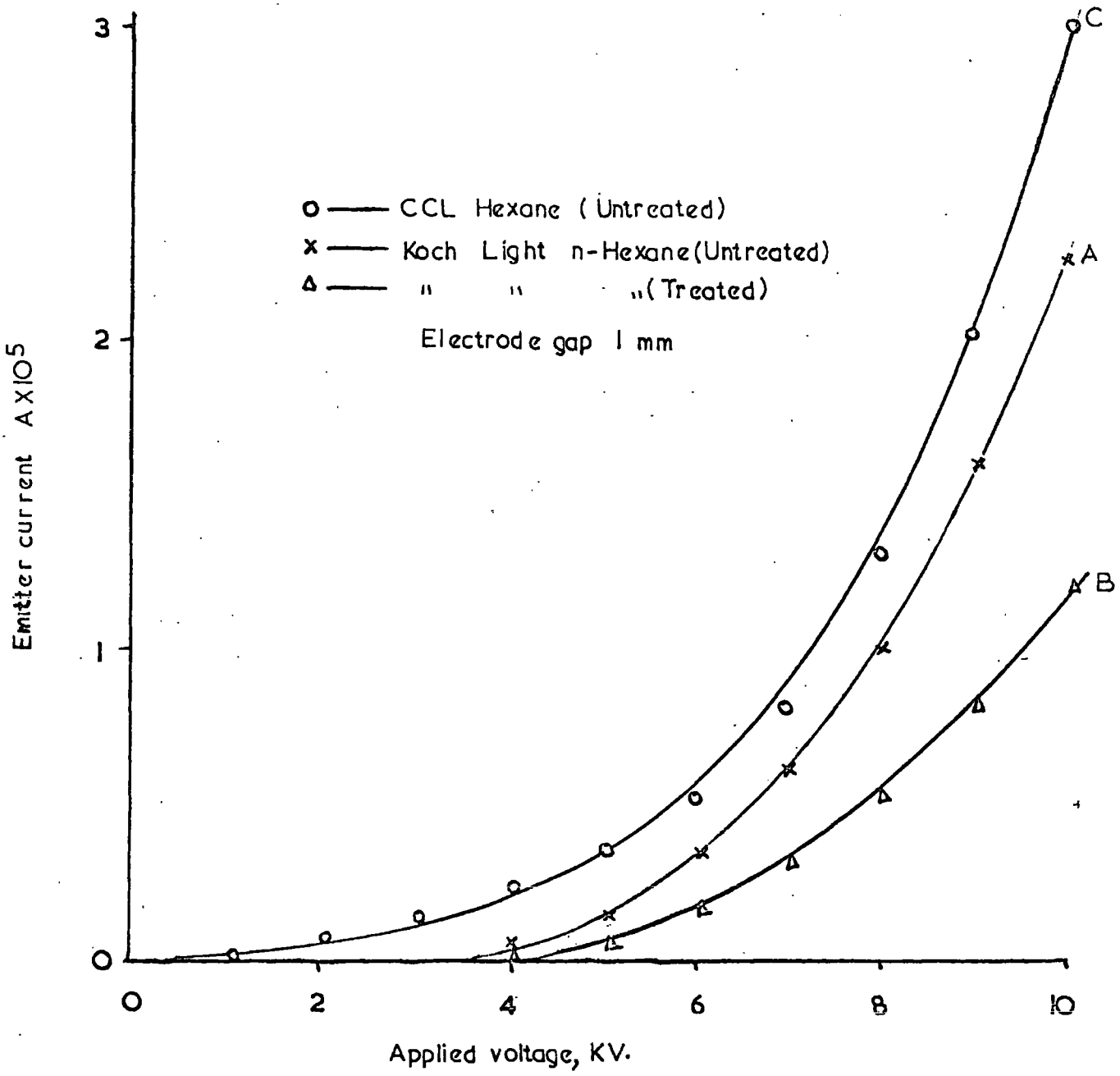

Figure 5.7 Showing the effect of different grades of hexane on emitter current from six blades to a grid anode.

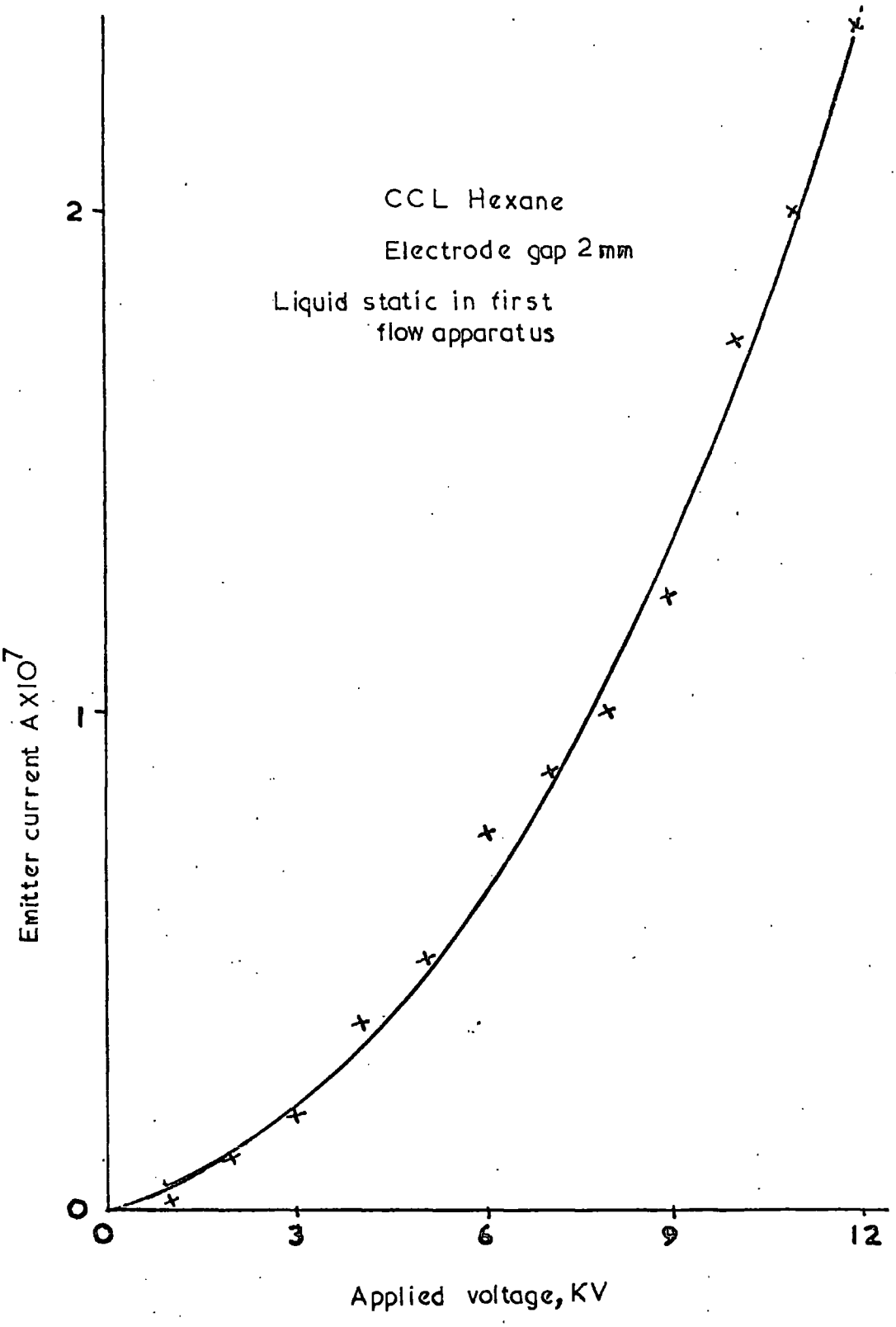

Figure 5.8 Variation of grid current with applied voltage for static liquid.

Measurements were made with the liquid flowing slowly as controlled by the valve below the cell. The pump maintained a constant head of liquid in the reservoir. The relation between emitter current and liquid velocity is shown in Fig. 5.9. In the flowing liquid the current was erratic and fluctuations of more than even 100% were observed. For applied voltages below 5 KV, the current was very small. With higher voltages the current increased rapidly to higher values than in the static liquid. As the velocity of the liquid was increased, the conduction current showed a steady increase up to about 10 cm/sec. This was followed by a decrease in the emitter current for higher flow-rates. As opposed to this the grid current decreased steadily with increase in liquid velocity as shown in Fig. 5.10. The grid current also fluctuated less than the emitter current. For a high liquid velocity (about 20 cm/sec) the grid current was about half the value in the steady liquid.

Because of the high impurity content of CCL hexane the next measurements were carried out in HWL hexane dried and filtered before use. The variation of the grid current for such a sample is shown in Fig. 5.11. The currents decreased with liquid velocity in a similar way to those in CCL hexane. On the other hand, the total current in this liquid was the same as in the steady liquid and was independent of flow-rate. This was a very important result which indicated that the increase of current with flow is due entirely to impurities. It meant that the effect of impurities on the flow-current became the main line of investigation in this work.

The static current was measured in this apparatus for various electrode spacings. The emitter current reached a value of the order of microamps for an applied voltage of 20 KV across an emitter-collector spacing of 3.5 mm and

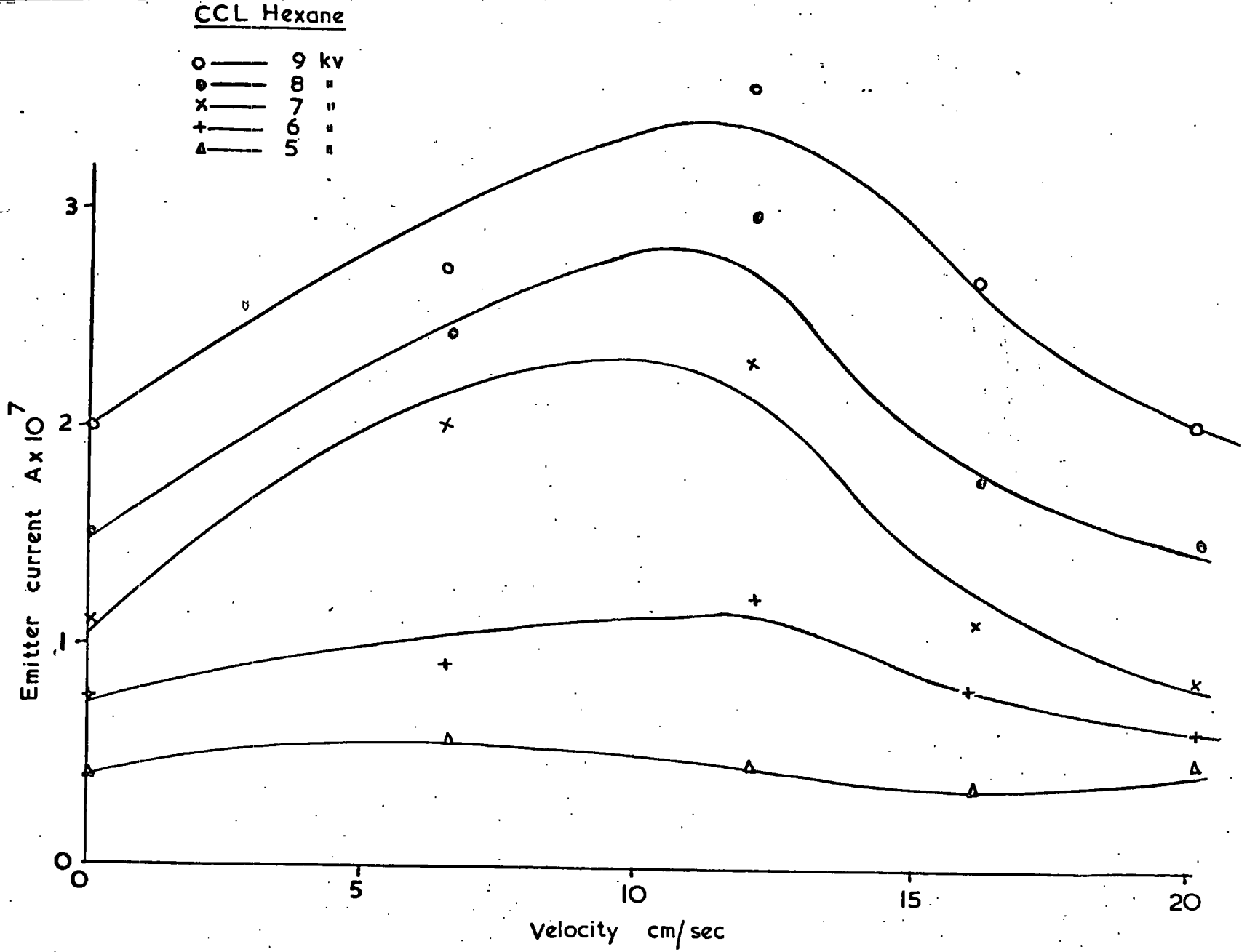

Figure 5.9 Initial results on the variation of emitter current with liquid velocity for different applied voltages.

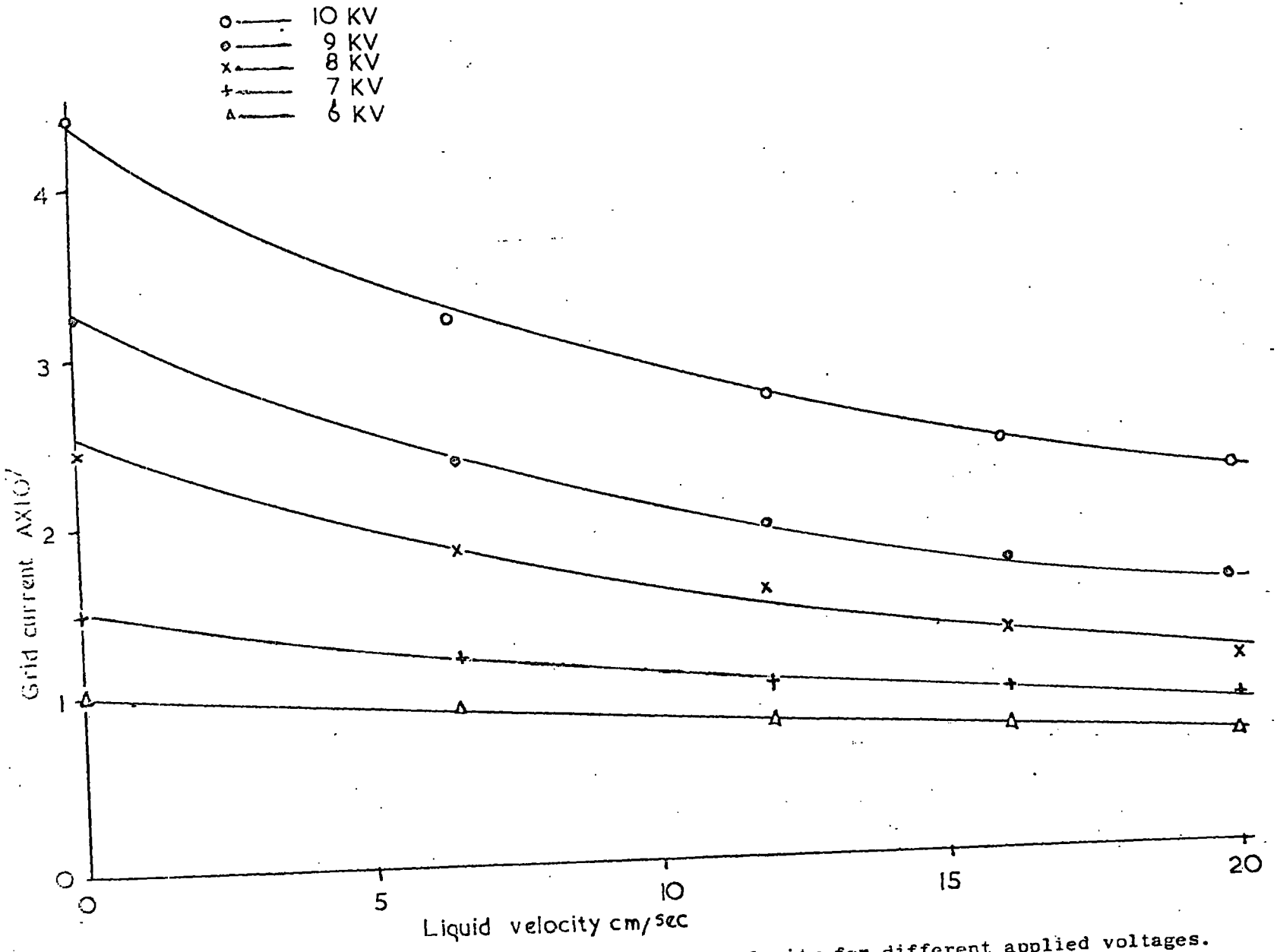

Figure 5.10 Variation of grid current with liquid velocity for different applied voltages. Same conditions as in Fig. 5.9, but not directly comparable.

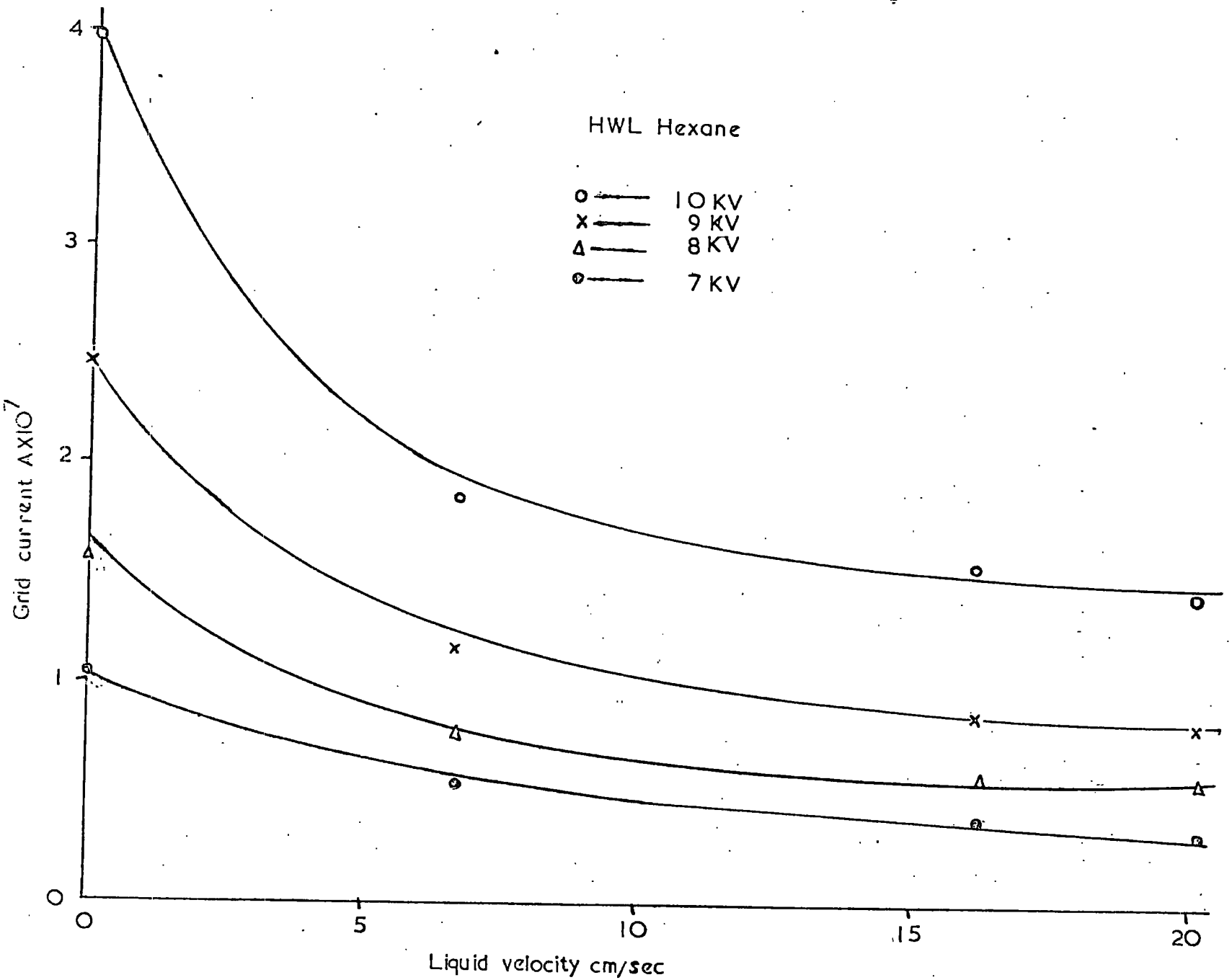

Figure 5.11 Variation of grid current with liquid velocity for different applied voltages. Same conditions as in Figure 5.9, except for HWL hexane

it showed no sign of saturation with higher voltages (Fig. 5.12, curve A). With smaller emitter-grid distances the conduction current was much greater for a given voltage probably because of the increased grid-emitter field. With an applied voltage of 20 KV, the emitter current was 4 μA (curve B) and 7.8 μA (curve C) for emitter-grid distances of 2.5 mm and 1.5 mm respectively.

Due to some inconsistencies in the measurements it was thought desirable to reduce the proximity of the cell walls and the PVC tube joining the emitter and grid was replaced by the enlarged PTFE cell shown in Fig. 5.2(c). The emitter-grid spacing was kept fixed at 3 mm. Static measurements were first made in CCL hexane as shown in Fig. 5.13, curve A. The more pure HWL hexane gave the considerably smaller currents shown in curve B. The magnitudes of the currents were almost the same as those obtained with the PVC tube as the emitter-grid connector. The same hexane, saturated with water, showed a sharp increase in the current, particularly below 12 KV, as shown in curve C, although the difference gradually became less at higher voltages. The currents measured in the water saturated HWL hexane showed large fluctuation and the currents closely resembled those in CCL hexane (compare curves C and A). When the water saturated HWL sample was filtered the current decreased again as shown in curve D. This was accompanied by a considerable decrease in the current fluctuations.

The effect of liquid flow on the conduction current in the hydrated HWL sample is shown in Fig. 5.14. The results are similar to those observed in CCL hexane earlier (Fig. 5.9). To obtain measurements in hexane with a water content below the saturation level, a range of mixtures was made of dried and water saturated samples. The water content is thus specified relative to the saturation value at room temperature. The effects of water concentration

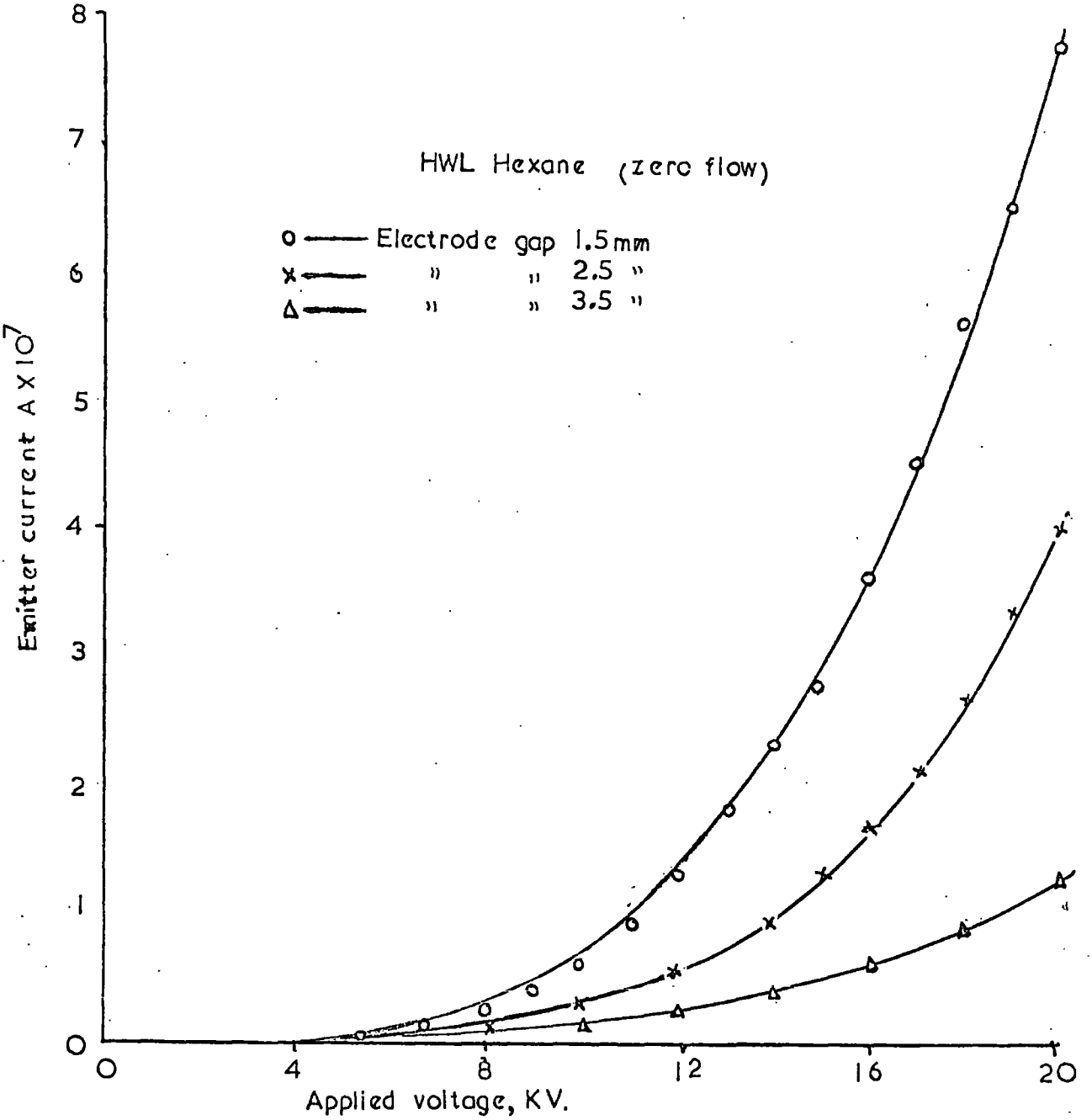

Figure 5.12 Variation of emitter current with applied voltage for different electrode spacing for HWL hexane and zero flow.

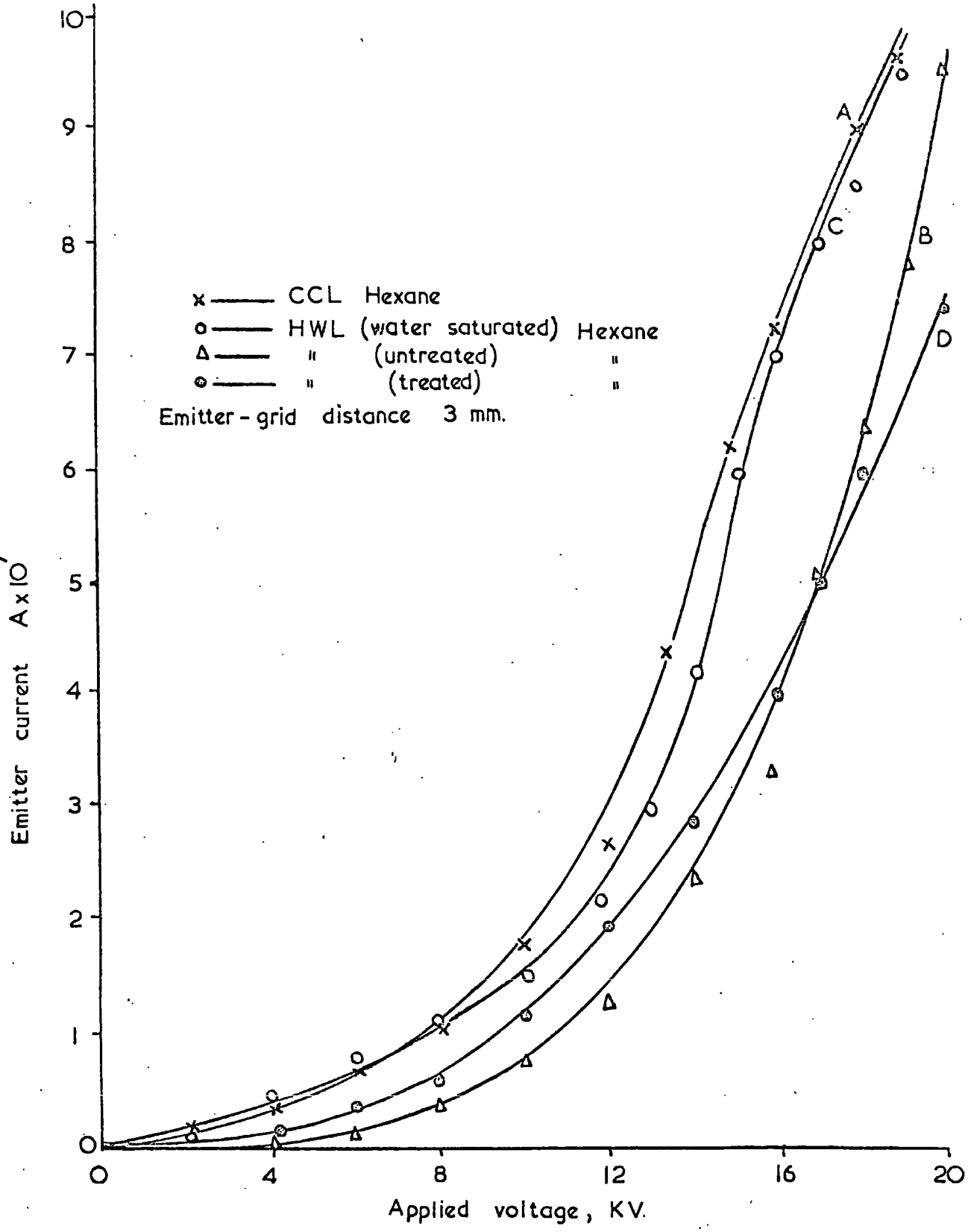

Figure 5.13 Showing the effect of impurity on emitter current with PTFE cell

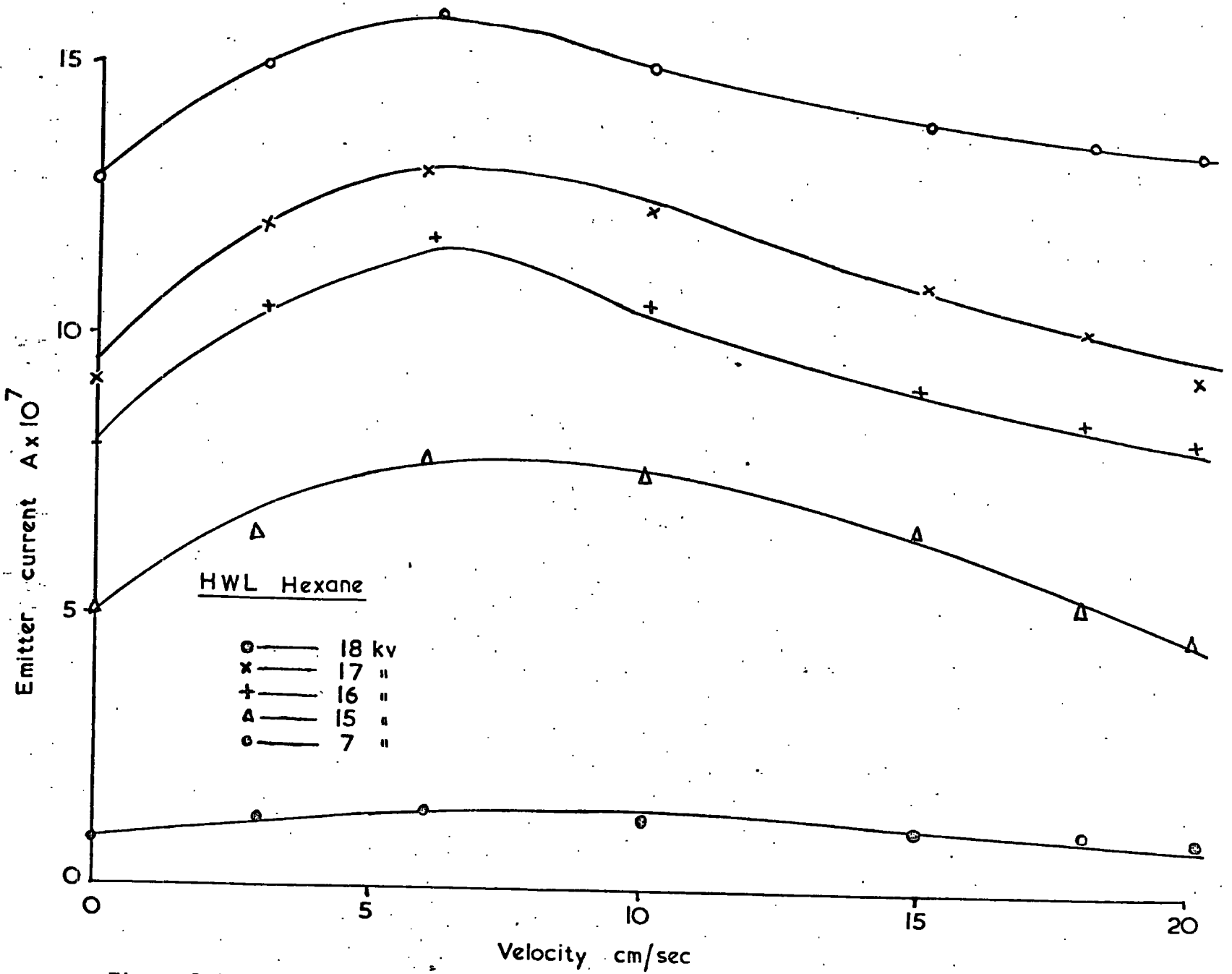

Figure 5.14 Variation of emitter current with liquid velocity in hydrated HWL hexane.

on the static and flow current in HWL hexane are shown in Figures 5.15 and 5.16 respectively. Both the currents are shown to increase with increase of water concentration,

The increase in the current with liquid velocity observed in CCL and hydrated HWL hexane led to the idea of doping hexane with something more suitable. Water is not readily soluble in hexane and there is difficulty in separating minute water globules from the saturated liquid. Alcohol, being miscible with hexane in all proportions, was selected as a much more suitable dopant that might show similar effects. The BDH hexane used in these measurements was dried before doping to the required concentration with 99 - 100% Ethyl alcohol (BDH).

The increase in the conductivity of hexane with alcohol doping,[14] gave a marked increase in the emitter current. A concentration of 1% by volume increased the current by nearly one order of magnitude with a steady rise beyond this up to the maximum concentration used, 8%. The I-V curves (Fig. 5.17) are of similar shape for each doping level. To measure the effect of alcohol concentration on the flow-current, a steady velocity of 10 cm/sec was maintained in the injector region for each doping level. The curves of Fig. 5.18 show the variation of flow-current with dopant concentration for fixed applied voltages. Although the currents continue to increase with alcohol concentration, they show a clear sign of saturation at the higher levels.

The effect of liquid velocity on the flow current was measured by varying the flow-rate in the injector region using hexane with an alcohol concentration of 4%. The relation between flow-current and liquid velocity is shown in Fig. 5.19. The curves rise initially but there is a drop in the flow-current at higher liquid velocities at low voltages.

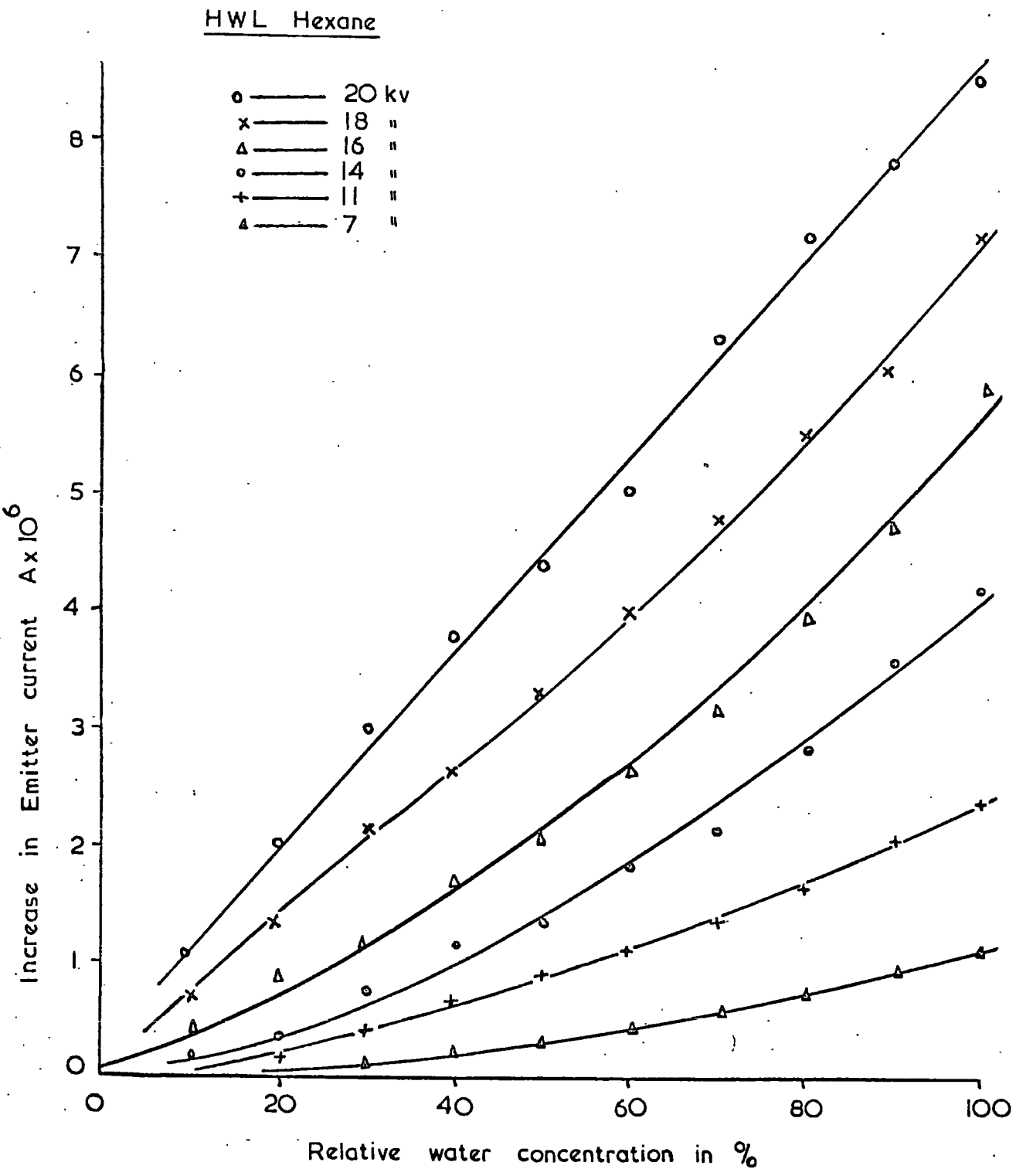

Figure 5.15 Increase in emitter current with water content in HWL hexane and zero flow.

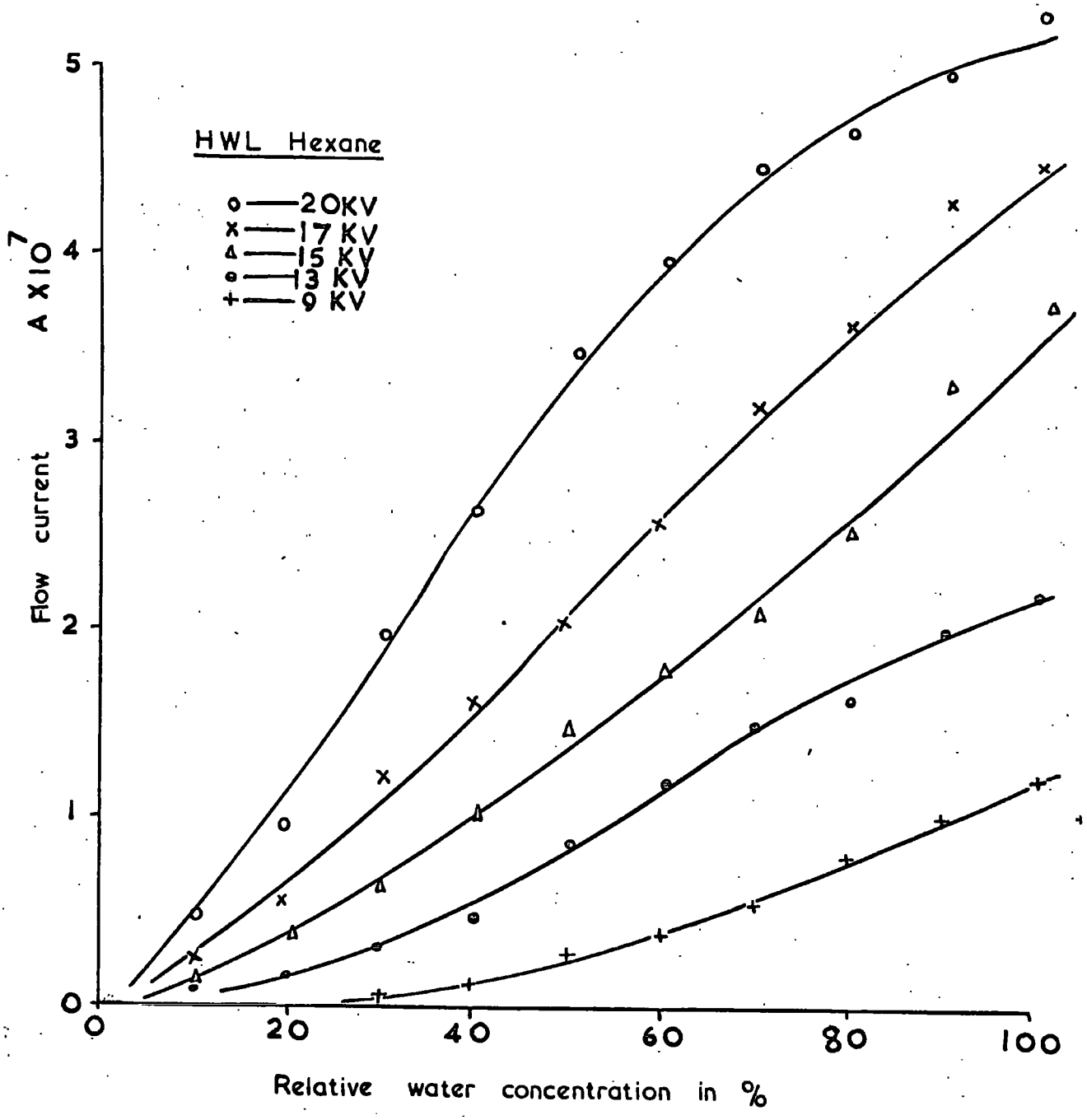

Figure 5.16 Variation of flow current with water content in HWL hexane. The liquid velocity = 10 cm/sec.

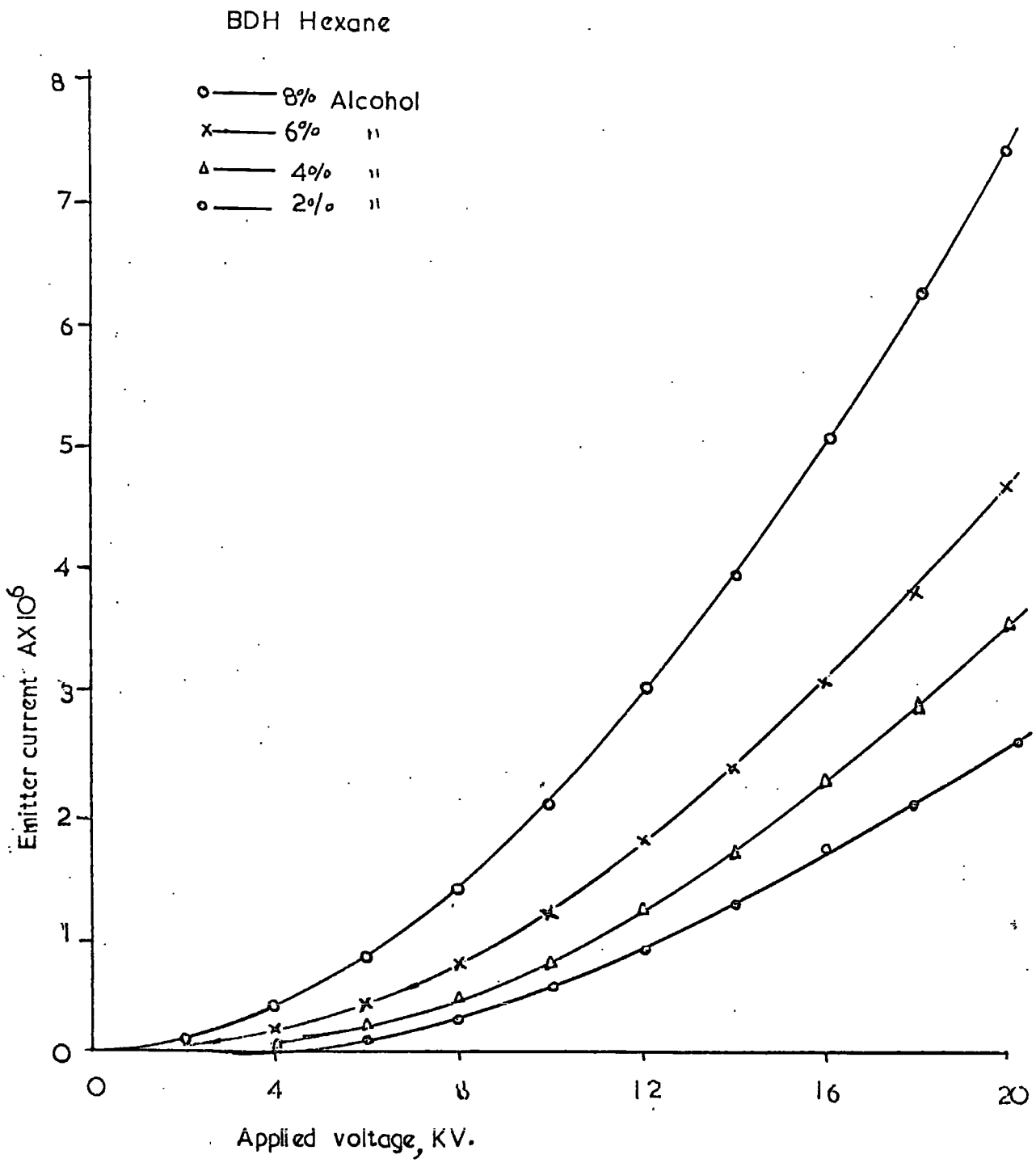

Figure 5.17 Variation of emitter current with applied voltage in static liquid for different doping levels in BDH hexane.

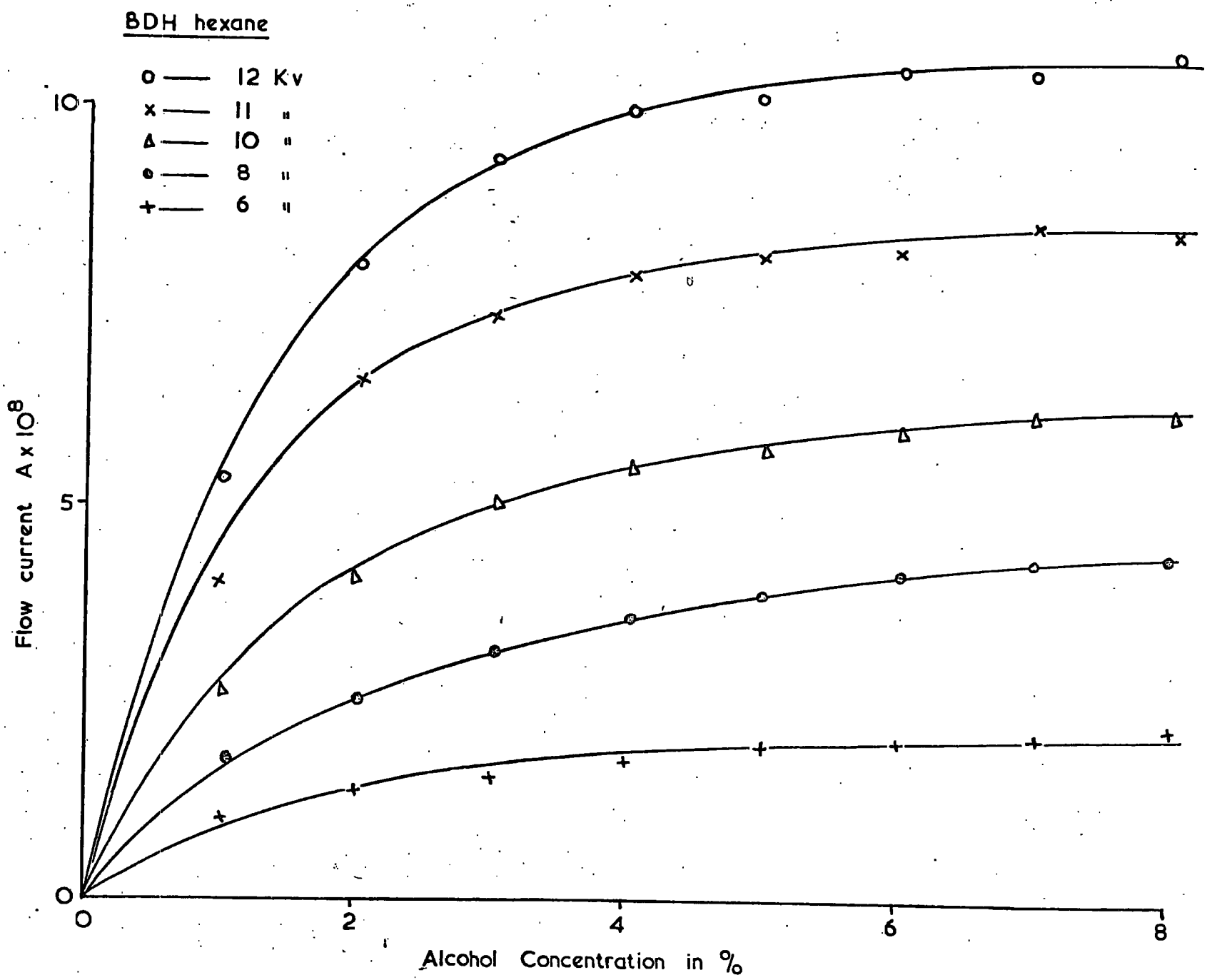

Figure 5.18 Variation of flow current with alcohol concentration in BDH hexane. The liquid velocity = 10 cm.

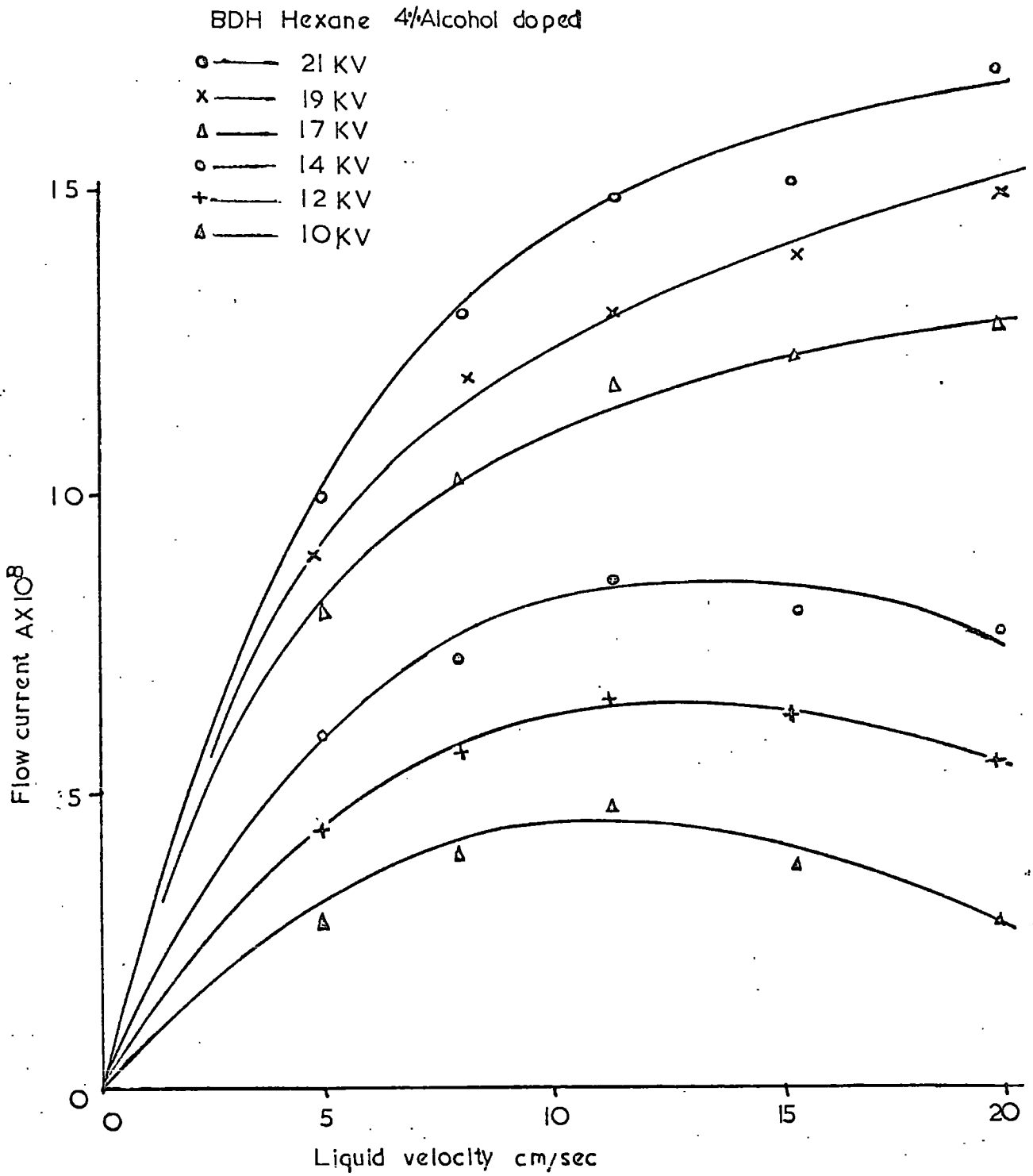

Figure 5.19 Variation of flow current with liquid velocity in BDH hexane, 4% alcohol doped.

The most important results with alcohol were the increase of the d.c. current and the reduction in the fluctuations, which made measurements much easier. For this reason all subsequent work used alcohol doping as a representative impurity.

5.2.3 Effect of fast liquid flow on conduction current

The results of the previous experiment showed an increase in flow-current with liquid velocity for the higher voltages. The slight decrease at the higher velocities below 15 KV was thought to be due to a change in the flow-pattern around the grid. An apparatus capable of maintaining a steady flow in the injector region up to a higher flow velocity was therefore devised as described in Sec. 5.1.3. The emitter and grid were basically the same as in previous experiment and were spaced at a distance of 3 mm. However, the flow into and out of the injector region was arranged to be more nearly streamlined as shown in the diagram of the cell (Fig. 5.3). The inclusion of the cell in the continuous circulating system enabled a high velocity smooth flow to be achieved.

Dried and filtered HWL hexane was used for the first experiment with the new system. The static conduction currents in pure and 1% alcohol doped samples are shown in Fig. 5.20 which are similar to the previous. However, Fig. 5.20 also shows the effect of polarity reversal, which is a considerable reduction in the conduction current. At lower voltages (< 4 KV) the currents were very small and almost equal for both polarities. At higher voltages, the currents with the blade negative were much higher than those with the blade positive. The ratio of the currents with the blade negative to the blade positive was 4 and 3 in the pure and doped hexane respectively.

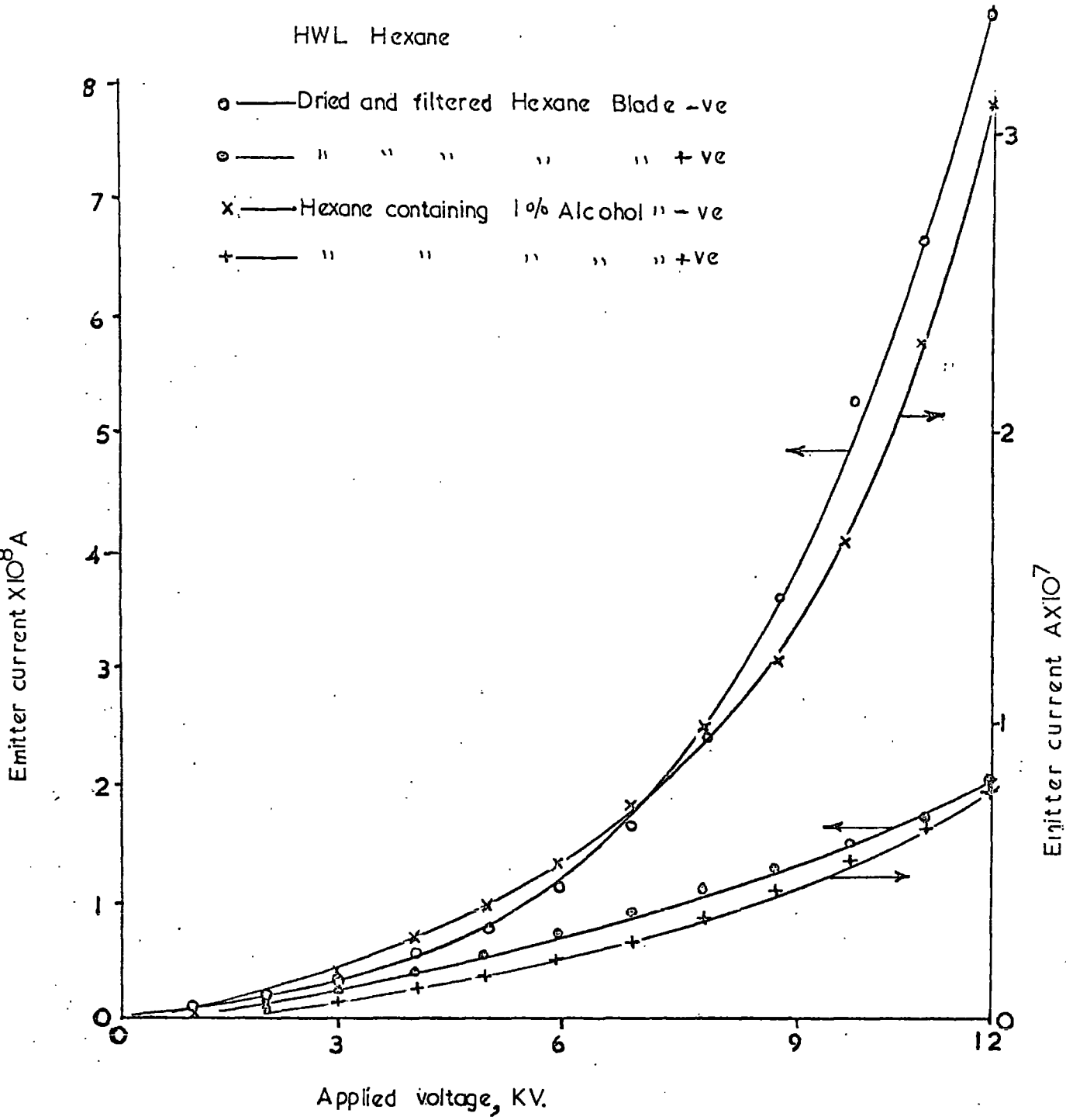

Figure 5.20 Showing the effect of impurity and polarity on static emitter current in circulating system.
Electrode gap = 3 mm

Later measurements were carried out in liquids with the doping level varied between 4% and 0.1%. The flow-currents were measured up to a liquid velocity of 2.6 m/sec which still gave an almost steady difference in the pressure heads of the Venturimeter. Also there was no sign of cavitation at the highest velocity.

The variation of the flow-current with liquid velocity in a sample containing 4% alcohol is shown in Fig. 5.21, where the maximum flow-rate is now ten times greater than in the earlier apparatus. The measurements were taken by increasing the velocity in steps of 20 cm/sec up to 2.6 m/sec. The current increased continuously with velocity and with the voltage across the emitter-grid region. At the higher voltages, measurements were limited by sudden spark discharges from the razor-blade tip and values higher than 15 KV resulted in high current pulses leading to breakdown of the gap.

To find the effect of the doping level, the alcohol concentration was decreased in the subsequent experiments. Fig. 5.22 shows the relationship between flow current and liquid velocity in a sample containing 2% alcohol. The current at a fixed applied voltage showed a reduction of about 25% compared to those in hexane with 4% alcohol content. A further decrease in the current was observed by reducing the doping level to 1% (Fig. 5.23) at which the current saturated at the higher liquid velocities. To see the reproducibility of the results, the same measurements (shown in Fig. 5.23a) were repeated after taking the apparatus to pieces and reassembling. The saturation was earlier with lower doping levels as shown in Figures 5.24 and 5.25, which are for 0.5% and.1% alcohol concentrations. The flow-current saturated at velocities as low as one meter/sec in the latter case. Decreasing the alcohol concentration decreased the conduction current and with

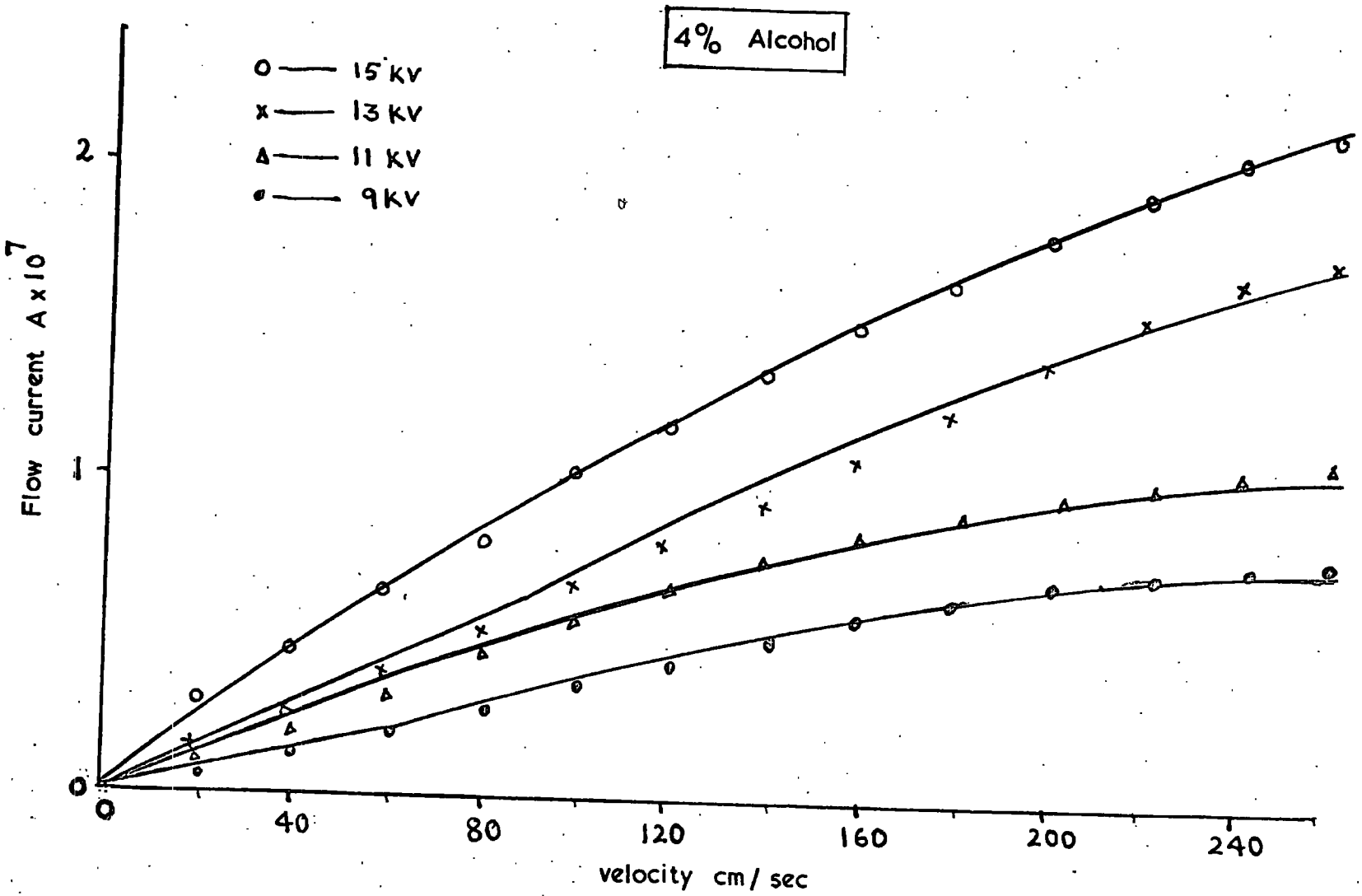

Figure 5.21 Variation of flow current with liquid velocity in 4% alcohol doped HWL hexane

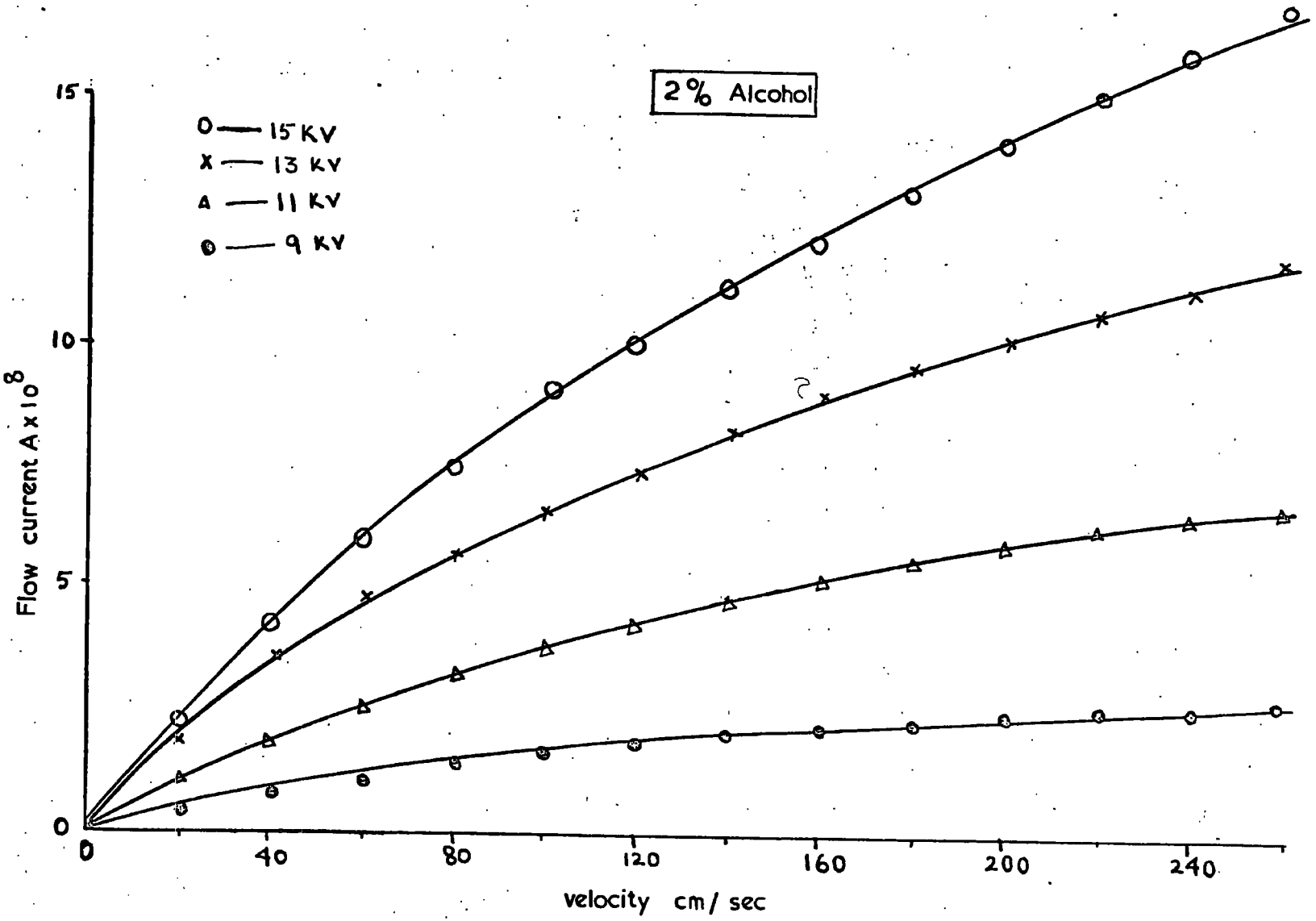

Figure 5.22 Variation of flow current with liquid velocity in 2% alcohol doped HWL hexane

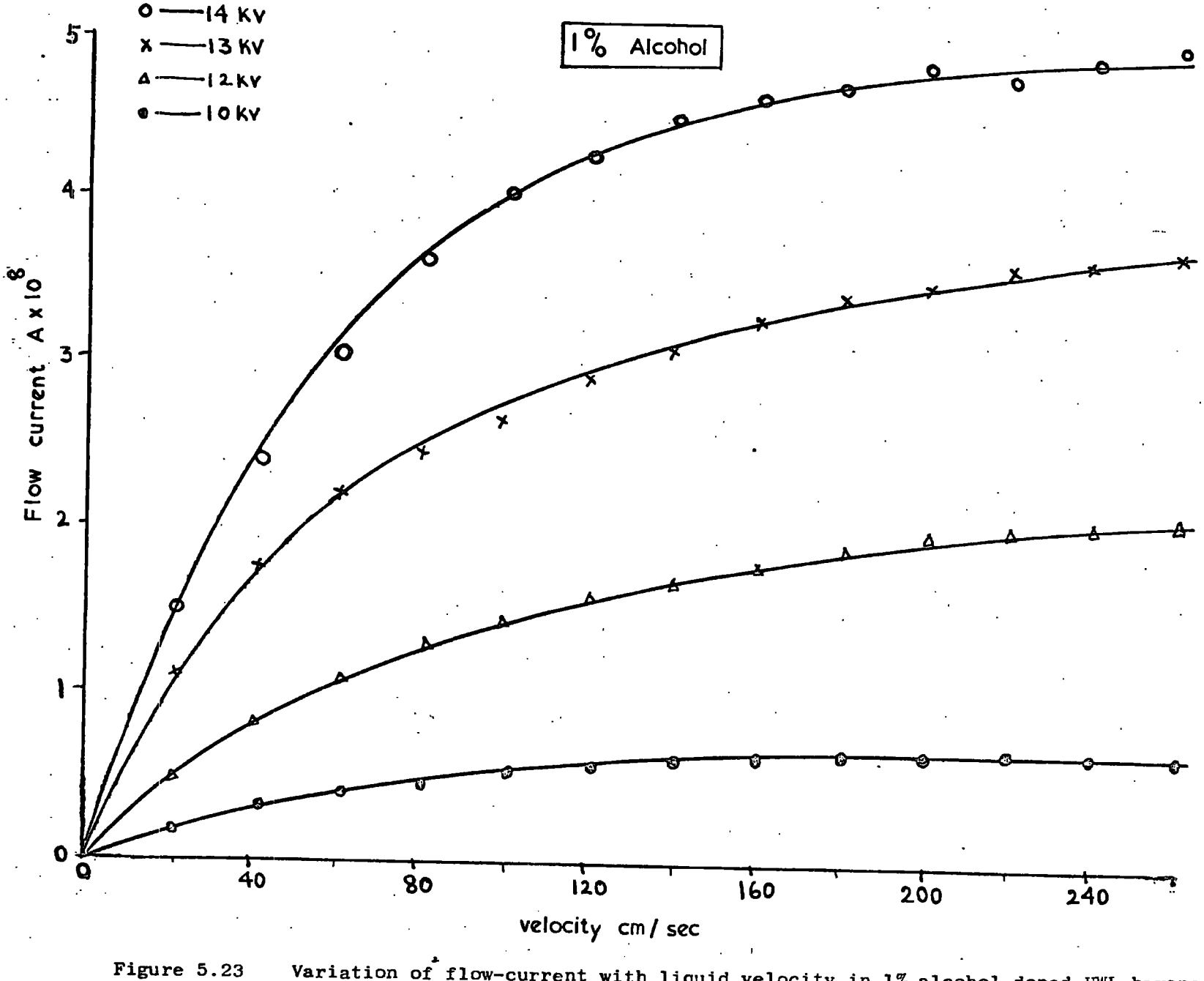

Figure 5.23 Variation of flow-current with liquid velocity in 1% alcohol doped HWL hexane

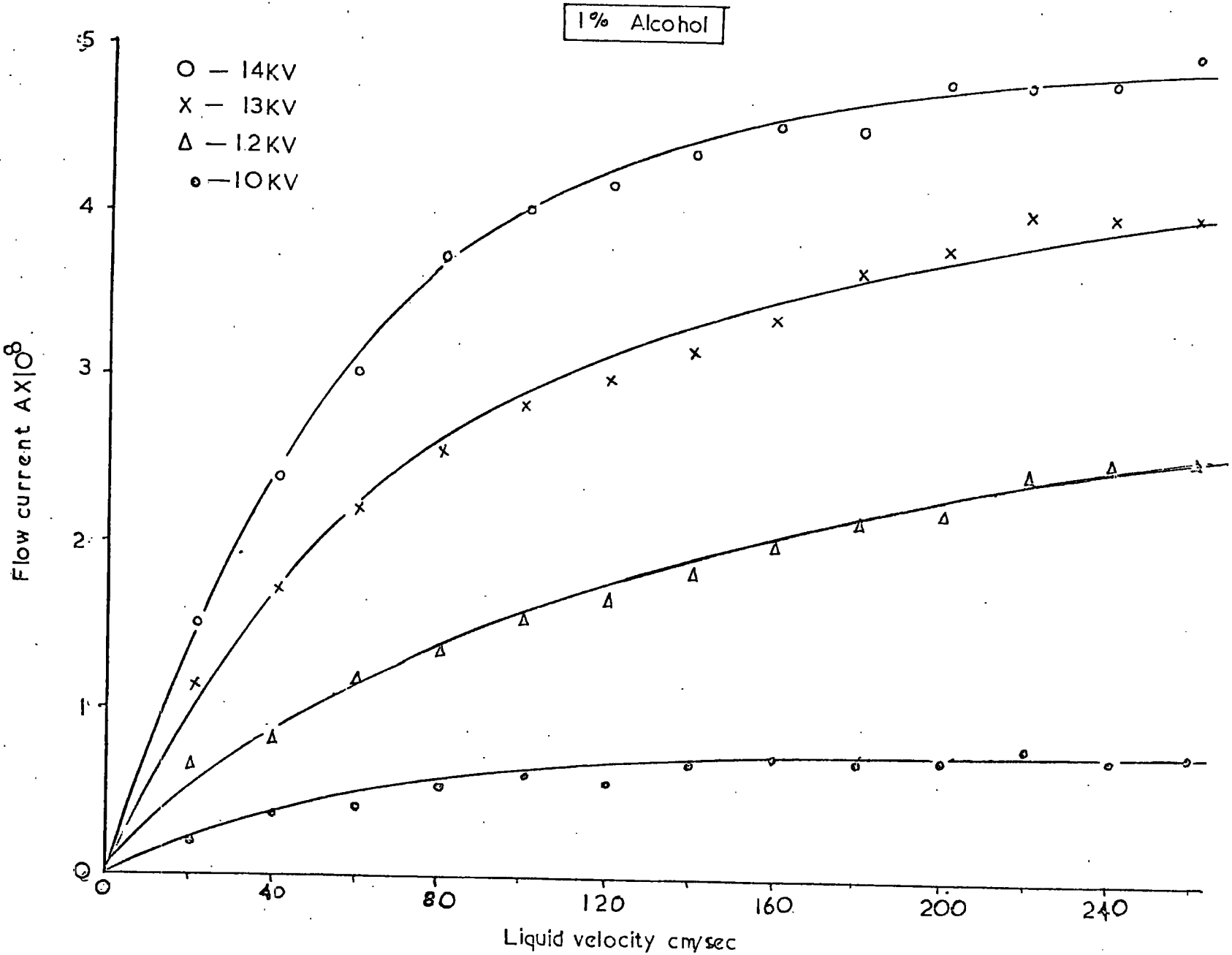

Figure 5.23a Same as in Figure 5.23; measured after taking the apparatus to pieces and reassembl...

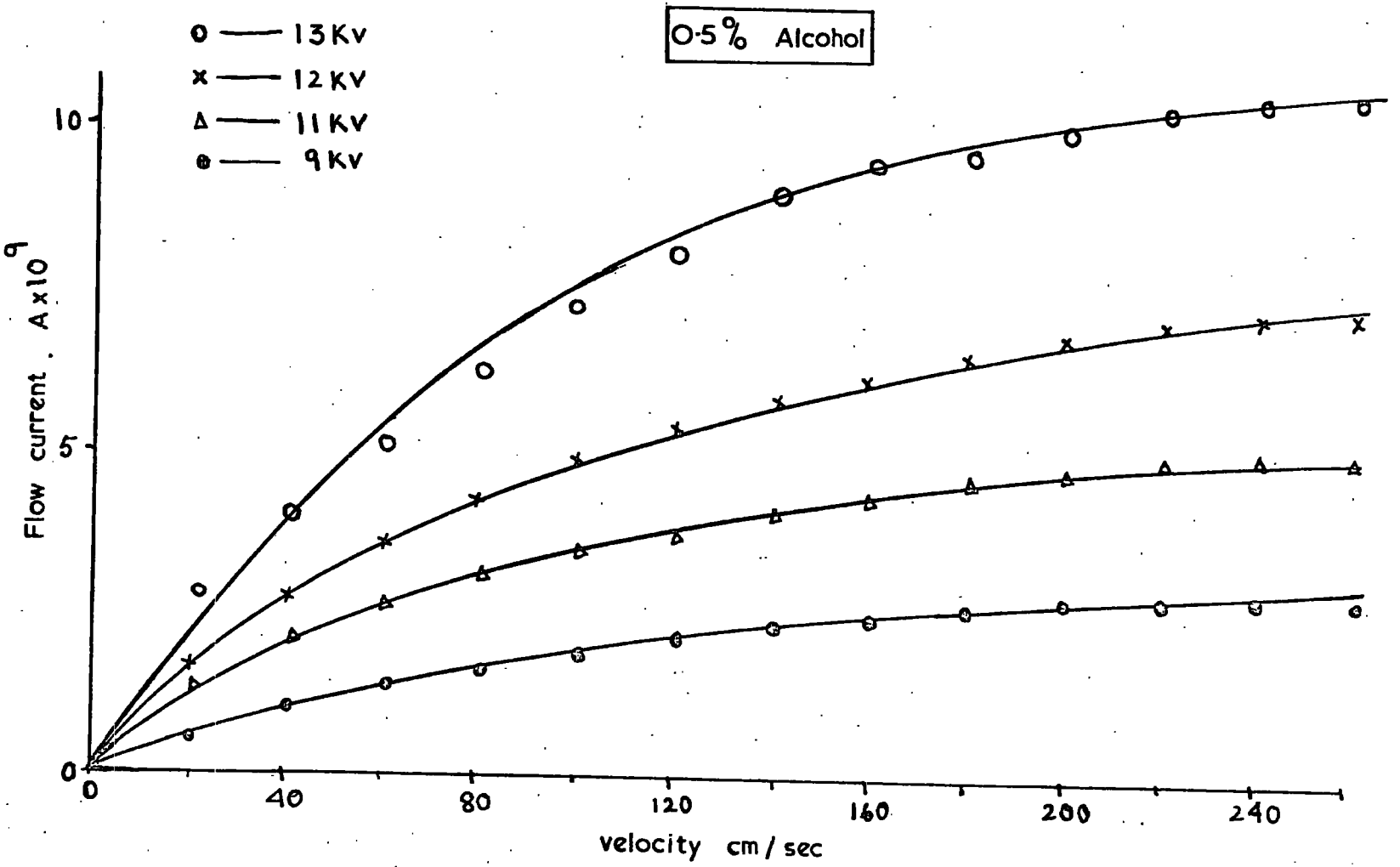

Figure 5.24 Variation of flow-current with liquid velocity in 0.5% alcohol doped HWL hexane.

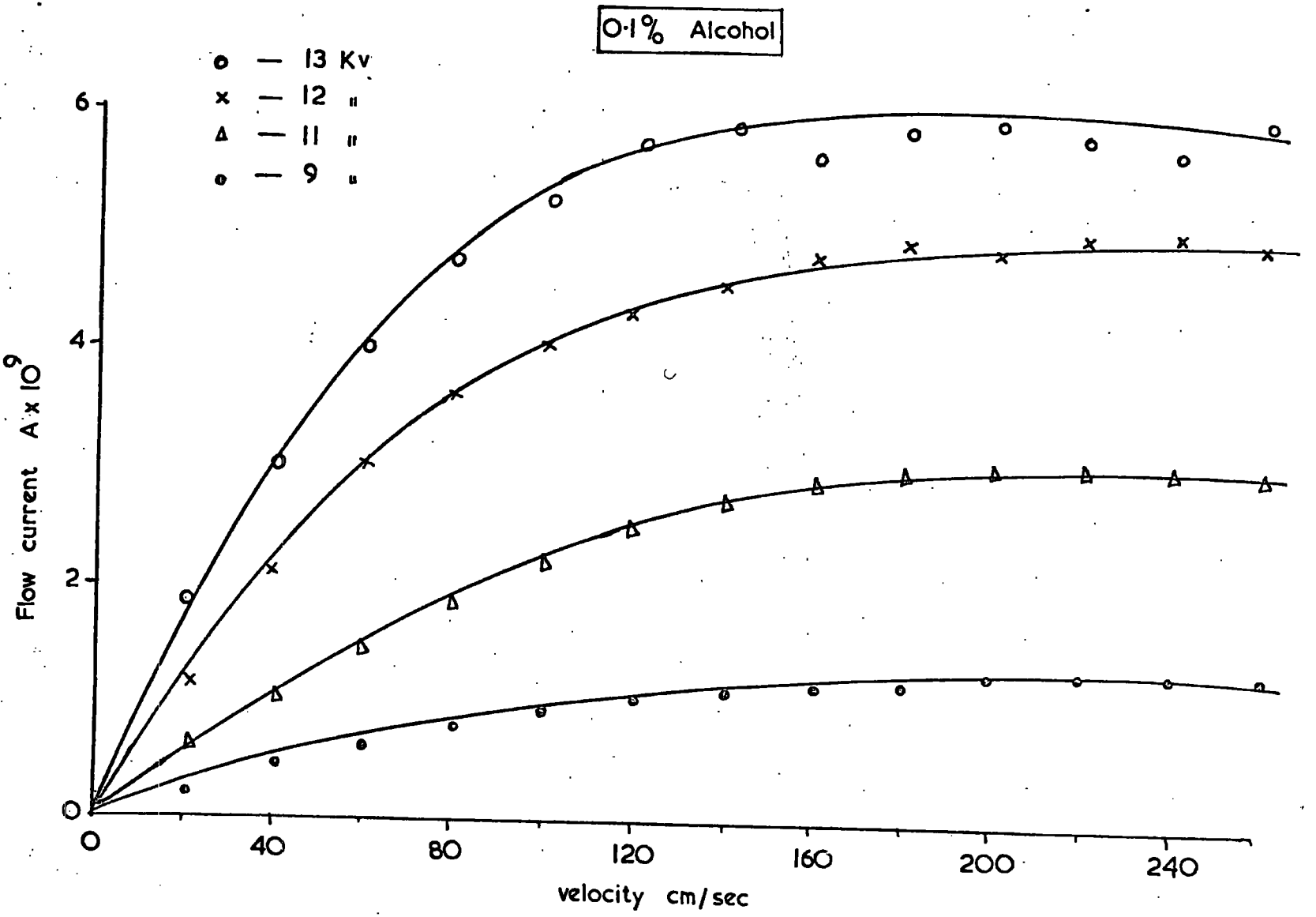

Figure 5.25 Variation of flow-current with liquid velocity in 0.1% alcohol doped HWL hexane

voltages below 7 KV, no measurable flow-currents were observed for the 0.1% doped hexane.

Currents measured in the flowing liquid with the blade positive were considerably less than even in the static liquid. This was most surprising and quite the opposite to the increase observed with the blade negative. The decrease was more pronounced with the higher applied voltages and also at the higher liquid velocities. Fig. 5.20 has already shown the static emitter current for both polarities in hexane containing 1% alcohol. Fig. 5.26 shows the corresponding flow-currents for both polarities. Note that the flow-current is negative (i.e. a decrease of the total current) with positive polarity. Measurements made with a sample of higher doping level showed a much bigger effect of liquid motion. The emitter currents with the blade positive were always found to decrease with liquid motion. Fig. 5.27 shows the flow-current with the blade negative and positive in liquid doped with 4% alcohol. The ratio of the steady currents with the blade negative and positive (approximately ' 2) also showed a considerable change compared to the value of approximately 3 for 1% alcohol doped sample.

Measurements of current at voltages higher than 17 KV, which was the maximum voltage applied in the previous measurements, were made by increasing the emitter-grid spacing to 5 mm. The results (Fig. 5.28) were similar to those obtained with a 3 mm spacing. At voltages exceeding 20 KV, the measurements were limited by high current pulses followed by breakdown of the gap. The increase in the emitter-grid spacing resulted in an overall decrease in the conduction currents and a corresponding decrease in the flow currents.

In the above measurements an increase in flow-current was observed with increasing doping level at constant applied voltage and liquid velocity. The

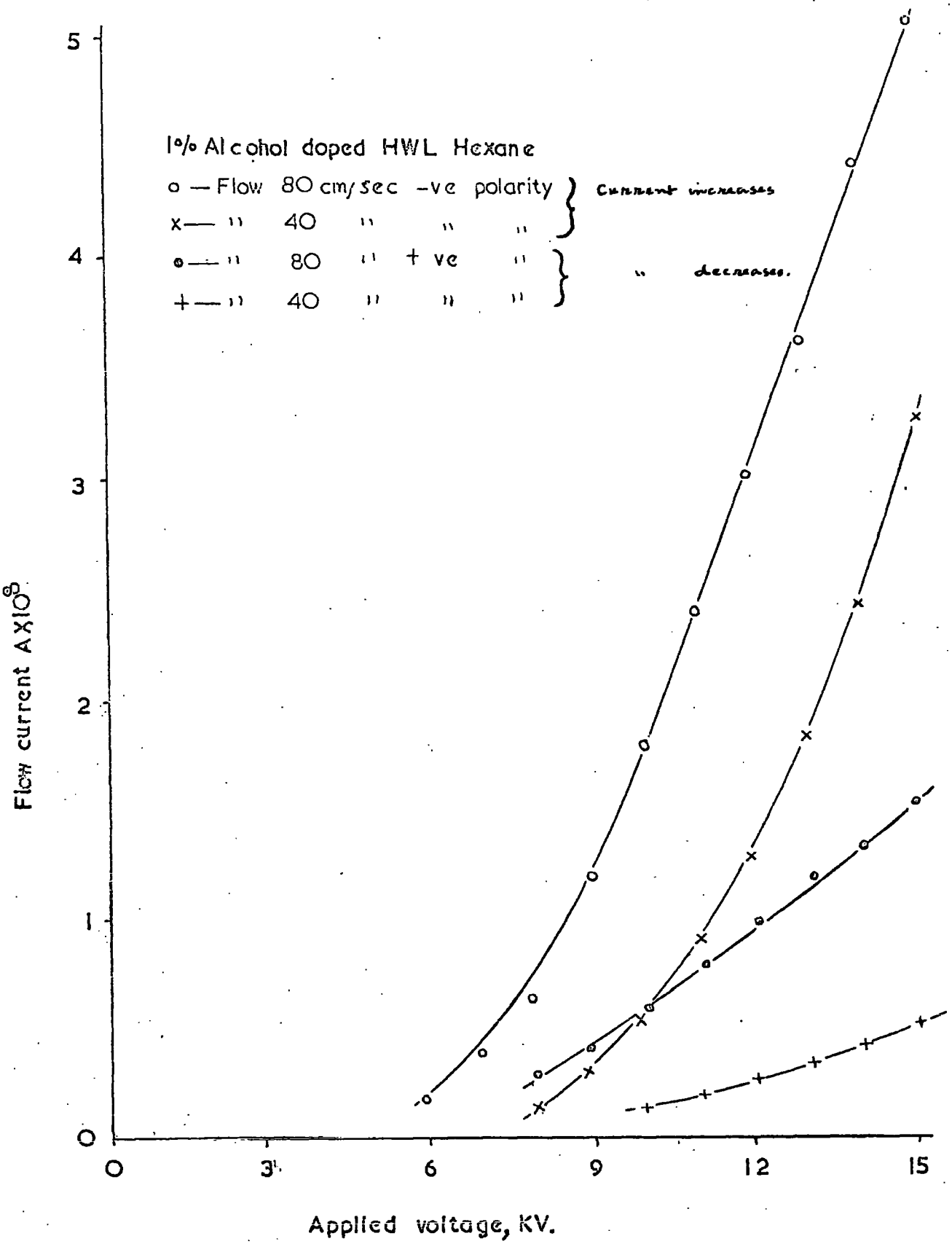

Figure 5.26 Variation of emitter current and flow-current magnitude with applied voltage in 1% alcohol doped HWL hexane.

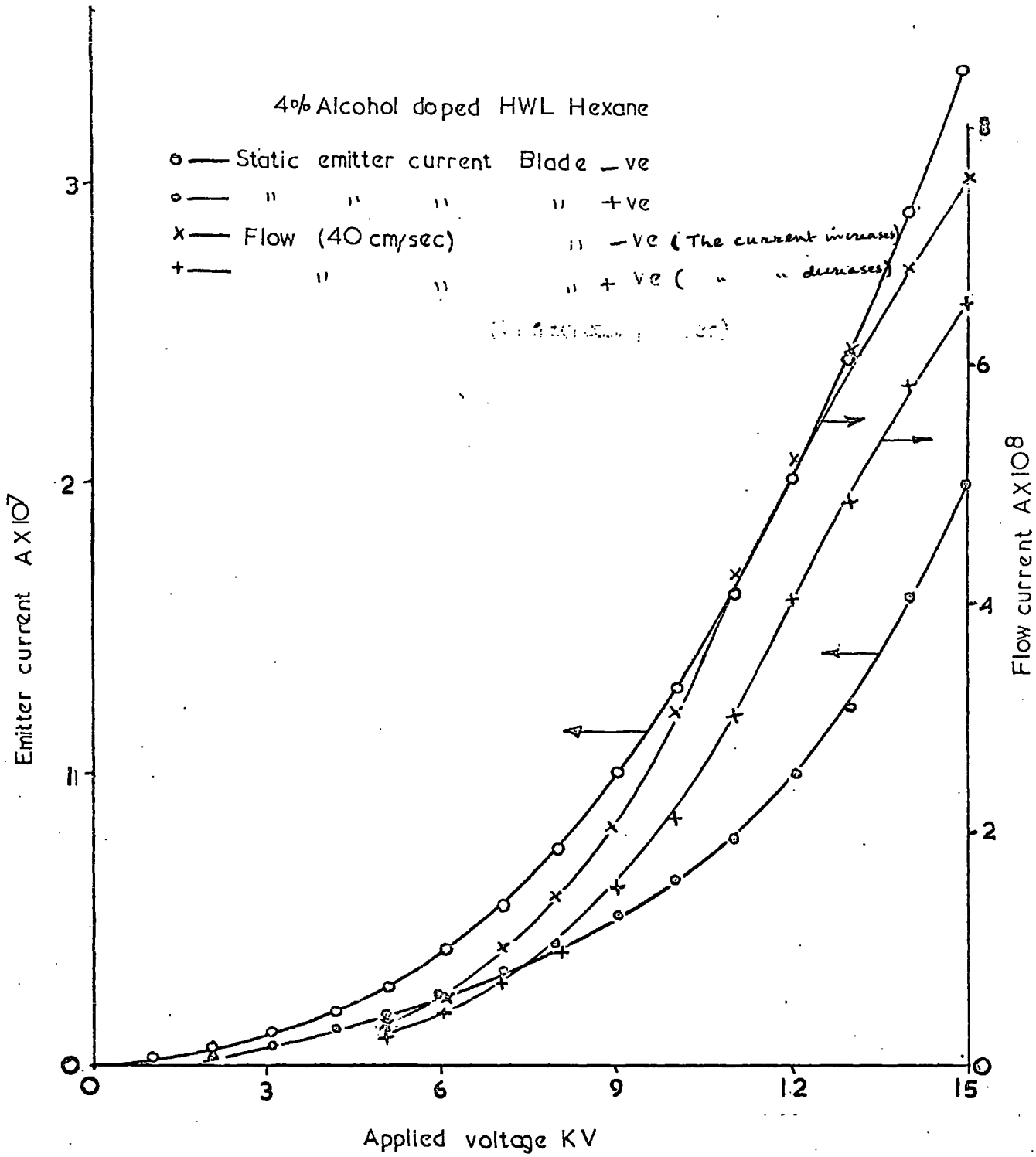

Figure 5.27 Variation of static emitter current and flow (40 cm/sec) current magnitude with applied voltage in 4% alcohol doped HWL hexane.

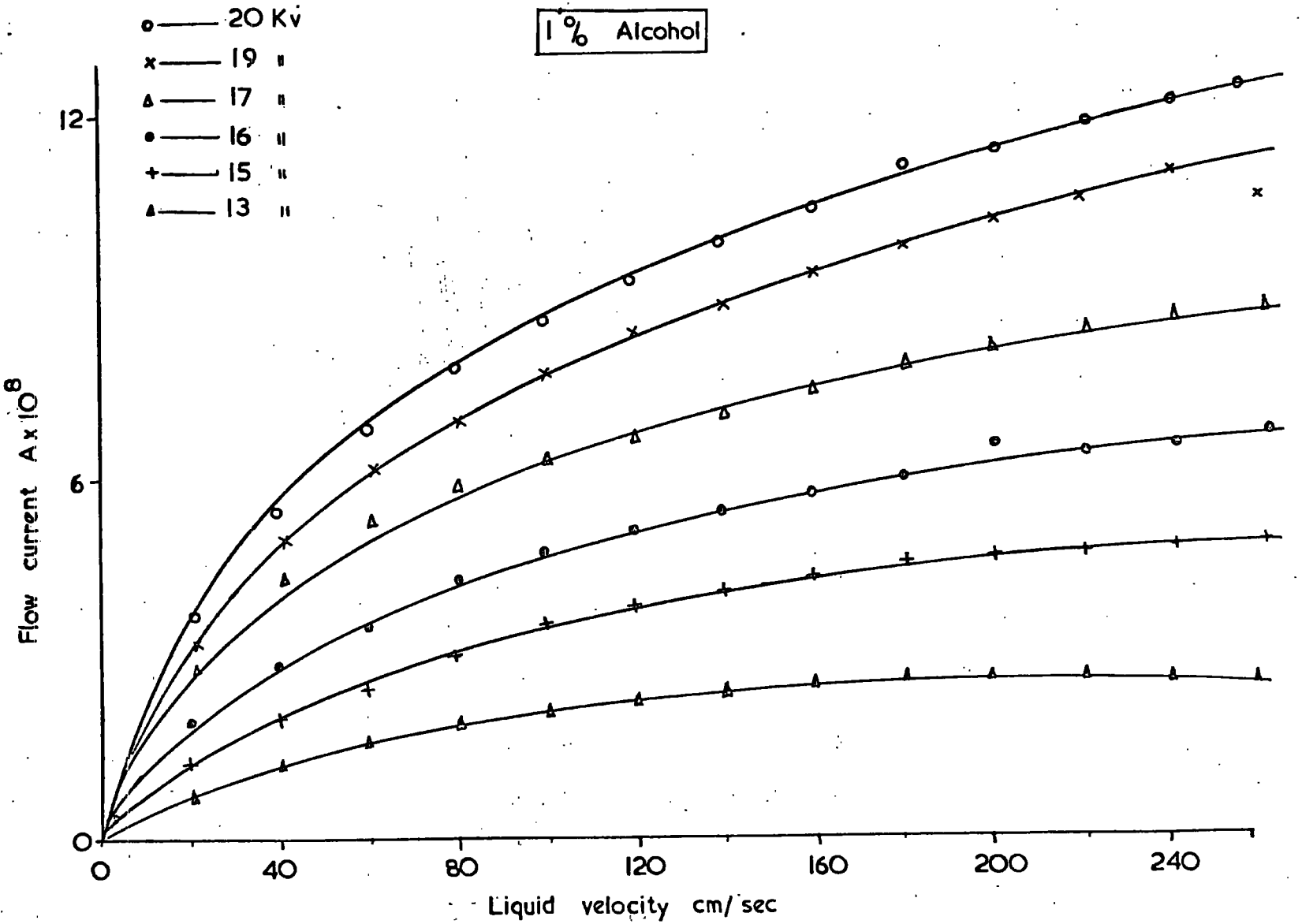

Figure 5.28 Variation of flow-current with liquid velocity in 1% alcohol doped hexane; for emitter-grid spacing of 5 mm.

increase was proportional to the alcohol concentration below one per cent but was less dependent on concentration above this. The saturation of flow current with liquid velocity was more definite; the lower was the doping level. With the blade positive, the flow-currents were measured for only two values of liquid velocity (40 cm/sec and 80 cm/sec). The doping level was also limited to values of 1% and 4% of alcohol in these measurements.

These measurements showed that impurities have a very large influence on the current in flowing hexane with a very non-uniform field. It was of interest to see whether this could be correlated with the low-field conductivity measured in uniform field conditions. These measurements were, therefore, made in usual conductivity cells, one of which was manufactured by Mullard and the other made in the Department.

The natural conductivity of well purified hexane is of the order of 10^{-18} - 10^{-20} mho/cm. Measurement of such low values was not required and it was limited in any case by leakage of the cells to conductivity values of 10^{-14} mho/cm for the Mullard cell and of 10^{-16} mho/cm for the one made in the Department. The conductivity of water saturated hexane was 3.0×10^{-4} mho/cm. Conductivity measurements for the alcohol doped samples gave values of 4.2×10^{-12}, 2.5×10^{-12}, 1.1×10^{-12}, 6.0×10^{-13} and 2.1×10^{-13} mho/cm for alcohol concentrations of 4%, 2%,1%, 0.5% and 0.1% respectively.

The possibility of chemical reactions or of significant dissociation occurring in the region around the blade tip at high voltages was investigated by vapour phase chromatography and ultra violet transmittance measurements on samples taken before and after use in the circulating system. Hydrogen abstraction by the alkoxyl radical from saturated hydrocarbons such as methane, ethane, propane and butane under suitable conditions has been

reported by Gray and Williams[88] and was a possibility here. A Perkin-Elmer Model 451 vapour phase chromatography apparatus was used by courtesy of the Chemistry Department for the analysis of hexane samples with different alcohol concentrations. The analysis did not reveal any new peaks that were not present in freshly prepared mixtures of hexane and the requisite quantity of alcohol. Measurements of u.v. transmittance made on a spectrophotometer also showed no change in the liquid after the experiment.

5.2.4 Dependence of conduction current on type of blade, counter electrode and liquid

The very much higher currents reported by Secker and Aplin,[55] compared to the present values, obtained in similar conditions but with dried and filtered hexane, led us to undertake a few measurements using different types of blade to see whether this could account for the difference. A piece of stainless steel Wilkinson blade, exactly the same length as the Personna one was next used as an emitter. The grid and collector assembly was the same as in previous experiments. Conduction currents were measured in both pure (dried and filtered) and doped hexane at voltages of both polarities up to 15 KV. The currents were smaller than those obtained using the Personna blade, as shown in Fig. 5.29, although the ratio of currents with the blade negative and positive was approximately the same. As in the previous experiments, there was no effect of liquid movement on the conduction current in pure hexane. In the doped samples the effect of liquid flow was measured for both polarities. The currents increased with flow for negative voltages but they decreased with the blade positive, as observed in previous experiments. The flow-currents were somewhat smaller than before. (Compare Figures 5.29 and 5.26)

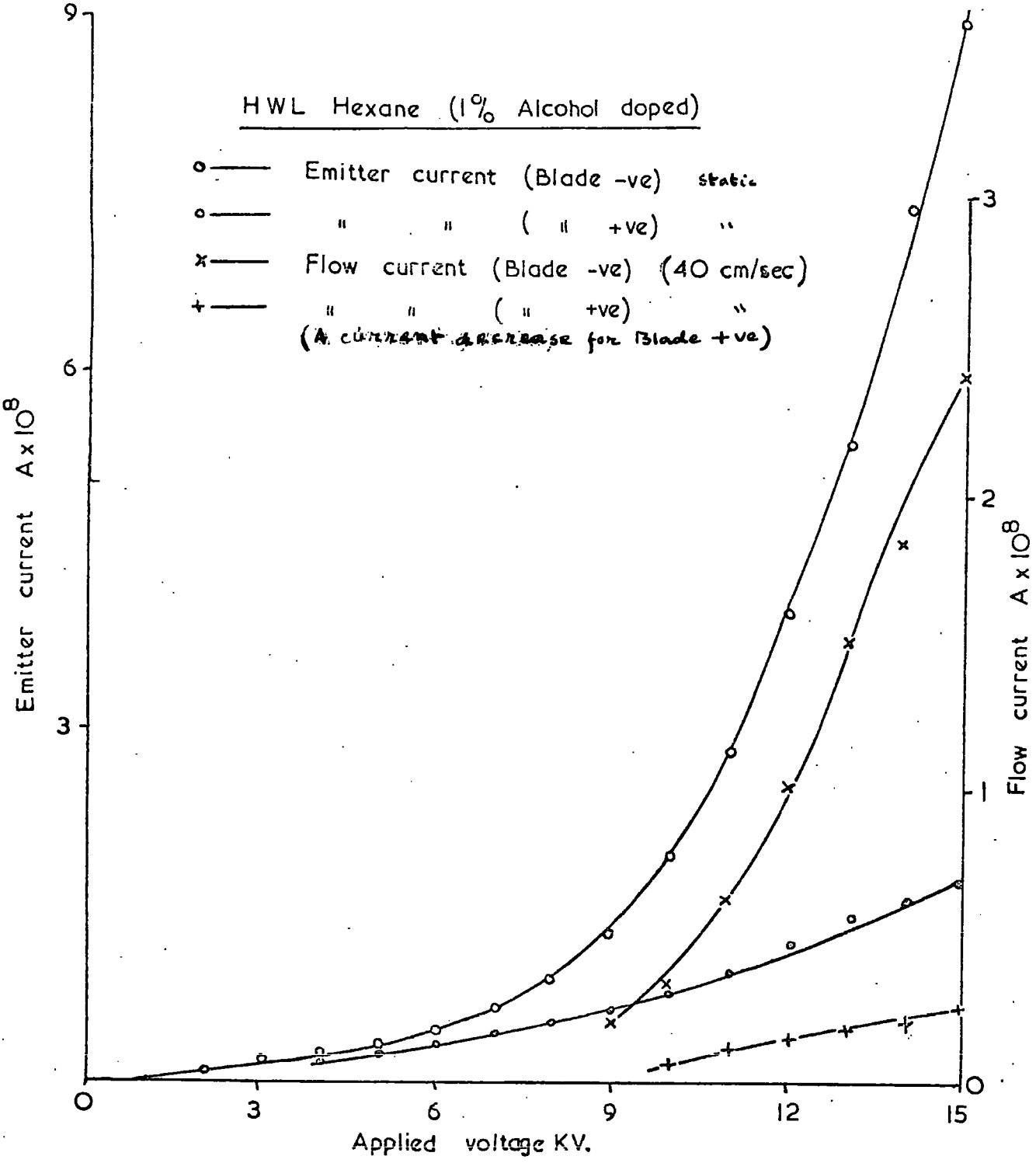

Figure 5.29 Variation of emitter current and flow-current with applied voltages in 1% alcohol doped HWL hexane with Wilkinson blade.

Replacing the Wilkinson blade with a Blue Gillette, which is the best blade for high-field injection according to Secker and Aplin[55], showed no increase in the conduction currents above those obtained with the Personna blade. However, the ratio of currents with the blade negative and positive increased from 4:1 (Personna) to 7:1 (Blue Gillette). The effects of dopant and flow were similar to those observed using the Personna and Wilkinson blades. For applied voltages below 6 KV the currents with both polarities were almost equal. The static characteristics of the different blades are shown on a log scale in Fig. 5.30.

The significant features of field-injection, namely high current level and high ratio of currents with the blade negative and positive, were still very different from those reported by Secker and Aplin.[55] A change of counter electrode from the grid to a solid disc was considered to be another possible way of increasing the current ratio. The cell described in the previous sections was removed from the closed loop and the grid was replaced with a brass disc of the same size, keeping the emitter counter electrode distance at 3 mm. This, of course, prevented further flow experiments from being made, although it was perfectly adequate for static measurements, for which the cell was placed vertically in a large glass beaker. With pure HWL hexane and the blade negative there was no increase in current over that obtained with the grid as is shown by comparing Figures 5.30 and 5.31. An increase in current was, however, observed with the blade positive and the ratio of the currents was thus decreased to two.

Another possible change to enhance the current with this electrode assembly was to change the experimental liquid. Accordingly, Puriss-grade hexane, obtained from Koch-Light laboratories, was used, as this had also been

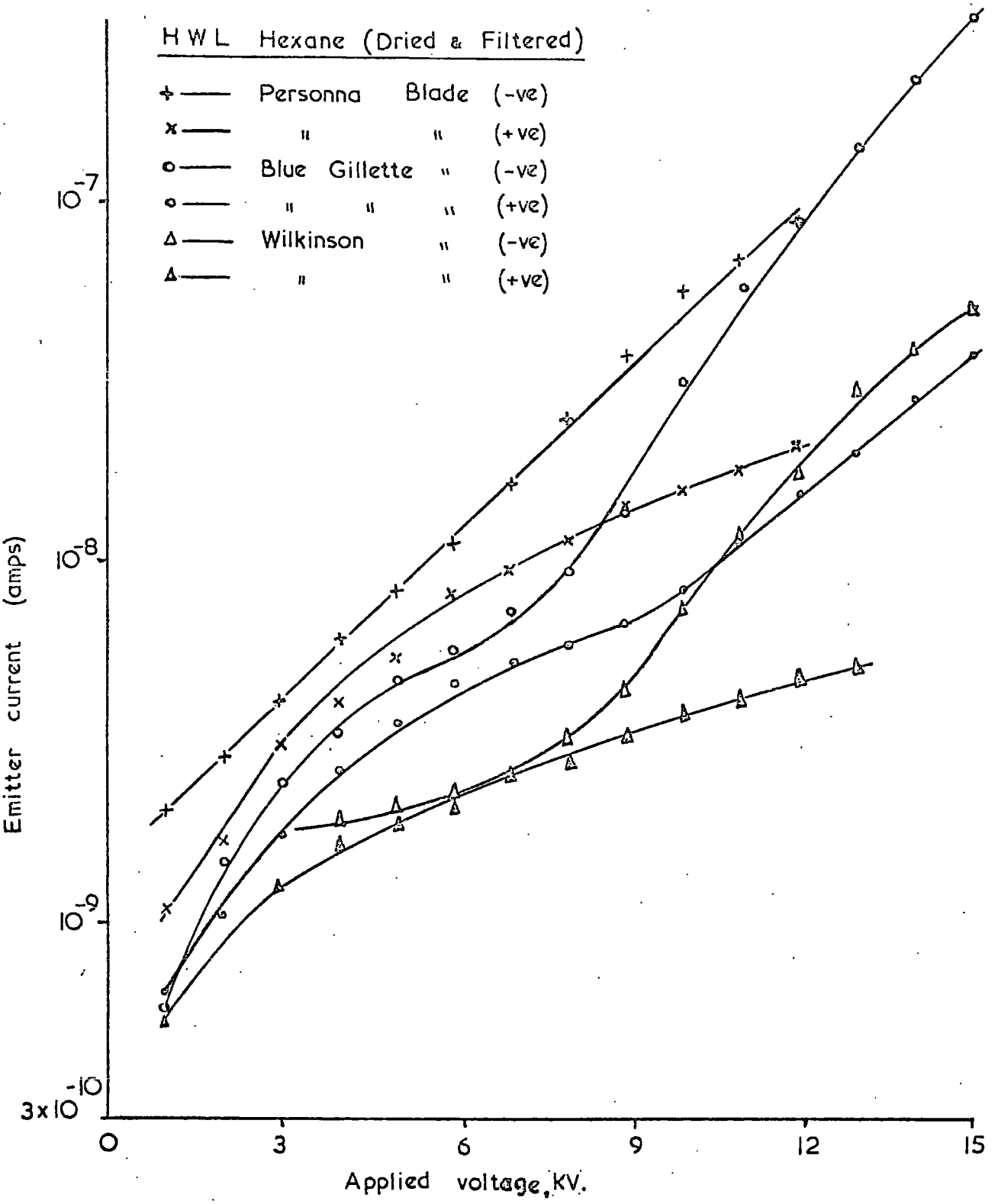

Figure 5.30 Static emitter current characteristics for various blades.

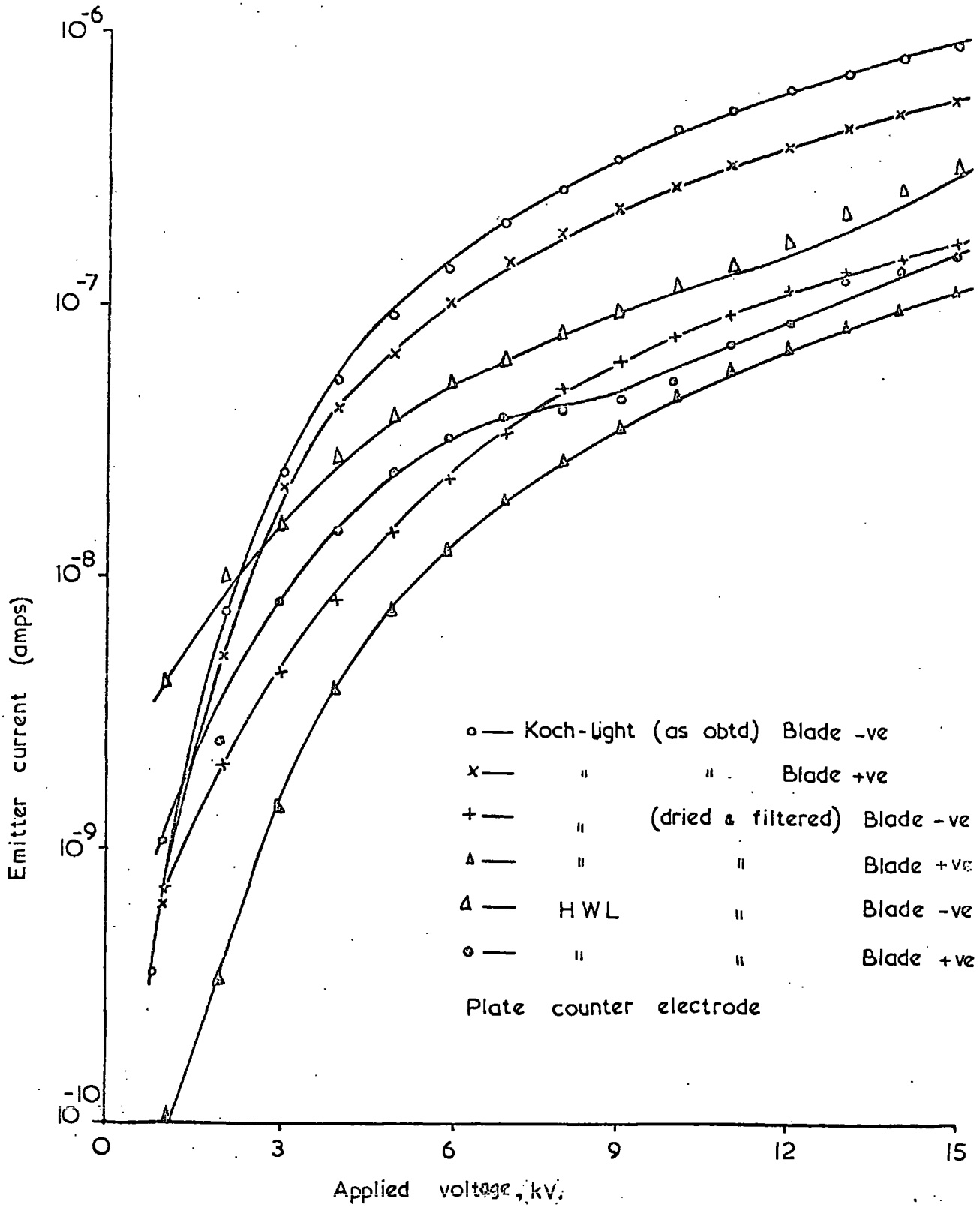

Figure 5.31 Static emitter current characteristics for different grades of hexane with Blue Gillette blade.

used by the above workers. With the hexane as supplied, a current of 8.5×10^{-7} A was measured for a negative applied voltage of 15 KV, with a Blue Gillette blade as emitter (Fig. 5.31). With the blade positive the current was 5.4×10^{-7} A for the same applied voltage. Aplin's currents with the blade negative are fairly close to this value, considering that he used a blade length of 38 mm and electrode gap of 1 mm as compared with a blade length of 8 mm and gap of 3 mm here. However, the ratio of the currents was far less in the present work. When the liquid was dried and filtered, the currents with the blade both negative and positive decreased to about one fifth of their previous values, so maintaining the same ratio. Fig. 5.31 shows the characteristics with these liquids and measurements taken in the same conditions for HWL hexane (pure) included for comparison.

It was concluded that we could not reproduce the measurements of Secker and Aplin although the experimental conditions were almost identical. Even the use of one of Aplin's blades did not give his results in the present apparatus. No explanation could be found for this.

5.3 Summary of Observations

The results described in this Chapter are fairly reproducible and the measurements in different sets of apparatus are similar in nature (e.g. compare Figures 5.19 and 5.21). Experiments carried out at different times in the same apparatus under similar experimental conditions gave almost the same results. (Compare Figures 5.23 and 5.23a which are for measurements deliberately taken to check the reproducibility.)

Field-injection currents in hexane will be shown in Chapter VII to be explained by a combination of (a) field emission and (b) field ionisation of impurities at the blade tip. Considerable information about the conduction mechanism can be obtained from a study of the effect of the movement of the liquid on the conduction current.

(a) Electrode limited currents.

The following were the main observations in filtered and dried hexane in which field ionisation of impurities was probably not important.

(i) With an assembly of six blades a current of 12 μA was measured for an applied voltage of 10 KV and tip counter electrode gap of 1 mm.

(ii) Using a single piece of blade, the current reached the order of a microamp for an applied voltage of 20 KV and an inter-electrode gap of 3 mm.

(iii) Beyond a threshold voltage the current varied at between the third and fourth power of the applied voltage. The threshold value was about 4 KV.

(iv) The ratio of the currents with the blade negative and positive was up to seven at the higher voltages. At voltages below 6 KV the currents were approximately the same for each polarity.

(v) There is no effect of liquid movement on conduction current in pure hexane.

(vi) The emitter current increased with the decrease of emitter-grid distance.

(b) Field-ionisation of impurities.

The following were the main observations for impure hexane, most of which was deliberately doped with water or alcohol. The increase in the currents in CCL hexane (up to 30 μA compared to a (i)) and in Koch-light hexane as supplied (up to 23 μA compared to 12 μA in pure liquid) was thought to be due mainly to field ionisation of the impurities.

(i) Currents in CCL hexane were nearly of the same magnitudes as those in hydrated HWL samples. In alcohol-doped hexane the current increased with increase of doping level.

(ii) The large fluctuations in the currents observed in water saturated samples is probably due to water globules which can be filtered out (Sec. 5.2.2). Dissolved water is a common impurity in hexane. The measurements, however, showed that dissolved water behaves qualitatively like alcohol in hexane and the fluctuations with alcohol are very much less.

(iii) Hexane containing water or alcohol in solution showed a considerable effect of liquid movement on the conduction currents.

(iv) With the blade negative, the current increased with flow whereas with the blade positive the current decreased with flow. All the flow directions are from blade to grid.

(v) The flow-current became more pronounced at higher voltages, velocities and doping levels. At higher velocities it reached a saturation level.

(vi) The saturation was reached earlier for the lower concentrations of alcohol.

(vii) The ratio of currents with the blade negative and positive decreased from 7 in pure hexane to 2 in a sample containing 4% alcohol.

(viii) Analysis of alcohol-doped hexane after the experiments did not show any chemical change.

Measurements of currents at higher voltages were limited by spark discharges from the tip. An increase of emitter-grid distance from 3 to 5 mm increased the voltage limit by only 3 KV (from 17 KV to 20 KV). No remarkable change was observed in the magnitude of the conduction currents with stainless-steel blades from different manufacturers. In all cases the currents were independent of liquid movement in pure hexane but depended considerably

on flow after doping the liquid. When the grid was replaced by a solid disc as the counter electrode, the ratio of currents with blade negative and positive decreased considerably.

These observations, together with the supporting results, will be discussed in detail in Chapter VII.

CHAPTER VI

DISCUSSION AND THEORY OF PHOTOCONDUCTION

Charge injection into hexane by photo- and high-field injection has been studied in the present work. In this Chapter the results on photoconduction are discussed in detail. Attempts have been made to put forward a semi-quantitative model of the photoinjection process on the basis of the experimental results.

6.1 Discussion of Photoconduction Results

The photoconduction in hexane may be due to several competing processes at the electrodes and within the liquid. A discussion of the results is therefore necessary to identify the true cathode injection component due to the u.v. radiation. The experiments used the same grade of hexane as Pugh[2], degassed at a similar pressure, but the different method of cathode irradiation may account for slight differences in the results. The main features are discussed in the different sub-sections below.

6.1.1 Forward current and its decay

The main features of the forward photocurrents are:-

(a) Their magnitudes are not precisely reproducible. The initial currents measured in each run gave some variation.

(b) The larger the photocurrent, the more upward curvature there is on the Ip-V characteristic.

(c) The photocurrent always decreases with time and the Ip-V curve becomes flatter and finally curves downwards.

Pugh explained the photocurrents in these conditions as a mixture of cathode injection and bulk ionisation which may still occur in spite of careful purification of the liquid. The decrease of current with time, also observed in the present work, is probably due to a decrease in the activity of the photocathode. This phenomenon, commonly known as 'fatigue', may be caused by residual gases in the photocathode itself or in the liquid or desorbed from the cell walls[89], even with the very low degassing rates measured. On the other hand, the photocurrent due to bulk ionisation probably rises with time due to chemical changes in the liquid. It follows that the initial photocurrent measured just after the cathode preparation is the most characteristic of cathode injection.

The initial Ip-V curves (e.g. Fig. 4.10) are curved upwards more than those of Pugh, probably due to the better cell geometry used here. Downwards curvature is known to be a characteristic of the bulk ionisation current so that results with the greatest upwards curvature are probably more representative of the cathode injection mechanism. One can therefore conclude that the largest measured photocurrents, i.e. those of Fig. 4.10, curve A, are the most characteristic of cathode injection.

The lack of reproducibility between runs is probably due to variations in cathode quality between the different sets of measurements. The state of oxidation of the photocathode affects its photoemissive efficiency[3] and may partly account for the non-reproducible photocurrent measurements. The other, and possibly more important factor in achieving reproducible results, is the thickness of the photocathode. In the present work the film thickness was gauged only by looking through the film at the time of evaporation. The variation in thickness in the different runs would have changed the absorption

of u.v. radiation and also the electron emission probability to give a consequent change in the photoemission results.

The low-voltage measurement of photocurrent taken 13 days after cathode evaporation (Fig. 4.11) is considered to be mostly due to bulk current as the Ip-V characteristic shows downwards curvature.

6.1.2 Reverse characteristics

The photocurrents with reverse voltages could originate from photo-emission from the metal electrode or from bulk ionisation. During the evaporation of the photocathode, the anode surface also becomes coated with a fresh layer of aluminium, making it photosensitive. In the experiments, u.v. radiation passing through the photocathode and the liquid may therefore emit photoelectrons from such surfaces. The reverse photocurrents are therefore also dependent on the evaporation process and hence they are not reproducible. The reverse photocurrents have the following features:-

(a) they are of variable magnitude, e.g. compare Fig. 4.10 and Fig. 4.13,

(b) they have variable decay characteristics,

(c) they increase linearly with voltage or at a lower rate.

The decay of the reverse currents may depend on

(1) the deterioration of the metal electrode surface

(2) change of transparency of the film cathode, and

(3) possible rise of bulk current due to liquid deterioration.

All these factors are variable from run to run, so that the variability in the behaviour of the reverse photocurrent is not surprising. In other work[5,31,46] the reverse photocurrent was also affected by reflected or stray radiation but here the radiation was directed normally on to a small area of the photocathode (Sec. 4.2.5) so that unwanted reflections will be negligibly small.

The existence of the small reverse currents confirms that the forward current is largely due to photoinjection of negative carriers from the photocathode. The magnitude of the reverse current can easily be explained by the processes described above without pre-supposing any new phenomena beyond those which account for the forward photocurrent.

6.1.3 Miscellaneous results

After the second evaporation of a photocathode in a single sealed-off cell, the photocurrent shows a considerable increase in magnitude. This partial recovery confirms the cathode dependence of the forward photocurrent although, due to the increased thickness of the second film, a complete recovery cannot be expected. The photocurrent after the second evaporation was found to decay more rapidly and this may be due to a higher oxygen pressure in the sealed-off cell after the second evaporation, due to degassing of the aluminium source.

The fact that there is no change in the u.v. transmittance of hexane exposed to filtered radiation for a long period shows that, although there may be some residual short term bulk ionisation, there is no long term deterioration of the liquid as occurs with unfiltered radiation[2]. The increase of the dark current with time may be due to an increase in the undetectable impurity content of the liquid possibly due to bulk ionisation, gas pressure rise within the cell, or a slow chemical reaction arising from the impurities in the test cell.

6.1.4 Charge measurements

The preliminary results on pulse charge injection into hexane (Fig. 4.12) were obtained after the second evaporation of the photocathode. Unfiltered radiation had to be used to give a measurable charge with this inferior

photocathode. The better results shown in Fig. 4.14 were taken with a fresh photocathode and filtered radiation and they show the decay of charge injection with time. The decay is similar to that of the d.c. photocurrent (e.g. Fig. 4.13), due to the fall in the cathode injection. The shape of the corresponding curve of photocurrent shows that even after three days from cathode preparation the cathode injection is still predominant (Fig. 4.13). The pulse photocharge is therefore thought to be a genuine measurement of charge injection for at least this period of time.

The earlier measurements of Bloor[3] show an approximately linear increase of pulse photocharge with applied field strength (Fig. 4.1(b)). His measurements were mainly for much higher field strengths than in the present work. The slight curvature in the Q-V curves found here (Fig. 4.14) is probably noticeable only at lower field strengths.

The first simultaneous measurements of d.c. photocurrent, Ip, and pulse photocharge, Q, shown in Fig. 4.16, used unfiltered radiation for the latter so that they are not strictly comparable. The true relation between Ip and Q taken with identical conditions is shown in Fig. 4.17 which is based on Ip measurements that have been shown to be due to cathode injection in the forward direction and on the best Q measurements. The points in the figure (X for $1\frac{1}{2}$ hours after cathode preparation and O for times greater than 2 hours) all fit the same relationship equally well and this may be taken as a confirmation of similar decay processes for both Ip and Q. The significance of the linear relationship between Ip and Q will be discussed in Sec. 6.2.

6.1.5 Mobility measurements

The apparent mobility of the charge carriers, calculated from the 'transit time', τ, depends on the proper definition of τ for transients with

considerable curvature (Fig. 4.18). The reverse polarity transients are probably greatly affected by bulk ionisation which can account for their more curved shape. The 'transit time' calculated from such transients is therefore not characteristic of genuine charge transfer from cathode to anode, and the apparent mobility will not be the true value. On the other hand, the transients with forward polarity were less curved and similar to those obtained by Bloor[3] who made an extensive study of possible reasons for the shape of the transients and the correct transit time to be deduced from them. The range of mobility values ($6.0 - 6.9 \times 10^{-4}$ cm^2/volt sec) is in reasonable agreement with Bloor and is considered to be the genuine value.

No field dependence of carrier mobility was observed within the range of field strengths of 1.0 - 2.5 KV/cm used in the present work. Below this field range, the pulse injection levels were too small for accurate measurement and the field dependence, if any, could not be ascertained. The existence of such a field dependent carrier mobility at below 1 KV/cm has recently been observed in n-hexane[41]. Also the values are up to about two orders of magnitude higher than in the present work. Such high values (0.07 cm^2/volt sec), however, require further investigation in the light of liquid motion[90] and possible effects of impurities.

6.1.6 Conclusion

(a) The results can be explained in terms of a mixture of photoinjection from both electrodes and bulk ionisation. The present work has helped to sort out the characteristic of cathode injection.

(b) The best pure photoinjection characteristic, probably better than Pugh's, is the curve of Fig. 4.10 of measurements taken just after the preparation of this particular cathode.

(c) The Q-V characteristics for pulse cathode injection, shown in Fig. 4.14, closely follows the Ip-V characteristic.

(d) The true Ip-Q curve for the two types of cathode injection is shown in Fig. 4.17. The measurements made at different times confirm similar decay processes for both Ip and Q.

(e) The observed carrier mobility is consistent with Bloor's result of 7.6×10^{-4} cm^2/volt sec.

The development of a detailed physical model to explain the characteristics of photoinjection into hexane is considered to be most demanding. The following section gives an attempt at a possible mechanism.

6.2 The Physics of Photoinjected Currents

In the previous Section, the true characteristics of cathode photoinjection into hexane have been sorted out from the measurements. They are the variation of both the d.c. photocurrent Ip and the pulse photocharge Q with the applied voltage. It has been shown that the measurements soon after the preparation of a photocathode are most characteristic of cathode injection. The processes leading to current flow due to this cathode injection are discussed in this Section.

Similar variations of photoinjection with applied voltage were observed earlier by Pugh[2] and Bloor[3] in this laboratory. Pugh tried to develop a model of photoinjection but his explanation was inadequate in detail. Bloor did not put forward any new idea and his explanation on the basis of the Schottky effect was a failure, as will be shown in Sec. 6.3.1. The measured photocurrents in degassed hexane are very different from those observed in vacuum[2] and an understanding of the photoinjection mechanism requires a proper explanation of photoinjected currents.

In order to explain the photoinjectedcurrents, the following assumptions are made:-

(a) the photocurrents are due to negative carriers only.

(b) the carriers are formed by photoelectrons from the cathode but as they have low mobility the carriers are not themselves free electrons.

(c) there is only one type of negative carrier except very close to the cathode where free electrons must exist.

These assumptions are justified by work on the mobility of photo-injected charge carriers, for example by Bloor, who was particularly concerned with looking for evidence of free electrons in hexane. Bloor showed that, although electrons must be emitted from a photocathode, they do not contribute appreciably to charge transport in the gap which appears to be entirely by the slow negative carriers, the possible form of which has been discussed in Chapter III.

Although the photocurrent undoubtedly originates at the cathode, it is not necessarily the emission which limits its value. In general the photo-current may be either an emission limited current (ELC) or a bulk limited current (BLC), the carriers in both cases being supplied from the cathode itself. It will be assumed that the photocurrent cannot be limited by a mixture of both processes so that it is either simply ELC or BLC and it is necessary to determine which by examination of the results.

An ELC is controlled by the cathode itself. The photocurrent will therefore depend on the physical and chemical state of the photocathode. The ultraviolet radiation also limits the photocurrent in such a way that only the radiations of higher frequency than ν_0 (eqn.7) can give photoinjection. With ELC the carrier motion after emission does not affect the total current.

On the other hand, a BLC is controlled entirely by the movement of carriers in the bulk of the liquid. The cathode can supply as many carriers as are required depending on its nature and the incident radiation but the motion of the carriers in between the electrodes limits the current. With single carrier emission into an insulator a BLC is the same thing as the current (SCL) considered in Chapter III.

The theoretical SCL current in hexane has been calculated on the basis of equation 10 (Chapter III) for the following conditions:-

(a) A single carrier mobility of 10^{-3} cm^2/volt sec

(b) An electrode gap of 1.2 cm and area of 1 cm^2. The equation neglects diffusion and assumes that the electric field is zero at the cathode, both of which are justified in this case.

The variation of the SCL current with applied voltage is shown in Fig. 6.1. Curve A is for stationary liquid and Curve B shows the effect of a considerable flow velocity (equal to the carrier velocity) from cathode to anode (equation 11, Chapter III). It is clear that the shape of the SCL curves (I proportional to V^2) is not the same as that of the observed photocurrents. The theoretical curves are tangential to the voltage axis and they have continuous curvature. As this is not a function of the numerical values used, it is clear that the results on photoinjection cannot be explained on the basis of space charge limitation. This disagreement between the experimental results and the theoretical SCL currents indicates an emission limitation to photoconduction, although its significance for the final model will be discussed further in Sec. 6.3.4.

The d.c. and pulse photoinjection measurements carried out in the present work must be totally different from the point of view of space

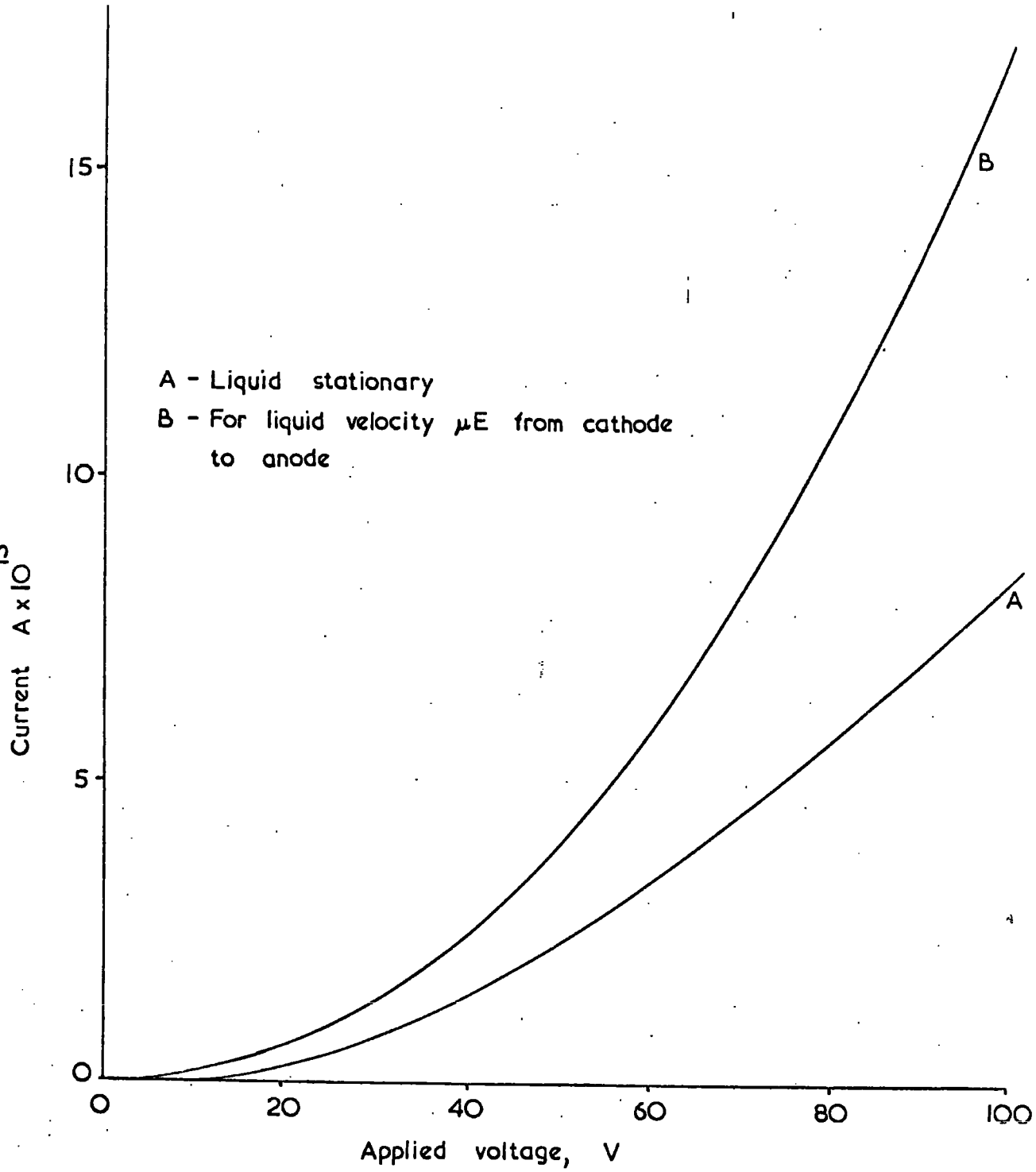

Figure 6.1. Theoretical variation of space charge limited current with applied voltage for stationary and moving liquid.

charge effects. In the case of the d.c. photocurrent measurements, the inter-electrode region is filled with charge carriers moving from cathode to anode. On the other hand, the pulse photocurrent is affected by the space charge of only the pulse of charge carriers moving in a space-charge free region. However, the results show that the variations of both Ip and Q with applied voltage are very similar. In fact, the graphs of Ip against the corresponding values of Q show that the points almost lie on one straight line for measurements taken at very different intervals of time. This shows that both Ip and Q vary in the same way with the experimental conditions over a wide range of current and voltage levels. Because of the widely differing space charge conditions over this range of experiments, the proportionality of Q to Ip may be taken as a proof that both these processes arise from the same cathode effect, i.e. both Ip and Q are emission limited.

This important result is believed to be the first time that cathode injection limitation of a current in hexane has been decisively proved. This was, in fact, one of the main objectives of the present photoconduction work and it is an important step in explaining the injection process.

Having shown the photoinjection to be a cathode limited effect, the next thing to explain is the photoinjection process itself. The proposed mechanism of photoinjection is thus dealt with in the next Section.

6.3 The Physics of the Photoinjection Process

The mechanism of photoinjection into dielectric liquids such as hexane has not yet been explained. A possible model for this field-dependant photo-effect is discussed in this Section.

6.3.1 Photoinjection as a modified Schottky effect

A review of previous work on the field dependence of the photocurrent in

dielectric liquids has been given in Chapter II. It has been generally observed that the photocurrent increases steadily with field strength without showing any sign of saturation. This increase of the photocurrent has sometimes been considered to be due to a modified Schottky effect.

Blâor[3] recently measured the pulse photocharge Q for different applied voltages V and obtained a linear relationship (Fig. 4.1(b)). He also tried to explain these Q-V characteristics in terms of the Schottky effect. Although he obtained a nearly straight line by plotting log Q against the square root of applied field E, this can be misleading because a semi-log plot does not give a complete picture of the actual variation of Q with E.

For photoinjection to be due to a modified Schottky effect, the current should obey the Schottky Law when plotted on linear scales also. The Schottky equation for the electron emission current into a medium of dielectric constant K is given by

$$I = Io \exp \frac{e^{3/2} E^{\frac{1}{2}}}{(4\pi \xi_o K)\, kT} \frac{1}{} \qquad (17)$$

where Io = zero-field current; ξ_o is the permittivity of the free space; k is the Boltzmann constant and T is the absolute temperature.

The theoretical Schottky relationship for T = 300°K and K = 1.9 (for hexane) is shown plotted on linear scales in Fig. 6.2. Comparison with the observed photocurrent clearly shows that the experimental results cannot be explained by the Schottky Law, which can account for only a small increase of current over the range of fields used here. Also, a Schottky model must have an appreciable zero-field current which is not found with photoinjection. The explanation of the results therefore needs a very different theory.

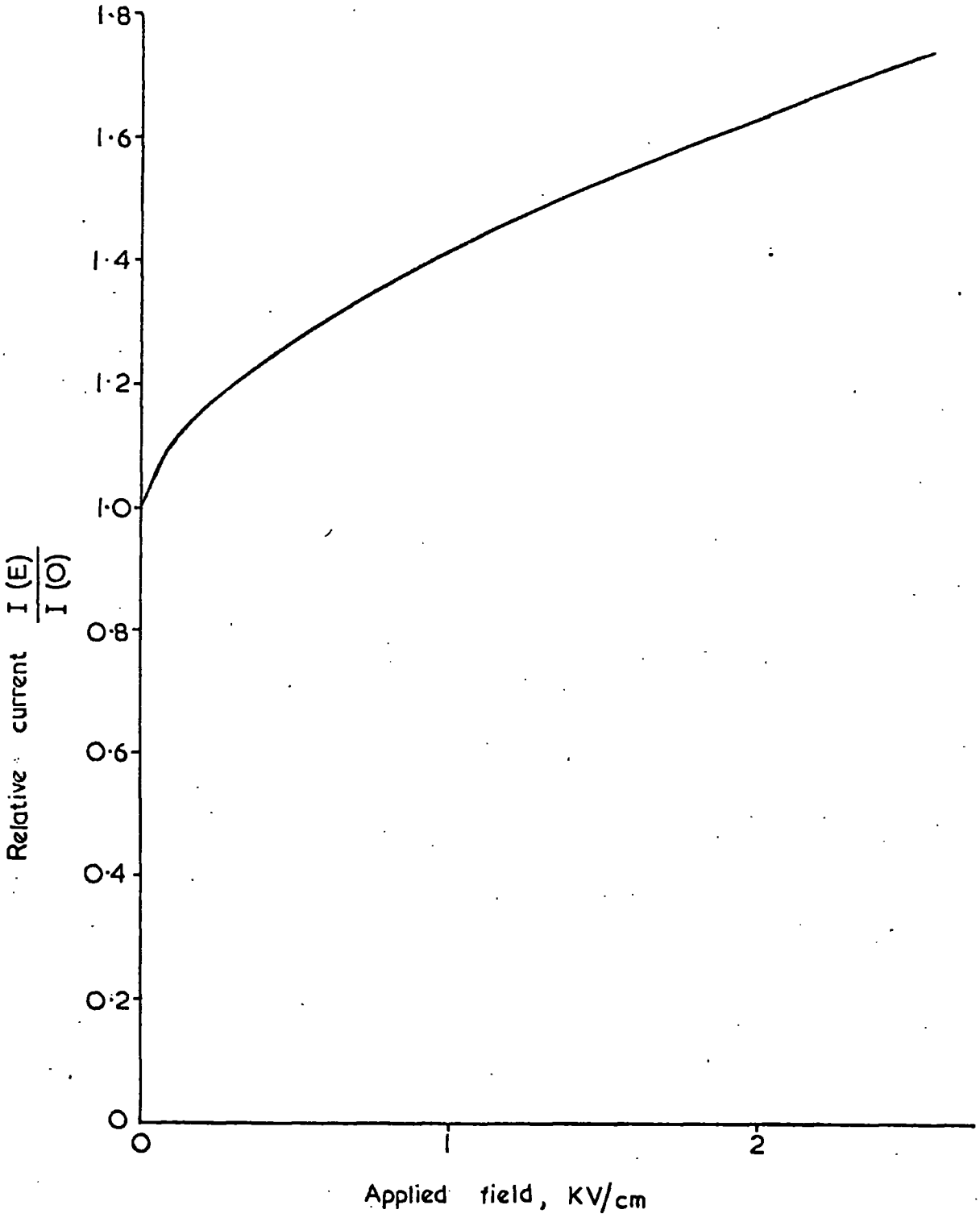

Figure 6.2. Schottky plot of the thermionic emission for room temperature (300°K).

6.3.2 Mechanism of photoinjection

The absorption of ultraviolet radiation in the cathode causes it to emit electrons with energies of the order of kT. These electrons must be trapped to form some kind of heavy negative carrier, as described in Chapter III. That the carriers in the liquid are not free electrons is proved by their low mobility, which would indicate an absurdly small mean free path.

Bloor concluded from his measurements that the photoelectrons are trapped within a very small distance of the cathode. To look for fast carriers he measured the pulse current transients for electrode gaps of the order of a millimetre. He could have detected fast charge transfer for only 1% of the gap distance but failed to observe any such carriers. Any model for photoinjection into hexane must obviously include the trapping process which is omitted with a modified Schottky theory. It must also account for the continuous rise of injection with cathode field strength and the lack of saturation.

The following model due to Dr. M.J. Morant, is used to describe the photoinjection into dielectric liquids. It will consider the photoemission of electrons and the formation of heavy negative carriers and their movement to the anode. As these processes are field dependent, the effect of applied field strength will be predicted. This method of explaining photoinjection is not entirely new. Pugh tried to explain his results with a similar model and more recently Silver et al[67] have put forward a similar model for hot electron emission current into liquid gases although the conditions there are rather different from hexane.

The main difference between electron emission into vacuum and into hexane is the severe scattering of the electrons in the latter case, even within the image barrier of the metal. As a consequence of this, many of the electrons that would be emitted into a vacuum lose energy and return to the cathode. Some of the scattering processes will lead to the formation of heavy negative carriers. Those formed within the image barrier will experience the image force returning them to the metal surface, where their energy above the Fermi level may give a large probability of discharge by loss of an electron to the metal. Heavy negative carriers formed outside the peak of the image barrier, by the few electrons that penetrate that far into the liquid, will move away from the cathode and constitute the photocurrent. It will be shown below that this model predicts a much smaller current in the liquid compared with vacuum photoemission and also that the photocurrent can be approximately proportional to the field.

The potential energy of an electron as a function of its distance from the surface and in the presence of an externally applied field is shown in Fig. 6.3. In this figure Φ is the work function of the metal, which may be slightly different from the vacuum valve due to the presence of the liquid and Xm is the distance of the potential maximum from the surface.

Only radiation of energy $h\nu$ (where ν is the frequency of the radiation) greater than Φ can give electron emission from the surface. The electrons leave the surface with energies (defined by equation 13) of the order of a few kT. Scattering with the neutral hexane molecules and with the heavy carriers causes some of the electrons to lose energy and return to the cathode (group a) so that the density of electrons capable of emission decreases. Other electrons form heavy negative carriers with

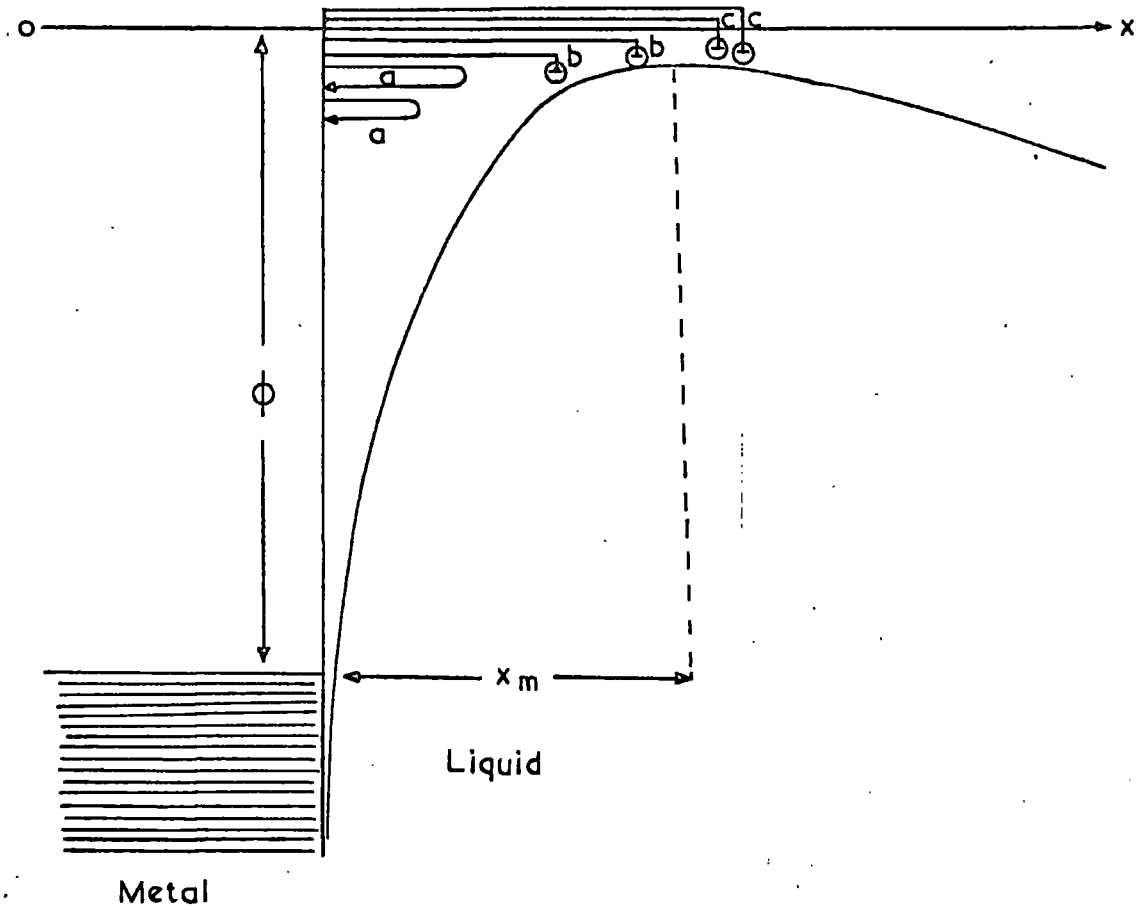

Figure 6.3. The image barrier into a dielectric for low applied field

with hexane molecules or with any impurity present. The resultant carriers will probably have energies lower than the potential maximum (group b) so that they can only return to the cathode. Thus only the carriers formed beyond Xm (group c) by electrons which reach that point with energies greater than the potential maximum (group d) can take part in conduction. The field dependence of the total electron emission will be discussed in the next sub-section.

6.3.3 Field dependence of photoemission

Guth and Mullin[91] have shown that the field dependence of photoemission from a metal is different from that of thermionic emission. For example they predicted a linear increase of photoemission with applied field from potassium and tungsten surfaces in vacuum for threshold radiation with slight differences for higher frequency radiation. They showed that photoemission varies with field according to:-

$$I \propto T^2 \left\{ \frac{\pi^2}{6} + \tfrac{1}{2} \delta^2 - \left[e^{-\delta} - \frac{e^{-2\delta}}{2^2} + \ldots \right] \right\} \qquad (18)$$

where T is the absolute temperature and the parameter δ for a medium of dielectric constant K comes out to be

$$\delta = \frac{h(\nu - \nu_0)}{kT} + \frac{e^{3/2} E^{\frac{1}{2}}}{4\pi K \varepsilon_0} \frac{1}{kT}$$

where ν is the frequency of the radiation, ν_0 the threshold frequency, ε_0 is the permittivity of free-space and k is Boltzmann's constant.

The threshold frequency of photoinjection into degassed hexane is not yet known. The threshold for bulk photoconduction has however been found by Morant[4] to be 3000 Å. Assuming that the threshold frequency of photoinjectinn

is the same as that of bulk photoconduction, ν_o was taken to be of 3000 Å wavelength. For calculations, the upper frequency ν was chosen as the frequency corresponding to a wavelength of 2300 Å, because in the present work the radiation was limited to the wavelength range of 2300 - 3000 Å by the combination of the lamp and OX-7 filter. The above frequencies thus correspond to the ends of the frequency range used and $h(\nu - \nu_o) = 0.05$ eV.

The above expression for the photoemission has been evaluated for room temperature and for $h(\nu - \nu_o) = 0$ and 0.05 eV. The results shown in Fig. 6.4 indicate that the photoemission is much greater for the shorter wavelength (curve B) and thus it will be assumed that the photoemission integrated over the wavelength range passed by the OX-7 corresponds closely to Curve B. The photocurrent due to those electrons will be studied in the next sub-section.

6.3.4 The probability of carrier formation

The electrons coming out of the cathode are scattered to lower energies and trapped to form heavy negative carriers. As a result, there will be an exponential decay in the number of high energy electrons on moving away from the cathode surface. The only electrons capable of taking part in photoconduction are those which reach the potential maximum without being trapped. If n is the number of electrons reaching the potential maximum per sec, then

$$n = n_o e^{-Xm/L} \qquad (19)$$

where n_o is the total number of electrons emitted per second from the cathode, Xm is the distance of the potential maximum from the surface for a field strength E, (Fig. 6.3) given by

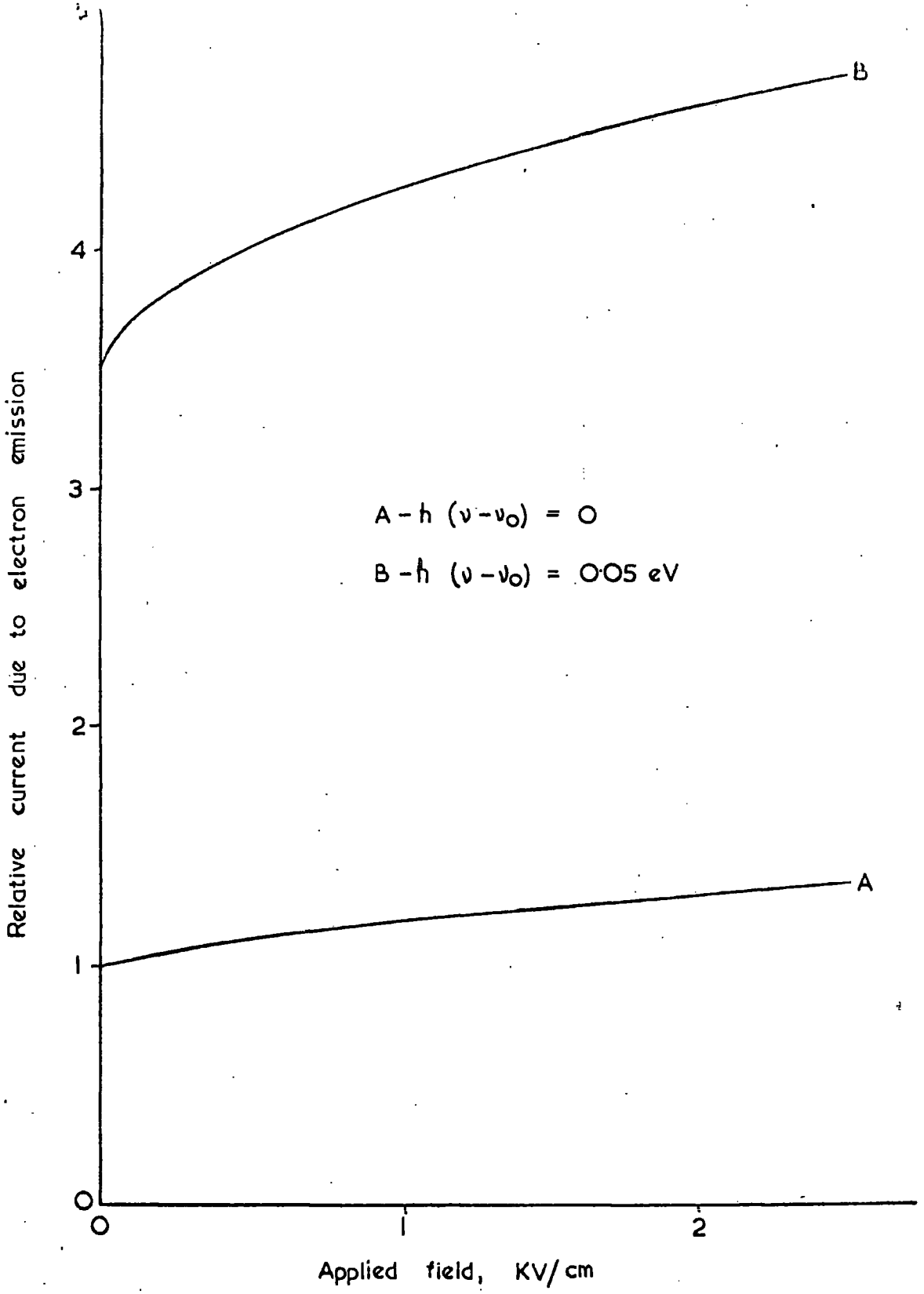

Figure 6.4. Variation of photoemission into hexane with applied field evaluated at T = 300°K for threshold and a higher energy radiation.

$$Xm = \left(\frac{e}{16 \pi K \xi_o E}\right)^{\frac{1}{2}} = \frac{1.376 \times 10^{-5}}{E^{\frac{1}{2}}} \text{ metres,}$$

where L is the average distance an electron will move before being scattered to an energy less than the barrier height, and where E is in volt/m.

Evaluation of the photocurrent by means of equations (18) and (19) for various values of L ranging from 50 Å to 1000 Å is shown in Fig. 6.5. It is seen that the current is zero for zero field and that it rises rapidly. Of the different values of L, the curve for L = 100 Å seems to give a shape most comparable with the experimental results.

Further examination of the experimental results shows that the photocurrents observed at low voltages are always higher than the space charge limited values even allowing for the effects of liquid movement (Fig. 6.1). All SCL curves are tangential to the voltage axis whereas the photocurrent curves are not. This discrepancy can only be explained by a second and independent source of current apart from photoinjection from the cathode and it is suggested that this different mechanism is probably a small amount of residual ionisation in the bulk of the liquid. Although bulk ionisation due to radiation of wavelengths shorter than 2300 Å was avoided by the use of a filter, this would not completely eliminate the possibility of a small amount of the most energetic radiation from being absorbed in the hexane. This is, in fact, confirmed by the shape of the reverse current characteristic.

If we consider that the current component due to bulk ionisation is about $^1/_5$ of the total current, and add a typical bulk component of this

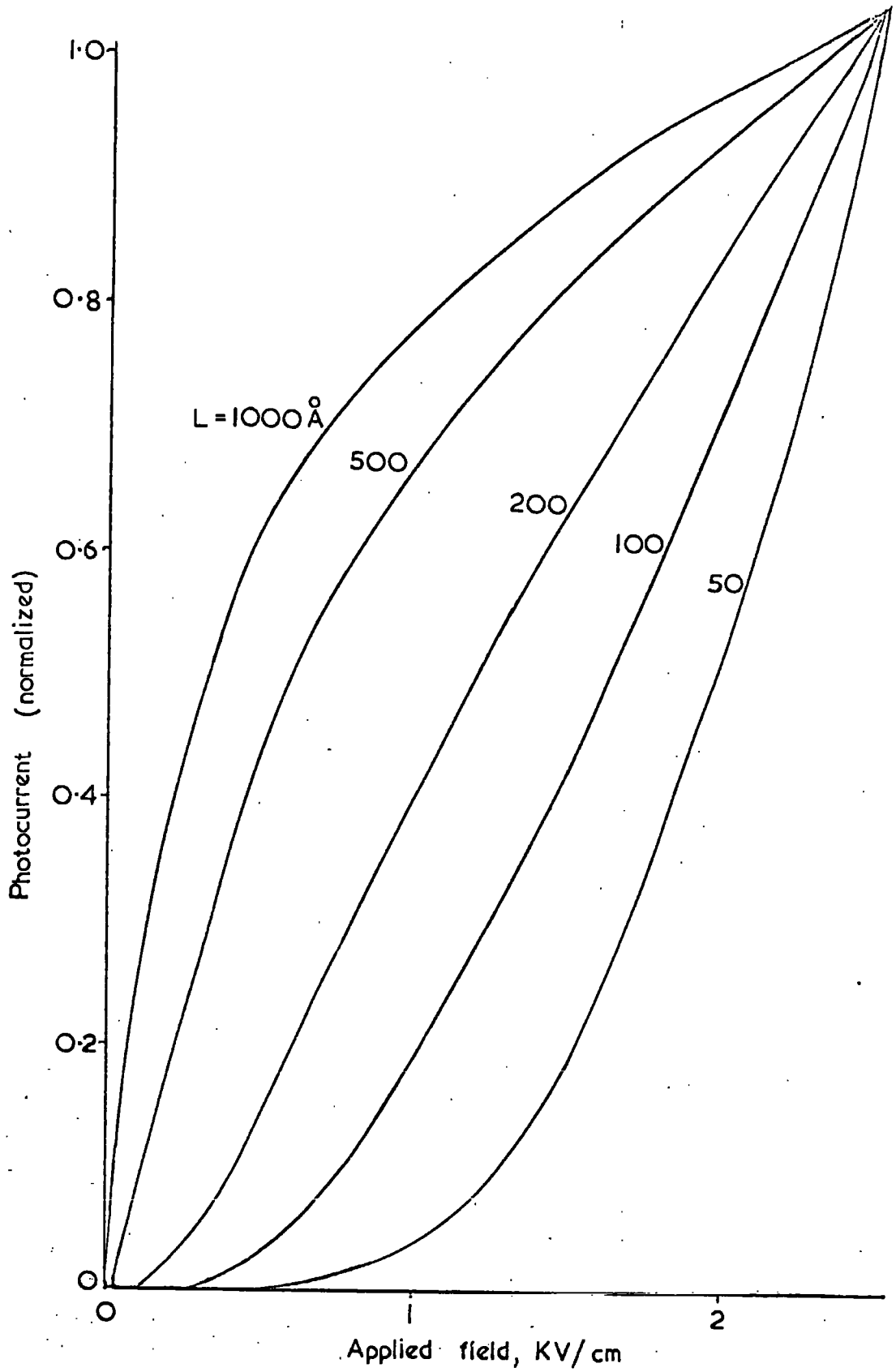

Figure 6.5. Theoretical variation of photocurrent with applied field for various values of L.

magnitude to the calculated result, then the resultant theoretical curve for L ≈ 100 Å takes the form shown in Fig. 6.6. Comparison of this curve with the best observed results (Fig. 4.10, Curve A) shows a very good agreement. The photocurrent in the present work can therefore be well explained by the above model together with a small amount of bulk ionisation.

Photoconduction in liquid gases due to energetic injected electrons has been explained elsewhere purely on the basis of a scattering mechanism,[67] without allowing for the image potential barrier. In liquid argon the quantity corresponding to L was found to be 1000 Å for such electrons. The present analysis shows that for hexane with L ≈ 100 Å, the image potential barrier is far from negligible. A lower value would be expected in hexane because of the difficulty in forming a slow carrier in argon so that the present work, although completely different in detail, appears to be consistent with the recent theoretical ideas on electron injection into liquid gases.

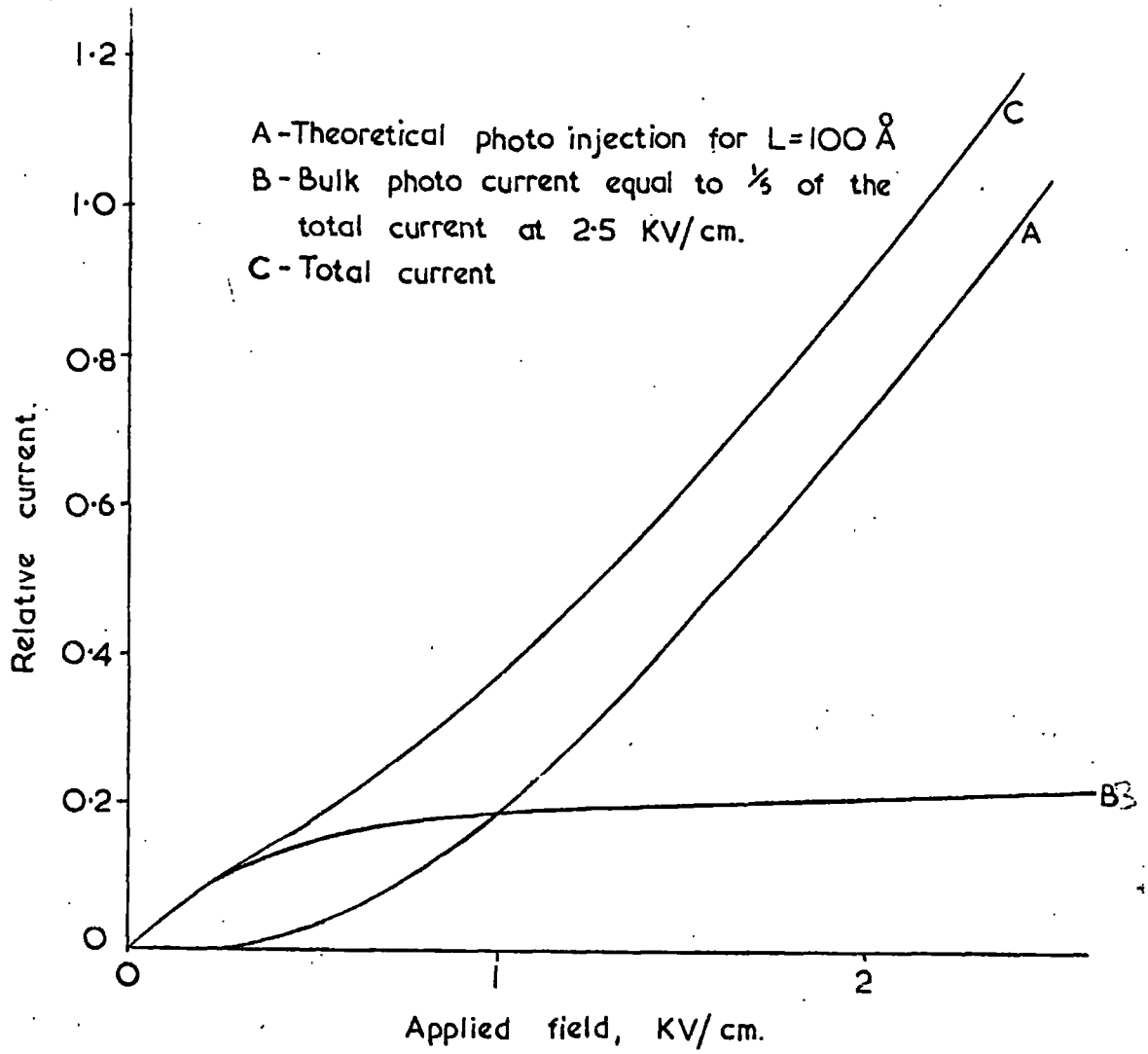

Figure 6.6. Theoretical variation of photocurrent with applied field for a combined photoinjection and photoionisation.

CHAPTER VII

DISCUSSION OF HIGH FIELD INJECTION

The large increase in the conduction current using razor blades as field emitters and the observed effect of impurities on the current led to an extensive study of high field injection in various grades of hexane, as described in Chapter V. Most of the earlier work was exploratory in nature and was carried out in simple apparatus. These preliminary results are discussed in Section 7.1. The important final measurements were made in a well designed cell and are discussed in Section 7.2. Section 7.3 gives a possible explanation of high field injection in pure and doped hexane.

7.1 Discussion of Preliminary Results

A large number of measurements was made on high field emission from razor blades without deliberate liquid flow. The main observations were:-

(a) the high currents obtained with comparatively low applied voltage;

(b) the large dependence of these currents on the purity of the liquid.

Each of these observations is discussed in detail in the following sub-sections.

7.1.1 High field injection

For a comparatively small voltage applied to the emitter, the conduction currents were much higher than the photocurrent measured earlier. These high currents (shown in Figures 5.5 and 5.8) are possibly due to field ionisation of the impurities or field emission of electrons due to the high field developed at the tip of the blades, or a mixture of both processes. The

field at the tip increases to a very high value for a small voltage applied to the emitter, as has been mentioned in Chapter III (equation 12). The increase in the current with decrease of the emitter anode distance (Fig.5.5) also shows the effect of an increased field.

At lower voltages, the conduction current is found to be almost independent of polarity (Fig. 5.6) which may be taken as an indication of field ionisation rather than field emission. The differences in the currents with different grades of hexane (Figure 5.12) may also be mainly due to variations in the impurity contents of the samples.

7.1.2 Effect of impurities on the conduction current

The increase of emitter current in flowing liquid, reported earlier by Hughes and Secker[54], led to the present measurements with apparatus capable of maintaining a steady flow in the emitter-grid region (Sec. 5.1). The effect of flow on the emitter current (Fig. 5.9) first observed in CCL hexane may be taken as being due to the presence of impurities. Among the various impurities in commercial grade hexane, dissolved water may be the most important. Although the solubility of water in hexane is very small (Chapter II), the presence of water greatly affects the conduction measurements, as shown in Fig. 5.12. The large fluctuations of the current observed in water saturated hexane may be due to minute water globules as subsequent measurements after the filtration of the sample showed a great reduction in the fluctuations. The later measurements of the effect of flow in pure (dried and filtered) and water saturated NWL hexane proved that the increase in emitter current with liquid movement (Fig. 5.14) only occurs in hexane containing impurities such as water.

Alcohol, being miscible with hexane in all proportions, served as a much better impurity for the investigation of the flow effect. The observed currents were much more steady in alcohol doped hexane than in water saturated samples but the effect of flow was similar in both cases. In general the emitter current increased with flow velocity, although a slight decrease at the higher liquid velocities and voltages (Figures 5.14 and 5.19) may be due to a change in flow-pattern round the grid. More reliable results were obtained later.

A decrease of grid current with liquid velocity was observed in both pure and water saturated samples (Figures 5.10 and 5.11). The decrease is likely as the grid is unable to intercept all the carriers moving towards it and some are swept away to the earthed collector before discharging. A larger decrease of grid current was thus observed at higher liquid velocities.

The PVC tube connecting the emitter and grid was later replaced by a PTFE cell for reasons mentioned earlier. The static currents measured in both arrangements were comparable for the same electrode spacing, thus showing no effect of the proximity of the PVC tube on field emission from the blade.

The increase in the static current with the increase of impurity content is due to the larger effect of ionised impurities. The increase was a linear function of water concentration (Figures 5.15 and 5.16) as would be expected[12] for such a low density of ions. The increase in emitter current with impurity concentration was also observed in alcohol doped hexane (Fig. 5.17) but with a tendency towards saturation for the higher flow currents at high alcohol concentrations (Fig. 5.18). This may be due to the large ion density affecting the flow current. This effect of flow on the emitter current will be discussed in more detail in Section 7.3.

7.2 Discussion of Final Results

Having found the basic characteristics of highfield injection and the effect of impurities on the emitter current, a flow cell (Sec. 5.1.3) was designed for precise measurements of field injection in hexane using a wide range of impurity contents and a liquid velocity of up to 2.6 m/sec. The important results are discussed in this Section.

7.2.1 Effect of polarity on emitter current

In pure hexane, the static emitter current with negative applied voltages was found to increase steadily with voltage. When the emitter was positive, the current was considerably less, particularly at the higher voltages. This effect of polarity on the conduction current is probably due to electron emission from the blade with the negative applied voltage. Adding alcohol to the pure sample, gave rise to a sharp increase in current for both polarities (Fig. 5.20). The fact that the emitter current in pure hexane is independent of liquid velocity suggests that the highfield injection is purely an electrode limited process in this case.

In doped samples with the blade negative, the emitter current was found to increase with liquid velocity (Figures 5.21 - 5.25). The increase is dependent on the impurity content of the liquid being greater in samples with a high impurity content for the same applied field and liquid velocity. This increase continues up to the limit set by complete field dissociation. This limit, or saturation level, is thus reached earlier at a low impurity content. In a sample with 4% alcohol, the saturation is beyond the maximum liquid velocity of 2.6 m/sec (Fig. 5.21) whereas for alcohol doping of 0.1% the saturation of the flow current occurred for liquid velocities even below one metre/sec (Fig. 5.25). These measurements are reproducible to a large

extent under similar experimental conditions, as shown by comparing Figures 5.23 and 5.23a.

The measurements of emitter current with the reverse polarity gave altogether different results. With the blade positive the emitter current was found to decrease with liquid movement in the same direction, i.e. towards the collector (Fig. 5.26). The decrease is more pronounced with the higher impurity content and at high liquid velocities (compare Figure 5.26 and 5.27). This effect is possible due to space charge build up around the emitter tip and it will be discussed further in Section 7.3.

7.2.2 Miscellaneous results

Low field conductivity measurements on well purified samples were limited by leakage of the cells used and they could not be made accurately. Measurements were, however, possible with doped samples. The value of conductivity obtained for water saturated hexane (3×10^{-14} mho/cm) is in good agreement with that reported by Standhommer and Seyer[12] (2×10^{-14} mho/cm). The conductivity of hexane doped with 4% alcohol is somewhat higher than that obtained by Secker and Scialom[14]. The values for concentrations lower than 4% are, however, smaller than would be obtained by extrapolating the latter workers' results. (Unfortunately no other data has been found for the conductivity of hexane containing less than 4% alcohol.) However, considering the varying impurity contents of the different grades of 'pure' hexane used, the observed conductivities of 4.2×10^{-12}, 2.5, 1.1, 0.6 and 0.2×10^{-12} mho/cm for 4, 2, 1, 0.5, and 0.1 per cent of alcohol, agree reasonably with those extrapolated from the work of Secker and Scialom, which give 2.0, 0.5, 0.2, 0.1 and $< 0.1 \times 10^{-12}$ mho/cm respectively.

The conductivity σ of an electrolytic solution with an impurity concentration C is theoretically proportional to $\sqrt{C.K(E)}$, where K is the field dependent dissociation constant (see Appendix B). Contrary to this, the conductivity was found to increase linearly with alcohol concentration in the present measurements (Fig. 7.1) and according to a power law at higher concentrations[14]. Bearing in mind that the theoretical relation is only valid for solutions below one-tenth of normal (4% alcohol makes approximately a normal solution in hexane) the linearity between σ and C is an intermediate case between a half-power law and a power law greater than unity. Thus, although the present measurements bridge the gap, they are still not easy to understand theoretically.

Some of the used hexane-alcohol mixture was analysed by vapour phase chromatography and u.v. transmittance to look for the formation of new products, if any[88]. No such products were found, which shows that there were no significant chemical reactions between the hexane molecules and either the alcohol or its dissociated fragments.

Measurements using different blades, liquid grades and a plate electrode (Figs. 5.30 and 5.31) were made in an attempt to obtain the high emitter current reported by Aplin. However, comparison of these results with those of Aplin[56], reproduced in Fig. 7.2, does not show the same features of field emission (e.g. high current level and high ratio of currents with the blade negative to positive) in the present work. The results of Aplin could not be reproduced even using his own blade and a satisfactory explanation for this disagreement could not be found.

The proposed highfield injection mechanism based on a general explanation of the results will be described in Section 7.3.

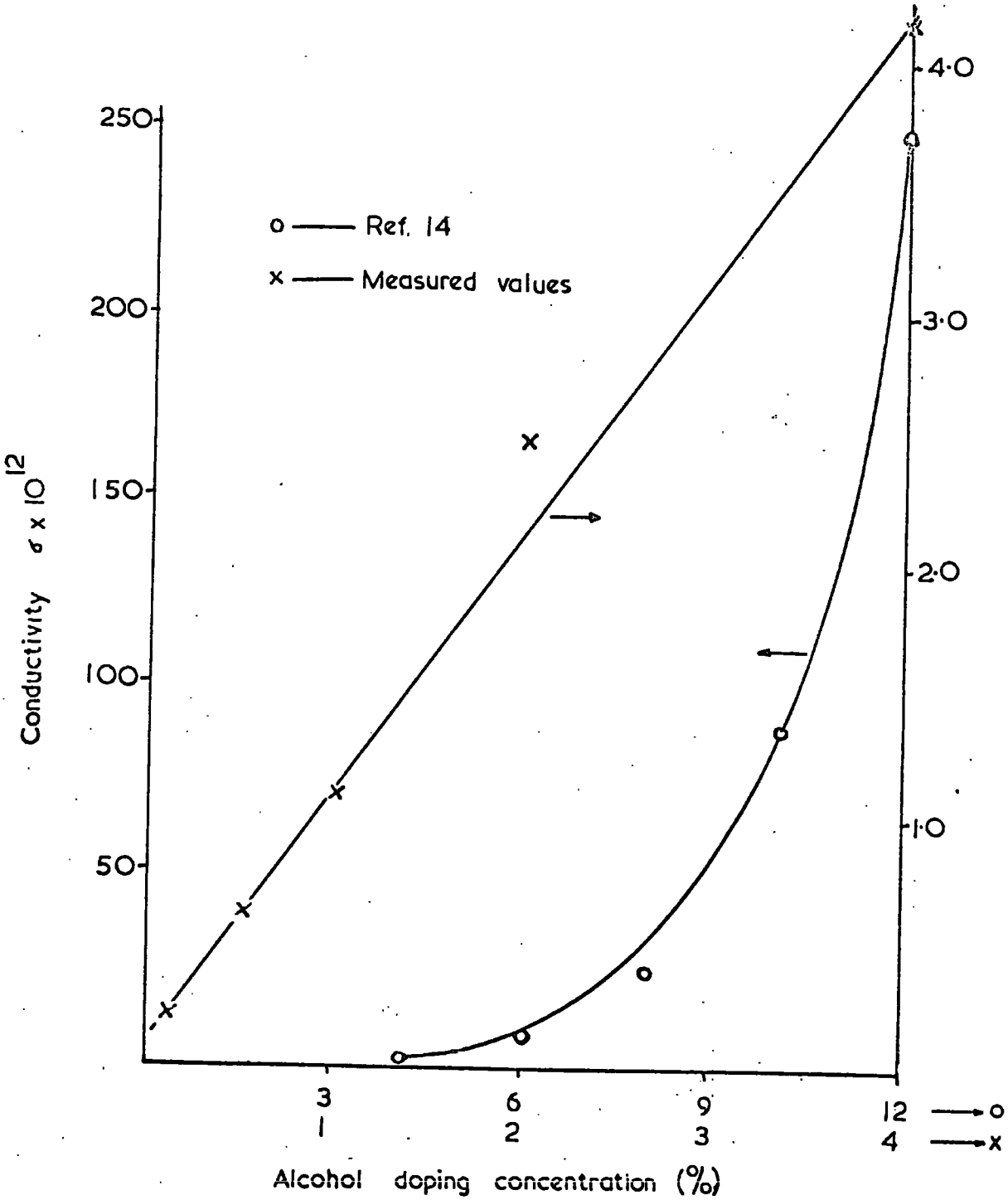

Figure 7.1. Variation of conductivity of hexane with alcohol concentration (per cent by volume).

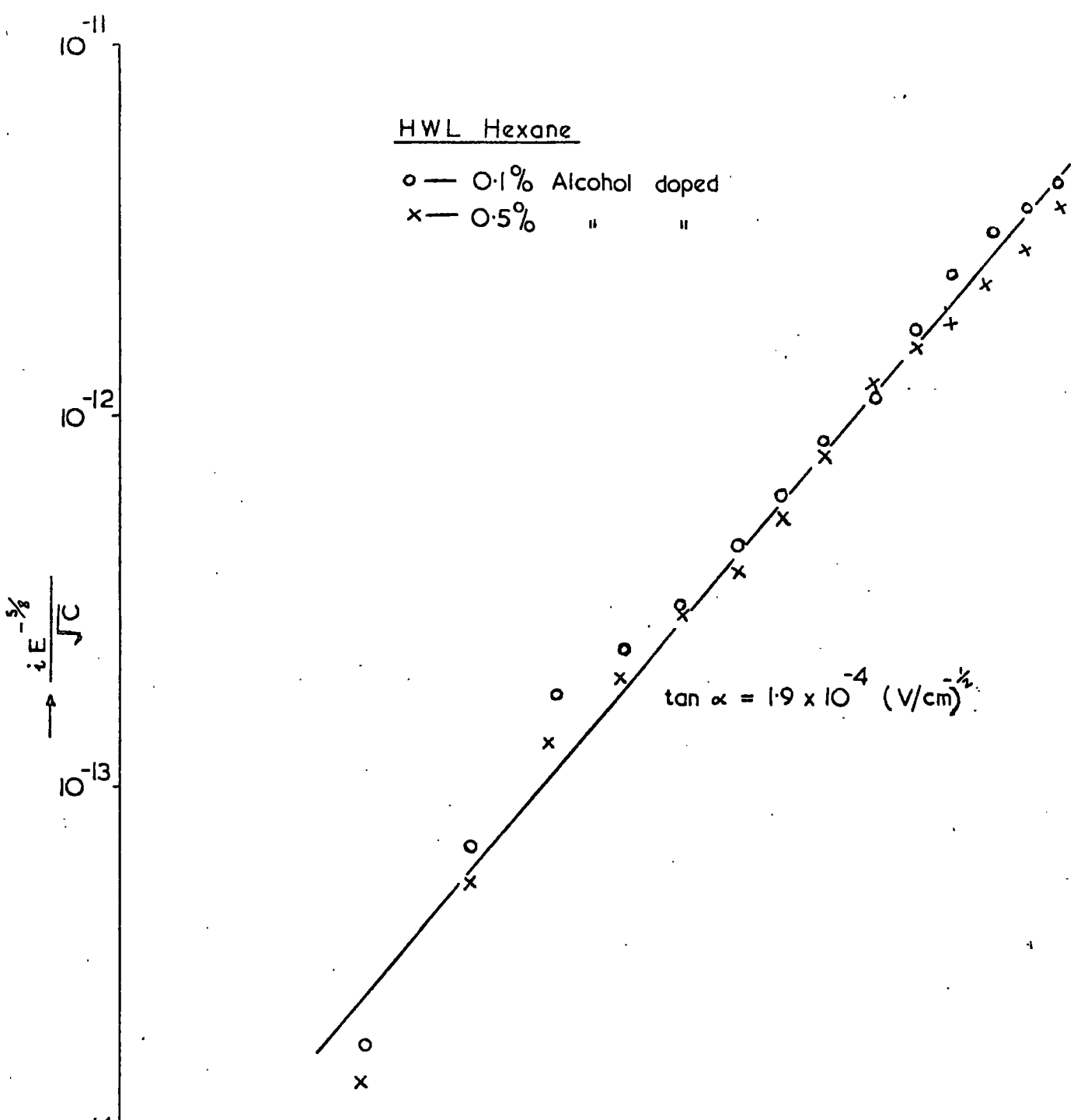

Figure 7.3. Variation of impurity current with applied field in alcohol doped hexane.

7.3 High-field Injection in Hexane

Previous workers on high field injection have argued that the higher current with the blade negative indicates electron emission from the tip (tip radius < 600 Å). For pure field injection, the conduction current should therefore satisfy the Fowler-Nordheim relation. Although Secker and Aplin[55] tried to explain their results by such a plot (e.g. $\log_e \frac{i}{V^2} \propto \frac{1}{V}$), the high values of the conduction current with the blade positive cast doubt on a pure field-injection process in their experiments. We therefore need to consider what controls the conduction current in more detail.

As with photoinjection, the conduction current due to high field injection is either (a) Electrode limited (ELC) or
(b) Bulk limited (BLC).

A study of the effect of bulk movement on the conduction current gives a great deal of information on the process limiting the current. In ELC, the flow of liquid will have no effect on the current magnitude as the current in such cases will not depend critically on the movement of the charge carriers. Limitation by the rate of emission of electrons at the cathode and the subsequent formation of negative charge carriers (as with photo-injection) will give rise to a conduction current that remains unchanged with bulk movement. When the blade is made positive the electrode process is electron extraction at the anode. This is a new process in the high field work which was not considered in the case of photoinjection because of the comparatively low applied field used there. Electron extraction from the hexane molecules is equivalent to dissociation with the current carried by the movement of the positive charge carriers formed, or of electron vacancies away from the point. The rate of carrier formation and <u>not</u> the

velocity of the carriers may determine the current, i.e. the current can be electrode limited for positive polarity also.

On the other hand, a bulk limited current is controlled either by the space charge (SCL) or by the formation of carriers in the bulk of the liquid. In the present case the additional carriers are believed to be ions formed by the field ionisation of the impurities present. In any case the movement of the bulk will always greatly affect a BLC. In the photoinjection experiments, the impurities in the hexane could be removed and bulk ionisation could be shown to be largely eliminated, to leave an ELC current. In the field-injection work, the field dissociation of impurities in commercial or doped hexane gives rise to additional charge carriers. The current due to these additional charge carriers (possibly ions) is bulk limited and the conduction current will therefore be effected by the movement of the bulk. The processes in pure and impure hexane will now be discussed in greater detail.

7.3.1 Current in pure hexane

One of the most important results of this work is that in dried and filtered hexane the high field injection current is independent of bulk movement. The current in such liquids is therefore ELC. With the blade negative the controlling electrode effect must be electron emission from the tip because field dissociation with transfer of a positive charge to the metal is not possible. The existence of free electrons in hexane is difficult to visualize for reasons described in the discussion of the photoinjection experiments. Electrons introduced into the bulk probably form negative carriers within perhaps 100 Å of the tip by attachment to neutral

hexane molecules or to dissolved gas molecules (Sec. 6.3). These carriers move towards the opposite electrode under the action of the applied field, with the electrons possibly jumping to other individual molecules by any of the processes mentioned in Chapter III. It should be noted that the formation of a negative carrier at the negative tip, in the way described above, is indistinguishable from its formation by field dissociation in the ELC case.

When the blade is made positive, the high field developed at the tip can only remove electrons from the neutral molecules to form some sort of positive ions which move towards the opposite electrode. This may be equivalent to electron vacancy movement[40] towards the cathode if electrons from neutral molecules jump into vacancies in the neighbouring positive ions. Although these positive carriers carry the current, it cannot be either the carrier velocity or the space charge that determines the amount of current in the ELC case.

On the above argument it would be expected that negative polarity on the blade would give a slightly larger current than for positive polarity as observed. There are many electrons in the metal and their emission into the liquid due to negative polarity is independent of the configuration of the surrounding hexane molecules. For positive polarity, on the other hand, the hexane molecules must probably be in the correct orientation before an electron can be extracted into the metal.

It is felt that the simple fact that the current injected into pure hexane is independent of flow enables the simple model proposed above to be substantiated. It is certainly capable of explaining the general

features of the experimental results for pure hexane and proves the electrode limitation in this case.

7.3.2 Current in impure hexane

As opposed to the case of pure hexane, the high field injection current into impure liquid changes considerably with flow. One of the most important of the present results is that the current increases with flow for the negative polarity point, but decreases for positive polarity. Flow dependence shows that the current magnitude must be determined by bulk processes in this case (i.e. BLC) even though the carriers may still originate at the high field electrode. The conduction process must therefore be considerably different from the ELC case considered previously.

It will be assumed that in impure hexane the impurities dissociate more readily in an electric field than do the hexane molecules themselves. The impurities are polarised by the applied field and those near the tip may easily become dissociated into positive and negative ions. The field dissociation of impurities may thus result in a higher conduction current. It has been shown that the increased conduction of impure insulating liquids is due to partial dissociation of the water content of the liquid even at low field strengths. The big increase in the high field injection current in water saturated hexane, compared with pure hexane, and the similarity of the current voltage curves between water saturated and commercial hexane (Fig. 5.13) may be taken as proof of additional dissociation in the high fields. For alcohol doping the current was measured for both high and low fields, and the increase in the high field injection current was considerably higher than that measured with plane electrodes.[25] This is

also a good indication of increased dissociation caused by the high field developed at the tip.

The ions formed by field dissociation move towards the opposite electrode. In the drift space some of the ions may be lost by recombination with those of opposite sign (Sec. 3.1.1). Depending upon the polarity of the blade either positive or negative ions approach the tip, where they may cause very different effects. With the blade negative, all the positive ions reaching the vicinity of the tip are assumed to be neutralised by electrons emitted from the tip. On the other hand, negative ions approaching a positive tip may not be discharged instantaneously so that they will form a space charge region around the tip. The consequences of this will be considered later.

A theoretical analysis of current due to impurity dissociation in liquids has been given by Onsager[79] and was applied to hexane by Coelho and Bono[76]. Assuming (a) that at the lower alcohol concentrations the effect of change in dielectric constant or viscosity on the conduction current is negligible and (b) that the theoretical conductivity concentration relation holds good for the high field region, the ionisation current is expected to vary according to equation (13) for alcohol concentrations up to about one tenth normal ($\sim$ 0.5%). Although a plot of log $(iE^{-\frac{5}{8}}/\sqrt{c})$ against $\sqrt{E}$ for 0.1% and 0.5% alcohol concentration gives a straight line with a large amount of scatter (Fig. 7.3), the wide difference between the slope of the line ($1.9 \times 10^{-4}(V/cm)^{-\frac{1}{2}}$) and the theoretical value ($4.6 \times 10^{-3}(V/cm)^{-\frac{1}{2}}$) casts doubt on the validity of the assumptions or of equation (13) for the range of field strengths used here. The agreement with theory is considerably worse than was found for Coelho & Bono, who used a cylindrical electrode arrangement.

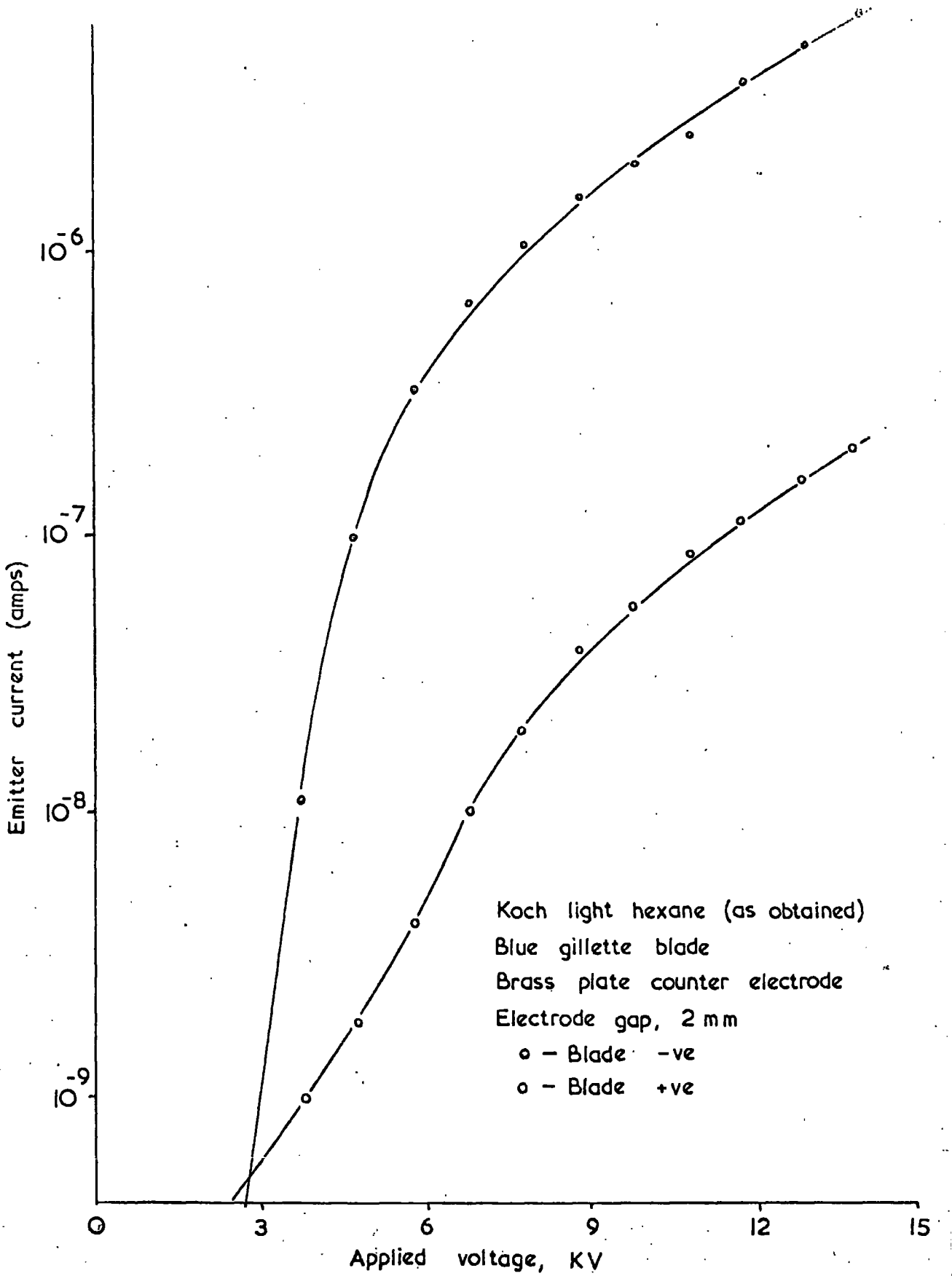

Figure 7.2. Variation of emitter current with applied voltage obtained by Aplin (private communication).

The charge carriers that have been considered above are more or less in equilibrium with the neutral molecules so that bulk motion of the liquid will result in the charge being transported in the same direction as the liquid flow. The effect of flow on the conduction currents observed in the present measurements has already been discussed theoretically in Section 3.2.2. With the blade negative, the positive ions attracted towards it are neutralised at distances of the order of 100 Å while the negative ions impart their charges to the other (large area) electrode. When the liquid is moving towards the grid, the negative ions are swept away more quickly from the high field electrode and more impurity molecules are brought into the high field region for dissociation. The flow thus leads to the formation of more ion pairs with a corresponding increase in the current. The current therefore increases with flow velocity up to a value corresponding to total field dissociation of the impurity in the high field region. At a lower concentration of impurity, this limit will be reached at a lower field strength and also at a lower liquid velocity (as is shown by comparing Figures 5.22 and 5.25). For the doping level of 4% of alcohol, the saturation point is probably well outside the range of the applied voltage and the liquid velocity used, but for low concentrations it can clearly be seen.

When the blade is made positive, the negative ions formed by field dissociation may not be discharged instantly at the tip. A negative space charge layer is therefore formed around the tip and this will partly limit the current. With liquid flow, the positive ions are removed more quickly from the high field region while the number of non-neutralised negative ions increases. This increase in the negative carrier density around the

tip decreases the field outside the space charge region so that, although more impurity molecules are available for field dissociation, the overall result is a reduction in the dissociation with a consequent decrease in the current. The decrease becomes more pronounced at the higher impurity concentrations and also with higher liquid velocity (e.g. Figures 5.26 and 5.27) because of the larger space charge build-up at the tip. The experimental results all agree with this model.

This discussion has shown that it is possible to explain the general features of injection into pure hexane and of the effect of flow in impure hexane comparatively simply in spite of the most surprising result which was a decrease in the current for the positive polarity. However, it has not been possible to account in detail for the impurity concentration dependence or for quantitative features of the results. Both of these will require much more detailed understanding of electrolytic processes in hexane.

CHAPTER VIII

CONCLUSIONS

The original aim of this work was to obtain the injection of large concentrations of charge carriers into pure hexane for electron spin resonance measurements. The experiments showed that the required charge density for such measurements cannot be obtained in pure samples. The large carrier injection currents that have been achieved are due to impurities in the hexane and there is considerably less incentive to examine impurity charge carriers by ESR. The aim of the work was therefore changed to an investigation of the injection processes themselves.

Injection of charge carriers into dielectric liquids can use either photoelectric or high-field effects. Injection by the photoelectric method requires a good photocathode, highly pure and degassed liquid and a proper selection of the radiation wavelength. Under these conditions, photoelectrons are emitted from the cathode. The current is then limited simply by the rate of emission of photoelectrons and their conversion into heavy carriers as has been proved by the simultaneous measurements of the d.c. photocurrent and the pulse photocharge.

The emission of electrons from the photocathode does not follow the Schottky effect although the field variation of the observed current has been explained in terms of a similar image barrier together with the probability of a photoelectron forming the unidentified heavy charge carrier. Although ionisation in the bulk hexane due to the u.v. radiation

cannot be totally neglected in spite of the great care taken in purification, the u.v. transmittance measurements show that there is no detectable long term photoeffect in the liquid. The photocurrent just after the evaporation of a fresh cathode in a highly degassed cell is shown to be most characteristic of photoemission from the cathode and is thought to be a great improvement on earlier work.

Now that a model for photoinjection has been established, there is a great deal more work that should be done on the details of the process. For example, more comparative measurements into vacuum and into hexane with a single photocathode (as done by Pugh) would help in the quantitative evaluation of the model. Photoinjection measurements as a function of wavelength are required to give the photoelectric threshold and, hence, information on the work function change from vacuum to hexane.

The low value of carrier mobility suggests that the charge carriers are either

(a) ions formed by the photoelectrons combining with oxygen or other impurities present or

(b) polarons formed by the photoelectrons becoming surrounded by polarised neutral hexane molecules.

There appears to be no way of distinguishing between these at the present time.

Charge injection into hexane by the high-field effect gives a much larger current than photoinjection for the same applied voltage. Both the injection process itself and the variation of the conduction current with the applied voltage are however very difficult to explain quantitatively.

The conduction current is greatly affected by impurities in the liquid, water and unsaturated compounds probably being the most important. This was not suspected in work done elsewhere in which large charge injection into flowing liquids was thought to be due to electron emission from the high-field electrode. The present work, done independently, has shown that the injection current into pure hexane is comparatively small, although it is certainly electrode limited and due to electron emission when the tip is negative. The increase in the conduction current in either doped or commercial hexane is a result of impurity ionisation. It appears that the hexane molecules, however, do not take part in any chemical reactions with these ions.

The variation of the conduction current with liquid velocity can also be explained in terms of field ionisation of impurities present in the liquid. Recent work by Hughes[92] (reported since most of the present work was completed) also shows that the high carrier injection from a razor blade into hexane is only obtained if the liquid contains some foreign substances such as water in solution. The high conduction currents reported by Secker and Aplin[55] could not be reproduced in the present work. Their high values were possibly due to impurity ionisation (not present here) and not exclusively due to field emission of electrons as they claim. If large currents can only be obtained by impurity ionisation rather than electron emission, the prospects for the use of hexane in high voltage generators are considerably less favourable.

The mechanisms of charge injection into hexane, particularly by the high-field effect, seems to be very complicated. Because of its possible use in high voltage machines, further measurements are necessary on this

subject. Measurements on the field injection process should include an investigation of the mobility of field injected charge carriers in both pure and impure hexane in order to confirm the present model. The effect of liquid motion from the grid towards the emitter may also be of great assistance in understanding the conduction process. It may still be possible to use an electron spin resonance method to identify the charge carriers in the high-field conduction, although this would be a considerable technical undertaking requiring a highly sensitive spectrometer.

This investigation used the basic techniques employed by other workers for obtaining charge injection into hexane with the aim of finding out more about the processes involved. Although some of the results are similar to previous findings, it is thought that the present work makes some important original contributions to this particular field of study.

APPENDIX A

SPACE CHARGE LIMITED CURRENT

Neglecting the diffusion term, the expression for the current density J at a field strength E is

$$J = ne\,\mu E \tag{A1}$$

where n is the carrier density and μ is the mobility.

By substituting from Poisson's equation in one dimension, (A1) becomes

$$J = K\,\varepsilon_o\,\mu E\,\frac{dE}{dx} \tag{A2}$$

where ε_o is the permittivity of free space and K is the dielectric constant of the medium.

Equation (A2) after integration with respect to x becomes

$$\frac{Jx}{K\,\varepsilon_o\,\mu} = \frac{E^2}{2} + \text{constant.} \tag{A3}$$

Applying the boundary condition that E = Eo at x =0, the constant of integration is - $Eo^2/2$. Equation (A3) therefore becomes

$$\frac{2\,Jx}{K\,\varepsilon_o\,\mu} + E_o^{\,2} = E^2 \tag{A4}$$

Or, since $E = \frac{dV}{dx}$,

$$\left(\frac{2\,Jx}{K\,\varepsilon_o\,\mu} + E_o^{\,2}\right)^{\frac{1}{2}} = \frac{dV}{dx} \tag{A5}$$

Integration of equation (A5) leads tp

$$\frac{K\,\varepsilon_o\,\mu}{3J}\left(\frac{2\,Jx}{K\,\varepsilon_o\,\mu} + E_o^{\,2}\right)^{3/2} = V + \text{constant} \tag{A6}$$

Applying the further boundary condition that at x = 0, V = 0; the constant of integration equals $\frac{K\,\varepsilon_o\,\mu E_o^{\,3}}{3J}$. Equation (A6) after rearrangement then takes the form

$$\frac{K\,\varepsilon_o\,\mu}{3J}\left[\left(\frac{2Jd}{K\,\varepsilon_o\,\mu} + E_o^{\,2}\right)^{3/2} - E_o^{\,3}\right] = V \tag{A7}$$

Putting $E_o = 0$, equation (A7) reduces to the space charge limited form

$$J = \frac{9}{8}\,\frac{K\,\varepsilon_o\,\mu}{d^3}\,V^2 \tag{A8}$$

APPENDIX B

THE VARIATION OF CONDUCTIVITY WITH IMPURITY CONCENTRATION

The specific conductivity of a solution containing N moles per cubic centimetre of solute capable of dissociating into monovalent ions is given by [78]

$$\sigma = \Lambda N \tag{B1}$$

where Λ is called the 'equivalent conductivity', i.e. the specific conductivity per gram equivalent per cubic centimetre. This equivalent conductance is related to the degree of dissociation α by the relation

$$\alpha = \frac{\Lambda}{\Lambda_o} \tag{B2}$$

where Λ_o is the value of Λ at infinite dilution.

It is obvious however, that if the viscosity of a solution changes with concentration, the drift velocity of the ions, which accounts for the conductivity, will also very with concentration and the above relation becomes

$$\alpha = \frac{\Lambda}{\Lambda_o}\frac{\eta}{\eta_o} \tag{B3}$$

where η and η_o are the viscosities of the solution at the equivalent conductances Λ and Λ_o respectively.

The degree of dissociation is also dependent on the concentration of the solution. If c is the concentration of the electrolyte, the concentration of each type of ion will be αc and that of the undissociated molecules $(1 - \alpha)c$. Applying the law of mass action, the dissociation constant K is given by

$$K = \frac{\alpha c . \alpha c}{(1 - \alpha)c} = \frac{\alpha^2 c}{1 - \alpha} \tag{B4}$$

For weak electrolytes $\alpha << 1$, therefore

$$K \simeq \alpha^2 c = \Lambda \Lambda^2 c \tag{B5}$$

From which

$$\Lambda = \sqrt{\frac{K}{Ac}} \tag{B6}$$

Substituting the relation (B6) in (B1), the specific conductivity takes the form

$$\sigma = \sqrt{\frac{K}{Ac}} \cdot N = B\sqrt{Kc} \qquad (B7)$$

where A and B are constants.

The relationship (B4), which is known as Ostwald's dilution law, only holds if the solution is very dilute (below 0.1 Normal). As the concentration is raised, this law fails and K becomes a function of concentration.

REFERENCES

1. Adamczewski, I. — Ionisation, Conductivity and Breakdown in Dielectric Liquids. Taylor & Francis Ltd., London, 1969.
2. Pugh, D.R. — Ph.D. Thesis, Durham University, 1968.
3. Bloor, A.S. — Ph.D. Thesis, Durham University, 1970.
4. Morant, M.J. — Nature, 187, 48, 1960.
5. Hughes, J.F. — Ph.D. Thesis, University of Wales (University College of North Wales, Bangor), 1968.
6. Zaky, A.A., Tropper, H. & House, H. — Brit. J. App. Phys. 14, 651, 1963.
7. House H. — Proc. Phys. Soc. London, B70, 913, 1957.
8. Guizonnier, R. — J. Electrochem. Soc. 108, 519, 1961.
9. Guizonnier, R. — J. Phys. Rad. 20, 153A, 1959.
10. Taris, F. & Guizonnier, R. — Rev. Gen. Elect. 75, 1295, 1966.
11. Sharbaugh, A.H. & Barker Jr., R.E. — Proc. Conf. on Conduction Processes in Dielectric Liquids, Grenoble, Sept. 17-19, 1968, 349-361.
12. Standhommer, P. & Seyer, W.F. — J. App. Phys. 28, 405, 1957.
13. Kleinheins, G. — J. Phys. D : App. Phys. 3, 75, 1970.
14. Secker, P.E. & Scialom, I.N. — J. App. Phys. 39, 2957, 1968.
15. Stannett, A.W. — Brit. J. App. Phys. 2, 110, 1951.
16. Kahan, E. — Ph.D. Thesis, Durham University, 1964.
17. Felsenthal, P. & Vonnegut, B. — Brit. J. App. Phys. 18, 1801, 1967.
18. Krasucki, Z. — Proc. Conf. on Conduction Processes in Dielectric Liquids, Grenoble, Sept. 17-19, 311-323, 1968.

19. Liebermann, L. J. App. Phys. 28, 205, 1957.

20. Jachym, B. Acta Phys. Pol. 36, 469, 1969.

21. Jachym, A. & Jacym, B. Acta Phys. Pol. 36, 1053, 1969.

22. Lewis, T.J. Progress in Dielectrics, 1, 97, 1959.

23. Dornte, R.W. Ind. & Eng. Chem., 32, 1529, 1940.

24. Baker, E.H. & Boltz, H.A. Phys. Rev. 51, 275, 1937.

25. Kao, K.C. & Calderwood, J.H. Proc. I.E.E. 112, 597, 1965.

26. Green, W.B. J. App. Phys. 26, 1256, 1955.

27. Zein-El-dine, M.E., Zaky, A.A., Hawky, R. & Cullingford, M.C. Proc. I.E.E. 112, 580, 1965.

28. Croitoru, Z. Progress in Dielectrics, 6, 103, 1965.

29. Bloor, A.S. & Morant, M.J. Proc. Conf. on Conduction Processes in Dielectric Liquids; Grenoble, Sept. 17-19, 1968, 507-523.

30. Zein-El-dine, M.E. & Tropper, H. Proc. I.E.E. C103, 35, 1956.

31. Hesketh, T.R. & Lewis, T.J. Brit. J. App. Phys. 2, 557, 1968.

32. Hancox, R. Brit. J. App. Phys. 8, 576, 1957.

33. Kao, K.C. & Higham, J.B. J. Electrochem. Soc. 108, 522, 1961.

34. Sletten, A.M. & Lewis, T.J. Brit. J. App. Phys. 14, 883, 1963.

35. Sletten, A.M. Nature 183, 311, 1959.

36. Brignell, J.E. & House, H. Nature 206, 1142, 1965.

37. Goodwin, D.W. & McFadyn, K.A. Proc. Phys. Soc. London, B66, 85, 1953.

38. Crowe, R.W. J. App. Phys. 27, 156, 1956.

39. Metzmacher, K.D. & Brignell, J.E. J. Phys. D : App. Phys. 3, L5, 1970.

40. Gosling, C.H. J.I.E.E. Sept. 1963 pp 380-383.

41. Minday, R.M., Schmidt, L.D. & Davis, H.T. J. Chem. Phys. 50, 1473, 1969.

42. Essex, V. & Secker, P.E. Brit. J. App. Phys. 2, 1107, 1969.

43. Terlecki, J. & Gzowski, O. Acta Phys. Austr. 15, 337, 1962.

44. Terlecki, J. Nature 194, 172, 1962.

45. Le Blanc Jr., O.H. J. Electrochem. Soc. 30, 1443, 1959.

46. Swan, D.W. Nature 190, 904, 1961.

47. Chong, P., Sugimoto, T. & Inusi, Y. J. Phys. Soc. Japan 15, 1137, 1960.

48. Kalinowski, J. Proc. Conf. on Conduction Processes in Dielectric Liquids, Grenoble, Sept. 17-19, 1968, 295-310.

49. Stuetzer, O.M. J. App. Phys. 31, 136, 1960.

50. Jorgenson, G.V. & Will, E. Rev. Sci. Inst. 33, 55, 1962.

51. Coe, G., Hughes, J.F. & Secker, P.E. Brit. J. App. Phys. 17, 885, 1966.

52. Essex, V. & Secker, P.E. Brit. J. App. Phys. 1, 63, 1968.

53. Gray, E. & Lewis, T.J. Brit. J. App. Phys. 16, 1049, 1965.

54. Hughes, J.F. & Secker, P.E. Electronic Lett. 2, 175, 1966.

55. Secker, P.E. & Aplin, K. Paper presented at I.E.E. Lancaster Conf. on Dielectric Materials, Measurements and Applications, July 1970.

56. Aplin, K. Private communication.

57. Secker, P.E. Brit. J. App. Phys. 16, 1527, 1965.

58. Secker, P.E. & Lewis, T.J. Brit. J. App. Phys. 16, 1649, 1965.

59. Gzowski, O. & Chybicki, M. Z. Phys. Chem. 233, 117, 1966.

60. Sato, T., Nagao, S. & Toriyama, Y. Brit. J. App. Phys. 7, 297, 1956.

61. Halpern, B. & Gomer, R. J. Chem. Phys. 51. 1031, 1969.

62. Secker, P.E., Jessup, M. & Hughes, J.F. J. Sci. Inst. 43, 515, 1966.

63. Watson, P.K. & Clancy, T.M. Rev. Sci. Insti. 36, 217, 1965.

64. Savoye, ED. & Anderson, D.E. J. App. Phys. 38, 3244, 1967.

65. Green, N. M.Sc. Dissertation, Durham University, 1969.

66. Silver, M., Smejtek, P. & Onn, D.G. Private communication.

67. Silver, M., Kumbhare, P., Smejtek, P. & Onn, D.G. J. Chem. Phys. 52, 5195, 1970.

68. Frenkel, J. Kinetic Theory of Liquids, Clarendon Press, Oxford, 1946, Chapter V.

69. Swan, D.W. Proc. Phys. Soc. London, 82, 74, 1963.

70. Weiss, J. Nature 186, 751, 1960.

71. Lewis, T.J. J. App. Phys. 26, 1405, 1955.

72. Lewis, T.J. Proc. Phys. Soc. London, B68, 504, 1955.

73. Thomson, J.J. Conduction of Electricity through Gases, Cambridge University Press, 1928, Chapter XI.

74. Onn, D.G. & Silver, M. Phys. Rev. 183, 295, 1969.

75. Stuetzer, O.M. J. App. Phys. 31, 136, 1960.

76. Coelho, R. & Bono, M. J. Electrochem. Soc. 107, 94, 1960.

77. Gemant, A. Liquid Dielectrics, John Wiley, London 1933, Chapter IV.

78. Newman, F.H. Electrolytic Conduction, Chapman and Hall, 1930, Chapter III.

79. Onsager, L. J. Chem. Phys. 2, 599, 1934.

80. Strong, J. Phys. Rev. 43, 498, 1933.

81. Instructions - Edwards High Vacuum Coating Unit, Model 6E4, p-6.

82. Evans, D.F. J. Chem. Soc. 1, 345, 1953.

83. Munck, A.U. & Scott, J.F. Nature 177, 587, 1956.

84. Potts, W.J. J. Chem. Phys. 20, 809, 1952.

85. Kiselev, A.V. Quart. Rev. Chem. Soc. 15, 99, 1961.

86. Hughes, J.F. & Secker, P.E. Brit. J. App. Phys. 2, 1115, 1969.

87. Kay, J.M. An Introduction to Fluid Mechanics & Heat Transfer, Cambridge University Press, 1963, pp 24-25.

88. Gray, P. & Williams, A. Chem. Rev. 59, 239, 1959.

89. Hughes, A.L. & Du Bridge, L.A. Photoelectric Phenomenon. McGraw Hill, 1932. pp 49 - 50.

90. Gray E. & Lewis, T.J. Brit. J. App. Phys. 2, 93, 1969.

91. Guth, E. & Mullin, C.J. Phys. Rev. 59, 867, 1941.

92. Hughes, J.F. J. Chem. Phys. 53, 2598, 1970.

A C K N O W L E D G E M E N T

I would like to express my deep gratitude to Dr. M.J. Morant for his supervision and every possible help throughout the work and the preparation of this Thesis. I would like to thank the Ministry of Education, Government of Pakistan, for the award of a Scholarship under the Central Overseas Training Scheme and the University of Dacca for the grant of study leave during this period of my research. I would also like to thank Prof. D.A. Wright for providing the necessary facilities for research, the technical staff of the Department headed by Mr. F. Spence for making the apparatus, Mrs. C. Pennington for helping in the diagrams and Mrs. J. Geary for typing the Thesis.